# RADAR/RADIO TROPOSPHERIC ABSORPTION AND NOISE TEMPERATURE

Lamont V. Blake

Naval Research Laboratory
Washington, D. C.

30 October 1972

NRL Report 7461

# Radar/Radio Tropospheric Absorption and Noise Temperature

LAMONT V. BLAKE

*Radar Geophysics Branch*
*Radar Division*



October 30, 1972



NAVAL RESEARCH LABORATORY
Washington, D.C.

Security Classification

**DOCUMENT CONTROL DATA - R & D**

*(Security classification of title, body of abstract and indexing annotation must be entered when the overall report is classified)*

| | |
|---|---|
| 1 ORIGINATING ACTIVITY (Corporate author)<br>Naval Research Laboratory<br>Washington, D. C. 20390 | 2a. REPORT SECURITY CLASSIFICATION<br>Unclassified<br>2b. GROUP |

3 REPORT TITLE

RADAR/RADIO TROPOSPHERIC ABSORPTION AND NOISE TEMPERATURE

4 DESCRIPTIVE NOTES *(Type of report and inclusive dates)*
A final report on one phase of the problem.

5 AUTHOR(S) *(First name, middle initial, last name)*

Lamont V. Blake

| | | |
|---|---|---|
| 6 REPORT DATE<br>October 30, 1972 | 7a. TOTAL NO OF PAGES<br>84 | 7b. NO OF REFS<br>27 |
| 8a CONTRACT OR GRANT NO<br>NRL Problem R02-64.201<br>b. PROJECT NO<br>Project SF-11-141-005-15483<br>c.<br>d. | 9a. ORIGINATOR'S REPORT NUMBER(S)<br>NRL Report 7461<br>9b. OTHER REPORT NO(S) *(Any other numbers that may be assigned this report)* | |

10 DISTRIBUTION STATEMENT
Approved for public release; distribution unlimited.

| | |
|---|---|
| 11 SUPPLEMENTARY NOTES | 12 SPONSORING MILITARY ACTIVITY<br>Department of the Navy<br>Naval Ship Systems Command<br>Washington, D. C. 20390 |

13 ABSTRACT

Fortran digital-computer routines to calculate absorption loss for radiowave propagation in the troposphere have been developed, and machine plots of radar attenuation as a function of range have been made for a standard atmosphere, over the frequency range 100 MHz to 100 GHz. The tropospheric noise temperature has also been calculated and plotted. This work is an updating of earlier calculations that were less accurate, especially in the frequency range above 10 GHz. Separate curves for the oxygen and water-vapor components of the absorption loss are provided in addition to the curves for total loss; this allows the loss for values of water-vapor density other than the standard 7.5 g/m$^3$ to be found, by applying a simple multiplicative factor. The computer routines, listed at the end of the report, have also been used as part of a computer program to calculate the maximum range of a radar system.

1A

DD FORM 1 NOV 1473 (PAGE 1)

S/N 0101-807-6801

Security Classification

| 14 KEY WORDS | LINK A | | LINK B | | LINK C | |
|---|---|---|---|---|---|---|
| | ROLE | WT | ROLE | WT | ROLE | WT |
| Microwave atmospheric absorption<br>Microwave oxygen absorption<br>Microwave water-vapor absorption<br>Radio noise temperature<br>Radiowave propagation | | | | | | |



DD FORM 1 NOV 68 1473 (BACK)
(PAGE 2)

## CONTENTS

## ABSTRACT

Fortran digital-computer routines to calculate absorption loss for radio-wave propagation in the troposphere have been developed, and machine plots of radar attenuation as a function of range have been made for a standard atmosphere, over the frequency range 100 MHz to 100 GHz. The tropospheric noise temperature has also been calculated and plotted. This work is an updating of earlier calculations that were less accurate, especially in the frequency range above 10 GHz. Separate curves for the oxygen and water-vapor components of the absorption loss are provided in addition to the curves for total loss; this allows the loss for values of water-vapor density other than the standard 7.5 $g/m^3$ to be found, by applying a simple multiplicative factor. The computer routines, listed at the end of the report, have also been used as part of a computer program to calculate the maximum range of a radar system.



PROBLEM STATUS

A final report on one phase of the problem.

AUTHORIZATION

NRL Problem R02-64
Project SF-11-141-005-15483

Manuscript submitted July 13, 1972.

# RADAR/RADIO TROPOSPHERIC ABSORPTION AND NOISE TEMPERATURE

## INTRODUCTION

The objective of the work reported here was to develop a computer program for calculating the absorption of radio waves by the oxygen and water vapor of the earth's lower atmosphere – the nonionized region known as the troposphere. Resulting calculations have been used to produce machine-plotted curves of attenuation as a function of frequency and other parameters. The requirement that instigated this work was the need to know the magnitude of the absorption loss in calculating the maximum range of a radar. The computer subroutines to be described have in fact been incorporated into a larger program that computes radar maximum range (1). However, the results are equally applicable to radio systems of any type that use the troposhere as a propagation medium.

The frequency range considered is 100 MHz to 100 GHz. Below 100 MHz (and even somewhat above this frequency) tropospheric absorption is negligible. Above 100 GHz strong water-vapor resonance lines result in great absorption; this region is not of much current interest for radar.

The work described updates earlier work begun in 1958, described in various NRL reports and other writings (2-8). The original work (2,4,6) resulted in curves plotted manually from manual calculations for frequencies from 100 MHz to 10 GHz. Later (7,8), the NRL NAREC digital computer was used to recalculate the absorption and noise temperature more exactly and to extend the frequency range to 100 GHz. However in that work (as in the earlier work) the "centroid approximation" of Van Vleck (9) was used to calculate the oxygen absorption; hence the results were not accurate in and near the 60-GHz oxygen resonances, that is, in the region from about 50 to 70 GHz. Also, the so-called residual absorption below 100 GHz due to strong water-vapor resonances at higher frequencies was approximated by a formula suggested by Van Vleck (10), but the constant factor used has subsequently been shown to give absorption values that are too low.

In the current work, presented in this report, the oxygen resonances are explicitly and individually included in the calculation, so that the results are valid in the region from 50 to 70 GHz. The equations used are those of Meeks and Lilley (11) as slightly modified by Reber, Mitchell, and Carter (12). Improved numerical integration formulas are used for the cumulative-absorption and noise-temperature calculations. An improved expression is used for the residual effect of the millimeter-wavelength water-vapor resonances, with a constant based on experimental results near 100 GHz reported by Straiton and Tolbert (13). Also a more sophisticated equation for the absorption of the 22.235-GHz water-vapor line, due to Liebe (14), is used. Finally an improved model of the atmospheric water-vapor content is used. The numerical results of these improved calculations differ significantly from the previous results only above about 10 GHz. Below that frequency the differences are small.

Many authors have made absorption calculations, and it is therefore pertinent to state why it is necessary or desirable to publish these of the present report. Among others the reports and papers of Bean and Abott (15), Hogg (16), Schulkin (17), Le Fande (18), and Ulaby and Straiton (19) may be cited, in addition to those previously mentioned. This list is not exhaustive; in particular, it does not include all of the work published in other countries, some of which is referenced by the authors cited. The published results by these authors have been either limited to calculation of the absorption coefficient (absorption per unit distance) as a function of frequency rather than calculation of the cumulated absorption along a ray path or limited to calculation of the total absorption for paths traversing the entire troposphere. Some results are limited to specific frequency regions or absorption lines. Moreover the curves presented by most other authors cannot be read with sufficient accuracy to be useful for practical calculations of radio or radar system performance.

For radar detection-range calculations the absorption between two points within the troposphere is usually needed, rather than total absorption through the entire troposphere. This report, and its predecessors, present curves of the former type (as well as the latter), with coordinate grids and scales that permit reading values to at least two-significant-figure accuracy. The curves of the present report have been plotted using the NRL Gerber plotter (Gerber Model 875 automatic drafting machine) and special computer plotting subroutines. The coordinate grids as well as the curves are plotted in a single operation, to avoid registration errors. The plotting accuracy is of the order of 0.001 inch on the original plots, which have been photographically reduced to about 1/3 to 1/5 as large for reproduction in this report.

To the author's knowledge results published by others based on computer calculation have not been accompanied by listings of the computer programs used. The programs previously written for the NAREC computer, on which the author's previous reports were based, were written (by Maurice Brinkman, of the NRL Research Computation Center) in the NELIAC language, which was never widely used and is no longer much used at NRL. The newer routines, described in this report, have been written by the author in Fortran for the NRL CDC-3800 computer. Complete listings of these routines will be given in the last section of this report. Although versions of the Fortran language used with other machines may differ slightly, the differences are usually minor, so that the routines can be readily adapted to any computer that has a Fortran compiler.

Another feature of the curves presented in this report is the separation of the oxygen and water-vapor absorption losses, in addition to curves showing the combined absorption loss. The combined results are for a "standard" atmospheric water-vapor density of 7.5 grams per cubic meter. The oxygen component of absorption is relatively stable and insensitive to day-to-day changes in the atmosphere. For various atmospheric conditions however the water-vapor content may vary between roughly 2 and 20 grams per cubic meter. The water-vapor absorption is (except for a small and generally insignificant non-linearity) proportional to the water-vapor density. Consequently separate oxygen and water-vapor curves allow the water-vapor component to be adjusted for any water-vapor content other than the standard 7.5 grams per cubic meter by simply multiplying the 7.5-gram absorption value by $\rho/7.5$, where $\rho$ is the actual gram-per-cubic-meter water-vapor content. This corrected water-vapor absorption can then be directly added to the oxygen absorption to obtain the total absorption.

The curves presented for cumulative attenuation along a ray path are for the radar case of two-way traversal of the path. Consequently the decibel attenuations are exactly twice as great as they would be for the radio-communication case of one-way propagation. The curves can be used for one-way systems by simply taking half of the decibel attenuation values shown for the radar case.

## ABSORPTION COEFFICIENT FOR OXYGEN

As mentioned in the Introduction, the absorption coefficient for oxygen has been calculated using equations given by Meeks and Lilley (11), as slightly modified by Reber et al. (12). The theory was originally due to Van Vleck (9); later workers have refined some of the details. In particular Meeks and Lilley have formulated a refinement of the dependence of the line-breadth constant (which will here be denoted $\Delta f$) on altitude (pressure and temperature), and Reber et al. have made a slight further refinement of this factor.

The Meeks and Lilley equations are a summation of the absorption over many oxygen resonance lines in the vicinity of 60 GHz. These resonances occur for odd-integral values of the rotational quantum number N, that is, for N = 1, 3, 5, . . . . It has been determined (11) that the contribution of terms above N = 45 is negligible; hence 45 is the largest value included in the summation. For each odd value of N there are two resonance frequencies, denoted $f_{N+}$ and $f_{N-}$. These resonances are listed in Table 1, as given by Meeks and Lilley. The absorption at an arbitrary frequency f is the sum of contributions from each of these collision-broadened resonance lines, plus a nonresonant component. The broadened resonance lines are assumed to have shapes defined by the Van-Vleck-Weisskopf formula:

$$F_{N\pm}(f) = \frac{\Delta f}{(f_{N\pm} - f)^2 + (\Delta f)^2} + \frac{\Delta f}{(f_{N\pm} + f)^2 + (\Delta f)^2}. \tag{1}$$

The nonresonant contribution is of the form

$$F_0 = \frac{\Delta f}{f^2 + (\Delta f)^2}. \tag{2}$$

The terms summed over odd values of N are of the form

$$A_N = (F_{N+}\,\mu_{N+}^2 + F_{N-}\,\mu_{N-}^2 + F_0\,\mu_{N0}^2)\, e^{-E_N/kT}, \tag{3}$$

where

$$\mu_{N+}^2 = \frac{N(2N+3)}{N+1} \tag{4}$$

$$\mu_{N-}^2 = \frac{(N+1)(2N-1)}{N}, \tag{5}$$

Table 1
Oxygen Resonance Frequencies

| N | $f_{N+}$ (GHz) | $f_{N-}$ (GHz) |
|---|---|---|
| 1 | 56.2648 | 118.7505 |
| 3 | 58.4466 | 62.4863 |
| 5 | 59.5910 | 60.3061 |
| 7 | 60.4348 | 59.1642 |
| 9 | 61.1506 | 58.3239 |
| 11 | 61.8002 | 57.6125 |
| 13 | 62.4112 | 56.9682 |
| 15 | 62.9980 | 56.3634 |
| 17 | 63.5685 | 55.7839 |
| 19 | 64.1272 | 55.2214 |
| 21 | 64.6779 | 54.6728 |
| 23 | 65.2240 | 54.1294 |
| 25 | 65.7626 | 53.5960 |
| 27 | 66.2978 | 53.0695 |
| 29 | 66.8313 | 52.5458 |
| 31 | 67.3627 | 52.0259 |
| 33 | 67.8923 | 51.5091 |
| 35 | 68.4205 | 50.9949 |
| 37 | 68.9478 | 50.4830 |
| 39 | 69.4741 | 49.9730 |
| 41 | 70.0000 | 49.4648 |
| 43 | 70.5249 | 48.9582 |
| 45 | 71.0497 | 48.4530 |

$$\mu_{N0}^2 = \frac{2(N^2 + N + 1)(2N + 1)}{N(N + 1)}, \tag{6}$$

and

$$E_N/k = 2.06844N\,(N + 1). \tag{7}$$

The complete expression for the absorption coefficient is

$$\alpha(f, p, T) = CpT^{-3}\, f^2 \sum_N A_N \tag{8}$$

where p is the atmospheric pressure and T is the absolute temperature. For f and $\Delta f$ in gigahertz, p in millibars, T in degrees Kelvin, and $\alpha$ in decibels per kolometer, C = 2.0058. For $\alpha$ in decibels per nautical mile, C = 3.7148. (One nautical mile is 1852 meters exactly.)

Van Vleck (9) estimated that $\Delta f$ was approximately 0.6 GHz at 1 atmosphere pressure and standard sea-level temperature and that it was proportional to pressure and inversely

proportional to the square root of absolute temperature. Later workers have suggested, based on experimental evidence, that the dependence on pressure and temperature is more complicated. The Reber-Mitchell-Carter (12) modification of the Meeks-Lilley (11) model for this dependence is given in terms of altitude h above sea level:

$$\Delta f = g(h)\,(p/p_0)\,(T_0/T), \tag{9}$$

where $p_0$ = 1013.25 millibars (760 torr), $T_0$ = 300°K, and

$$g(h) = 0.640,\ 0 \leq h \leq 8 \text{ km}, \tag{10}$$

$$g(h) = 0.640 + 0.04218(h - 8),\ 8 \leq h \leq 25, \tag{11}$$

$$g(h) = 1.357,\ h > 25 \text{ km}. \tag{12}$$

These are the equations and constants that have been coded in Fortran in Subroutine ALPHA, listed in the last section of this report, for computation of ALPHØ2, the oxygen absorption coefficient.

## ABSORPTION COEFFICIENT FOR WATER VAPOR

The absorption due to water vapor in the frequency region below 100 GHz can be separated into two components, one due to the water-vapor resonance at 22.235 GHz and the other due to the residual effect of the many resonance lines above 100 GHz. The absorption coefficient due to the 22.235-GHz line, which will be denoted $\alpha_{22}$, has been computed from equations given by Liebe (14). The following equation is a combination of his equations 2a, 6, 7, and 8:

$$\alpha_{22} = \left(\frac{4\pi f}{c}\right)(10 \log_{10} e)\, S^0\, p_w \left(\frac{300}{T}\right)^{7/2} e^{2.144(1-300/T)}\, F \text{ dB/km}, \tag{13}$$

where the symbols are defined as

$c$ = 2.998 × $10^5$ km/sec,

$S^0$ = 13.92 Hz/torr,*

$p_w$ — partial pressure of water vapor (torr),

$T$ — temperature (degrees Kelvin),

$F$ — line-shape factor.

As was done for oxygen, F is taken to be the Van-Vleck-Weisskopf function (here including the factor $f/f_r$):

*The theoretical value (14) is 14.33 Hz/torr, but the author has been advised by Dr. Liebe (private communication dated June 6, 1972) that this value involves approximations and that the experimentally determined value 13.92 is probably more accurate.

$$F = \left(\frac{f}{f_r}\right)\left[\frac{\Delta f}{(f_r - f)^2 + (\Delta f)^2} + \frac{\Delta f}{(f_r + f)^2 + (\Delta f)^2}\right], \tag{14}$$

where $f_r$ = 22.235 GHz.

The equation given by Liebe for $\Delta f$ is

$$\Delta f = 17.99 \times 10^{-3} \left\{ p_w \left[ (300/T) + 0.20846(p_t - p_w) \right] (300/T)^{0.63} \right\}, \tag{15}$$

where again $p_w$ is the water-vapor partial pressure in torr and $p_t$ is the total atmospheric pressure in torr; T is, as before, the temperature in degrees Kelvin. The atmospheric pressure p in millibars is given by

$$p = 1.33322\, p_t, \tag{16}$$

and the water-vapor partial pressure in torr is given in terms of the water-vapor density $\rho$ in grams per cubic meter (for atmospheric concentrations) by

$$p_w = \rho T/288.75. \tag{17}$$

Combining all of the numerical constants, with f expressed in gigahertz, p in millibars, and $p_w$ in torr, results in

$$\alpha = 2.534 \times 10^{-3} \left[ f\, p_w\, (300/T)^{7/2}\, e^{2.144(1 - 300/T)} F \right] \text{ dB/km} \tag{18}$$

and

$$\Delta f = 17.99 \times 10^{-3} \left\{ p_w \left[ (300/T) + 0.20846\, (0.75\, p - p_w) \right] (300/T)^{0.63} \right\}. \tag{19}$$

These are the equations and constants that are Fortran coded in Subroutine ALPHA for the computation of ALPH22, the absorption coefficient for the 22.235-GHz water-vapor line, except that the constant 2.534 in Eq. (18) has been increased to 4.693 to give the absorption in decibels per nautical mile. The water-vapor parameter actually employed in the model atmosphere is the water-vapor density $\rho$ (grams per cubic meter) rather than the partial pressure in torr; it is converted to partial pressure by Eq. (17).

The residual effect of water-vapor absorption lines above 100 GHz has been assumed, following Ulaby and Straiton (19) and others:*

$$\alpha_{res} = C_R\, (\rho/\rho_0)\, (p/p_0)\, (T_0/T)^{5/2}\, (f/f_0)^2, \tag{20}$$

where $\rho$ is the water-vapor density (grams per cubic meter), p is the atmospheric pressure, T is the temperature, $\rho_0$, $p_0$, and $T_0$ are the zero-altitude values of $\rho$, p, and T, and $f_0$ is a reference value of f. The constant $C_R$ can be taken from experimental results at any

*Ulaby and Straiton attribute this exponent for the dependence on temperature to Van Vleck, although it is not given explicity in Van Vleck's paper on water-vapor absorption (10). It is probably deduced from the footnote on page 420 of his paper on oxygen absorption (9).

suitable frequency $f_0$. Based on measurements reported by Straiton and Tolbert (13), the value $C_R$ = 0.4 dB/km at $f_0$ = 100 GHz has been adopted here. For p in millibars, taking $p_0$ = 1023.23 millibars*, $T_0$ = 288.16°K, $\rho_0$ = 7.5 grams per cubic meter (the value for the standard atmosphere which will be described in a later section), and $f_0$ = 100 GHz, this formula becomes

$$\alpha_{res} = 7.347 \times 10^{-3}\, \rho p T^{-5/2} f^2 \text{ dB/km}. \quad (21)$$

This is the expression that has been coded in Fortran for the absorption coefficient (named ALFRES in Subroutine ALPHA) due to the residual effect of the water-vapor lines above 100 GHz except that the constant $7.347 \times 10^{-3}$ has been changed to $1.361 \times 10^{-2}$ to give the absorption in decibels per nautical mile.

## DISCUSSION OF ABSORPTION-COEFFICIENT FORMULAS

The total absorption coefficient of the troposphere is the sum of the oxygen and water-vapor coefficients, and the water-vapor coefficient is in turn the sum of the coefficients for the 22.235-GHz line and the residual effect of lines above 100 GHz. Of these components of the total absorption, the one that has the poorest theoretical basis is the residual effect of the above-100-GHz (millimeter-wave and infrared) water-vapor resonances. As has been well known for some time (10,14,18) the application of the theoretical line strengths and the Van-Vleck-Weisskopf collision-broadening formula, Eq. (14), give absorption values that are too low by a factor of at least 5. Other line-shape formulas have been proposed, but no fully satisfactory theoretical solution of the problem has been advanced, to the author's knowledge. Consequently the empirical formula and constant used here are believed to be as good a solution as can be applied at present.

The use of the Van-Vleck-Weisskopf line-shape formula (20) for oxygen and for the 22.235-GHz lines is similarly suspect for absorption prediction at frequencies far removed from the resonance frequencies. However this matter is not so serious for these lines, because at frequencies far removed from the 22.235-GHz line its contribution is dwarfed by the contributions of the oxygen and higher-frequency water-vapor absorption lines and because the oxygen-line contributions at frequencies above about 90 Ghz are similarly dwarfed by the contributions of the millimeter-wave water-vapor lines, except in a very narrow region about the isolated oxygen line at 118.75 GHz. The oxygen absorption is also small compared to the water-vapor absorption in the near vicinity of the 22.235-GHz water-vapor line. At frequencies well below the 22.235-GHz line the nonresonant component of oxygen absorption is the dominant factor. No criticism of the shape factor for this component (Eq. (2)) has been found in the literature by the author.

As mentioned in the Introduction, the results for oxygen and for water vapor are presented in this report separately as well as in combination, so that correction to the latter can be made for any desired deviation from the standard 7.5-gram-per-cubic-meter water-vapor content. It was there stated that a simple multiplicative factor $\rho/\rho_0$ could be applied, where $\rho$ is the desired water vapor density and $\rho_0$ = 7.5 is the standard value. As Eq. (19) shows, this is not quite true; there is a small nonlinear dependence of $\Delta f$ on

*This value of $p_0$ is the total pressure, consisting of the dry-atmosphere standard pressure of 1013.25 millibars and the water-vapor partial pressure of 9.98 millibars corresponding to $\rho$ = 7.5 g/m$^3$.

$\rho$ (through $p_w$) in addition to the linear explicit dependence of $\alpha$ on $\rho$, Eq. (18). A similar slight nonlinearity would appear in the residual contribution of the higher-frequency lines if an exact expression were used, but again the nonlinearity is slight, and in view of the empirical nature of Eq. (20) it was not thought worthwhile to include it.

## MODEL OF THE ATMOSPHERE

The absorption coefficients, for which formulas have been given in the preceding sections, describe the rate at which signals traversing an atmospheric path will be attenuated, as a function of the pressure, temperature, and water-vapor density. To find the altitude dependence of the absorption coefficient, it is necessary to have a model of the altitude dependence of pressure, temperature, and water vapor in the atmosphere.

### Pressure-and-Temperature Model

The model adopted here for the pressure p and temperature T of the standard atmosphere is the U.S. extension to the ICAO Standard Atmosphere (21); this is, for the altitudes considered here (up to 100,000 feet or 30.48 kilometers), the same as the ARDC model atmosphere.

The equations describing the temperature (degrees Kelvin) and pressure (millibars) of this atmosphere in terms of the geopotential altitude $h_g$ (meters) are*

$$\left.\begin{aligned} T &= 288.16 - 0.0065\, h_g \\ p &= 1013.25\,(T/288.16)^{\alpha} \end{aligned}\right\} h_g \leqslant 11000, \tag{22}$$

$$\left.\begin{aligned} T &= 216.66 \\ p &= (226.32/T)\exp\left[-\beta(h_g - 11000)\right] \end{aligned}\right\} 11000 < h_g < 25000, \tag{23}$$

$$\left.\begin{aligned} T &= 216.66 + 0.003\,(h_g - 25000) \\ p &= 24.886\,(216.66/T)^{\gamma} \end{aligned}\right\} 25000 \leqslant h_g < 47000, \tag{24}$$

where

$$\alpha = 5.2561222,$$
$$\beta = 0.034164794$$
$$\gamma = 11.388265.$$

The relationship between geopotential altitude $h_g$ and geometric altitude $h_a$ is

$$h_g = rh_a/(r + h_a), \tag{25}$$

*Reference 21, pp. 6 and 7, Eqs. (13) and (15).

where r is the radius of the earth, taken to 356,766 meters. This relationship, which is Eq. (10) of Ref. 21, is valid for the altitude range considered here.

The absorption losses were computed in terms of altitude in feet and decibels per nautical mile, to conform to the measurement units employed by Navy radars. The conversion from feet to meters is 1 foot = 0.3048 meter exactly; the conversion from nautical miles is 1 nautical mile = 1852 meters exactly.

This model of the atmosphere is incorporated into the absorption-coefficient computer subroutine ALPHA, as a table of values at 75 specified altitudes, in the form of Fortran DATA statements. The pressure is given by the dimensioned identifier PP and the temperature by TT. The 75 altitudes ($h_f$) range from 0 to 100,000 feet in steps $\Delta h$ that are graduated according to the following scheme:

$\Delta h$ = 100 ft, $h_f < 2000$ ft,

$\Delta h$ = 1000 ft, $2000 < h_f < 30000$ ft,

$\Delta h$ = 2000 ft, $30000 < h_f < 70000$ ft,

$\Delta h$ = 5000 ft, $70000 < h_f < 10000$ ft.

This graduation provides more closely spaced points at low altitudes, where absorption is greater and therefore where more accurate interpolation of the tabulated values is desirable. The interpolation is provided by the numerical integration subroutines used in computing the cumulative absorption. As will be discussed in detail later, the integration is done by a modification of Simpson's rule, so that the interpolation is more accurate than would be obtained by using the trapezoidal rule (linear interpolation).

### Water-Vapor Model

No accepted standard profile of water vapor has been universally adopted. The one used here is taken from a report by Sissenwine et al. (22). Their values for the water-vapor density up to 32 km (104,987 ft) are given in Table 2. As shown, the vapor density is specified at 2-km intervals, and the surface value is 5.947 g/m$^3$. The values corresponding to the 75 altitudes specified in Subroutine ALPHA were found by interpolating. These values were then multiplied by the factor 7.5/5.947 = 1.26114, to convert them to the surface water-vapor value of 7.5 g/m$^3$ that seems to have been adopted as a standard by workers in the field of water-vapor absorption. The interpolation was done by use of a special computer subroutine by a method equivalent to using a French curve on a plot of the data points. This method is described (in terms of curve plotting) in an NRL Memorandum Report (23). The resulting values of water-vapor density are incorporated in Subroutine ALPHA in the form of a DATA statement for the dimensioned identifier RR.

Subroutine ALPHA also has a COMMON statement containing a variable named RHOFAC. This quantity is set equal to 1 in a DATA statement, but may be set to other values by use of the COMMON statement in the main program or in another subroutine. All the values of water-vapor density in the model atmosphere are multiplied by RHOFAC in Subroutine ALPHA. Consequently if for example calculations of the attenuation and noise temperature for a surface water-vapor density of 15 g/m$^3$ are wanted, the desired result will be obtained by setting RHOFAC = 2.

Table 2
Midlatitude Mean Water-Vapor Densities*

| Altitude (km) | Density ($g/m^3$) |
|---|---|
| 0 | $5.947 \times 10^{0}$ |
| 2 | $2.946 \times 10^{0}$ |
| 4 | $1.074 \times 10^{0}$ |
| 6 | $3.779 \times 10^{-1}$ |
| 8 | $1.172 \times 10^{-1}$ |
| 10 | $1.834 \times 10^{-2}$ |
| 12 | $3.708 \times 10^{-3}$ |
| 14 | $8.413 \times 10^{-4}$ |
| 16 | $6.138 \times 10^{-4}$ |
| 18 | $4.449 \times 10^{-4}$ |
| 20 | $4.449 \times 10^{-4}$ |
| 22 | $5.230 \times 10^{-4}$ |
| 24 | $6.138 \times 10^{-4}$ |
| 26 | $7.191 \times 10^{-4}$ |
| 28 | $5.230 \times 10^{-4}$ |
| 30 | $3.778 \times 10^{-4}$ |
| 32 | $2.710 \times 10^{-4}$ |

*From Ref. 22, Table 3.

This procedure may result in vapor densities that exceed the saturation values for the temperatures assumed. However this is probably not a serious violation of realism. It means that the temperature values should also be adjusted when the water-vapor density is increased significantly. But since the water-vapor attenuation depends somewhat weakly on the temperature, the inaccuracy that results from failure to readjust the tropospheric temperatures to values compatible with the increased vapor densities is probably slight.

It is noteworthy that $\rho(h)$ does not decrease monotonically in this model. It does decrease up to 18 km, remains constant to 20 km, and then actually increases from 20 to 26 km; thereafter it again decreases. However, this nonmonotonic behavior is probably not too significant from the absorption viewpoint, because it occurs at a vapor-density level that is too small to contribute appreciably to the absorption.

## Absorption Coefficients in the Model Atmosphere

The variation of the absorption coefficients at zero altitude in this model atmosphere for oxygen, the 22-GHz water-vapor line, the residual effect of higher-frequency water-vapor lines, total water vapor, and combined oxygen and water-vapor absorptions are plotted for the frequency range 100 MHz to 100 GHz in Figs. 1 through 5. Figure 6 illustrates the behavior of the absorption coefficients with altitude at several frequencies in the most-used part of the radar frequency spectrum, from 100 MHz to slightly above 30 GHz. These curves have been machine plotted from computations made with computer subroutine ALPHA, which is listed in the last section of this report. The plots have been made in terms of decibels per kilometer to facilitate comparison with other similar curves, although the curves of cumulative absorption loss, shown later, are plotted to nautical-mile scales.

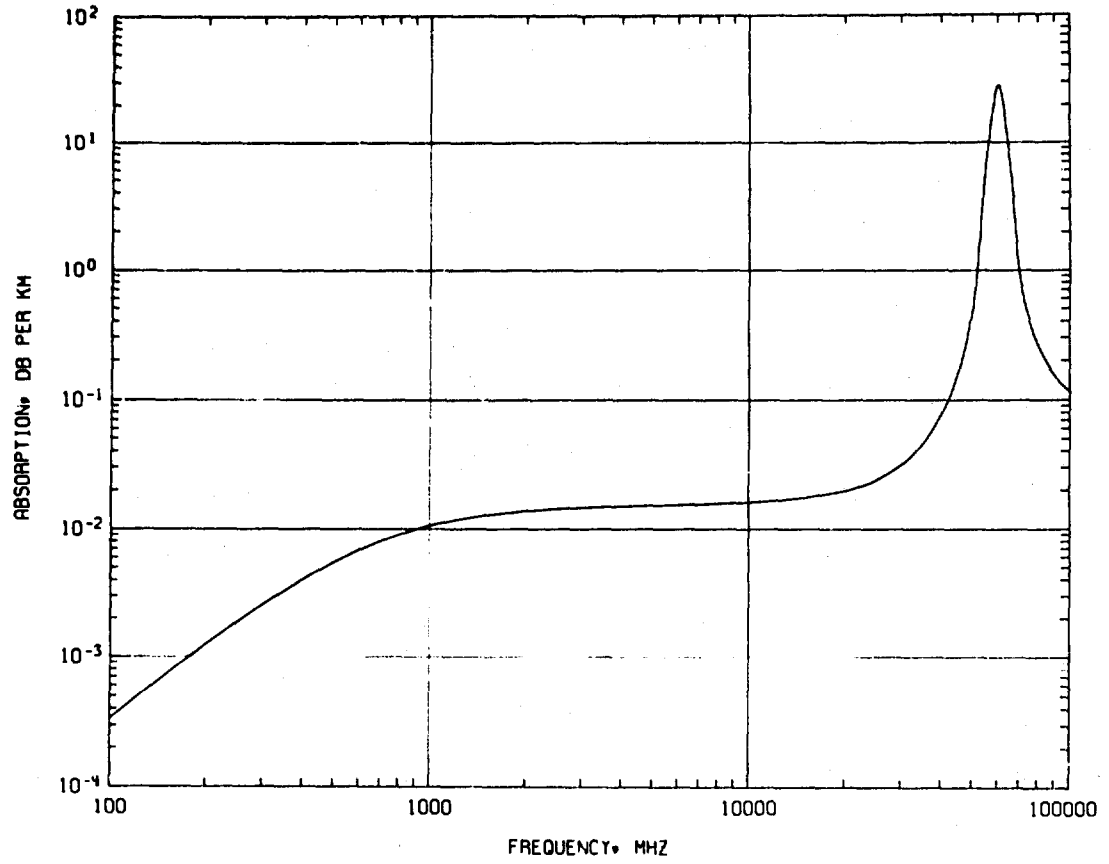


Fig. 1 — Absorption coefficient for oxygen at standard sea-level pressure and temperature

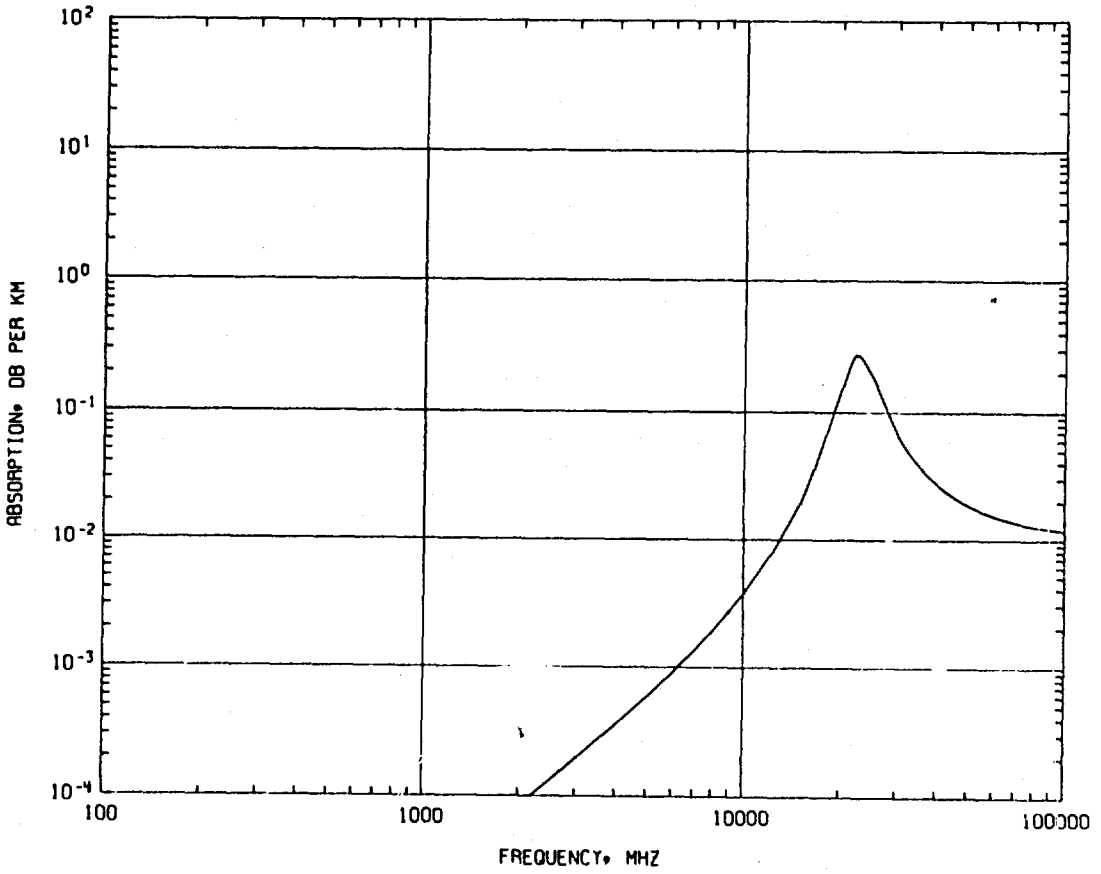


Fig. 2 — Absorption coefficient for the 22.235-GHz-resonance component of water vapor at standard sea-level pressure and temperature

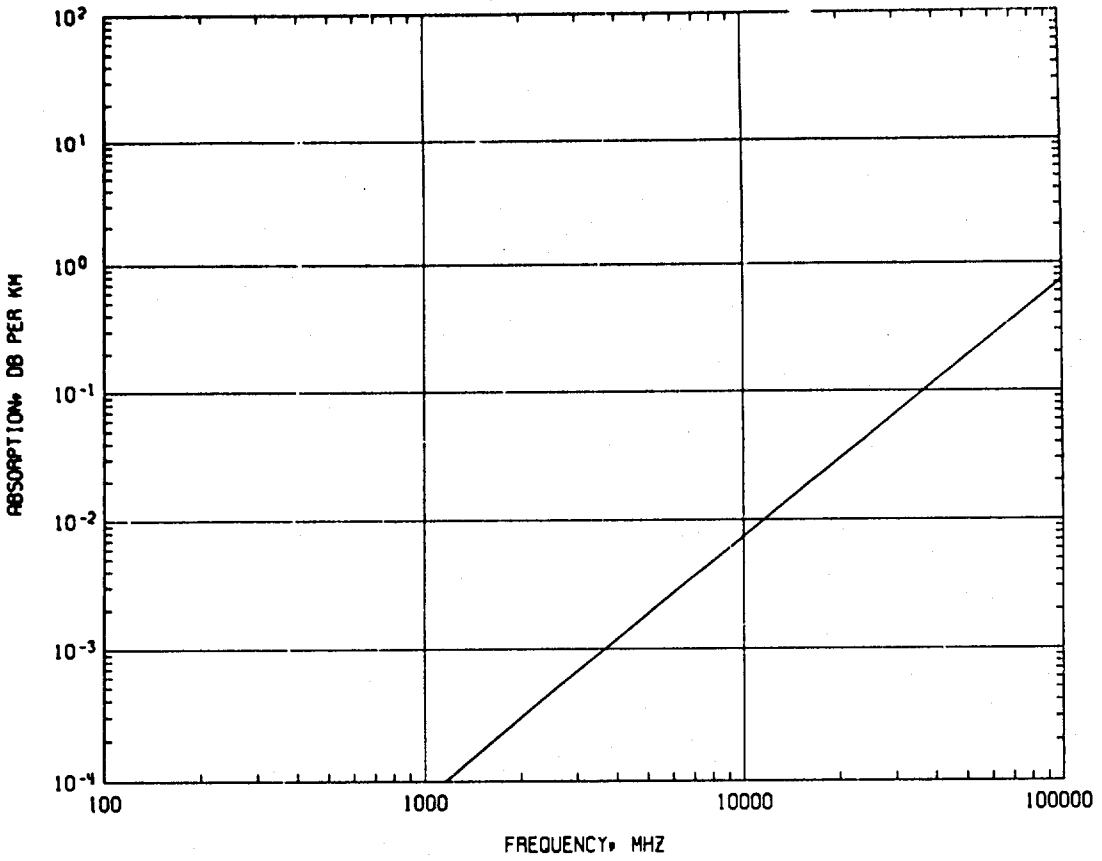


**Fig. 3 — Absorption coefficient for the residual effect of higher-frequency water-vapor resonance lines at standard sea-level pressure and temperature**

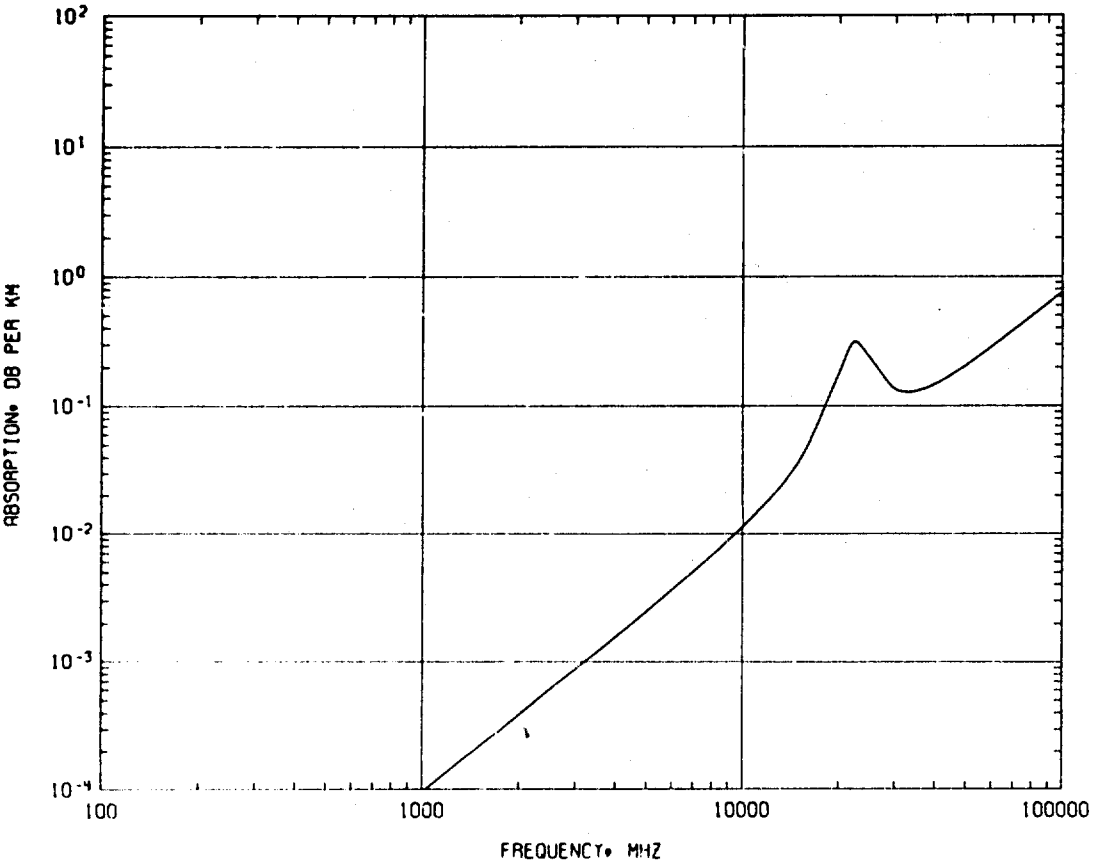


Fig. 4 — Total absorption coefficient for water vapor at standard sea-level pressure and temperature

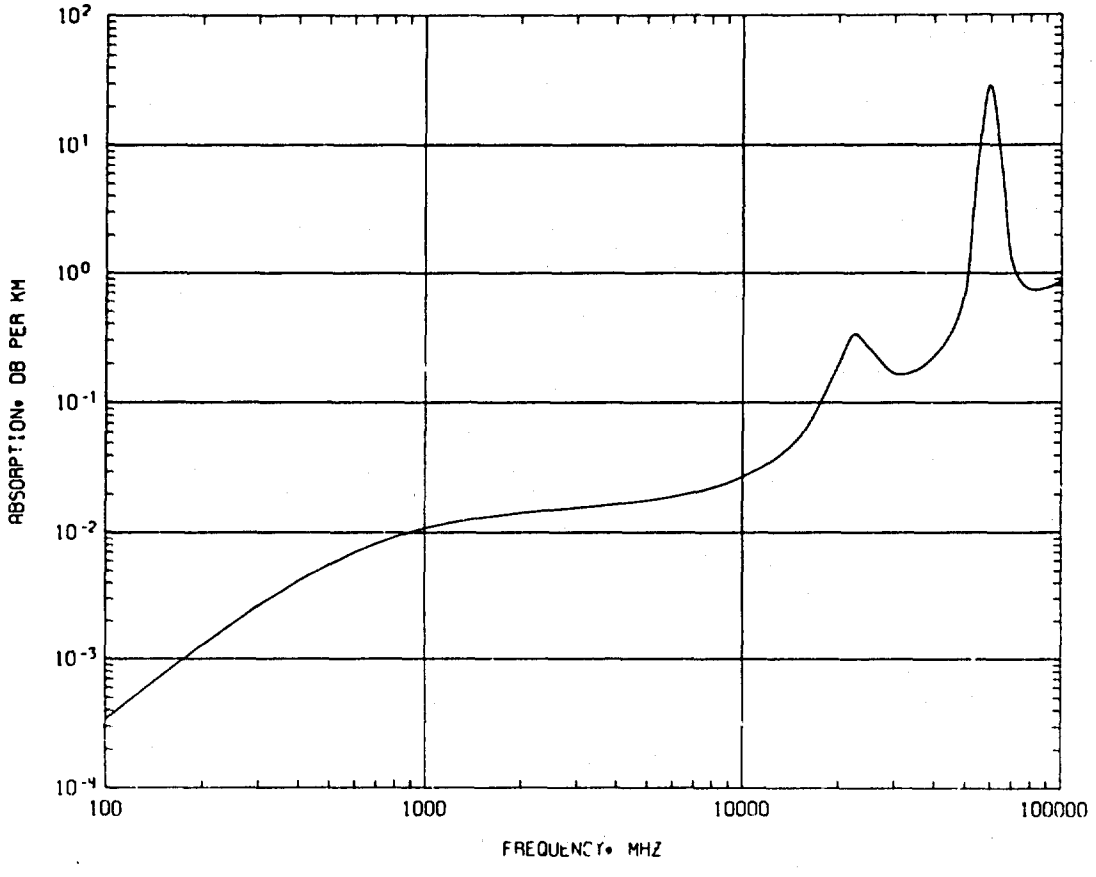


Fig. 5 — Absorption coefficient for oxygen and water vapor combined at standard sea-level temperature and pressure

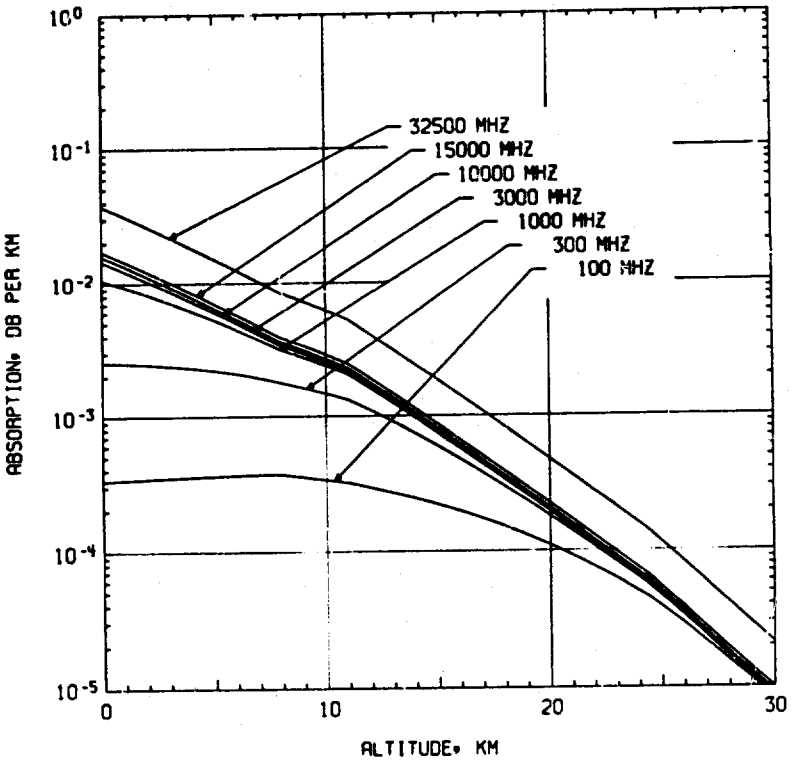


(a) oxygen component

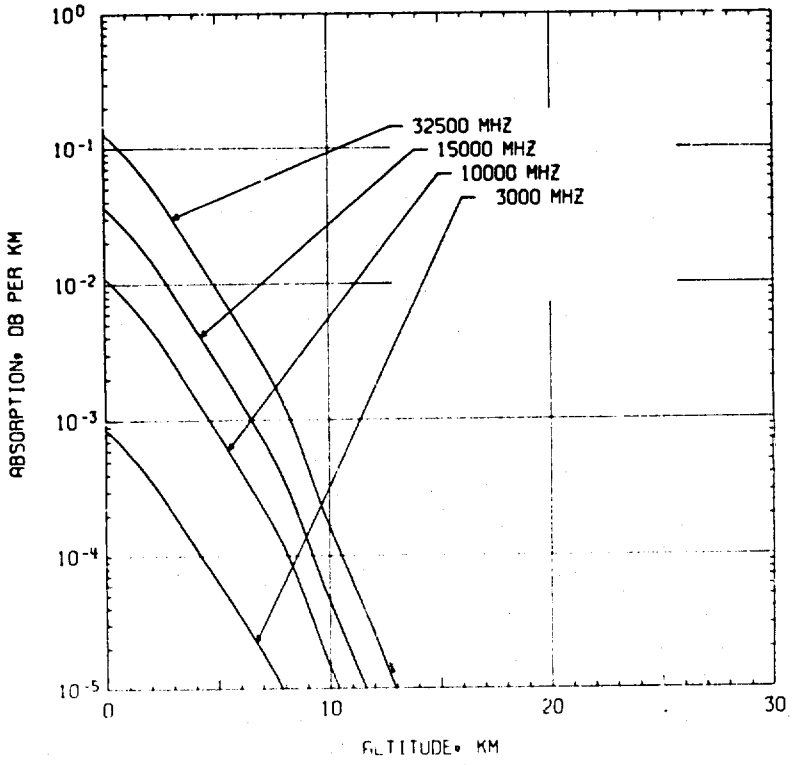


(b) water-vapor component

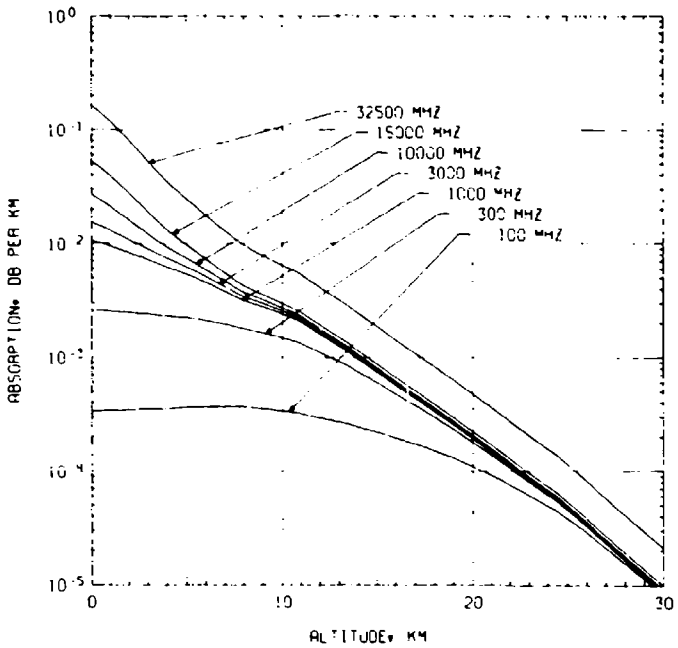


(c) oxygen plus water vapor

Fig. 6 — Variation of the total absorption coefficient in the standard atmosphere as a function of altitude for several frequencies

## EQUATIONS FOR CUMULATIVE ABSORPTION

To find the total attenuation along a ray path in the atmosphere, it is necessary to integrate the absorption coefficient along the path. This path is formally defined by the following relation between range R (as would be measured by a radar) and height h:

$$R(h_1) = \int_0^{h_1} \frac{dR}{dh}\, dh. \tag{26}$$

To calculate cumulative absorption along a ray path from the earth's surface to an altitude h, the bending of the ray path caused by refraction should be taken into account. This is a function of the ray elevation angle as well as the refractive index profile. The refraction is significant only at relatively low angles. In principle the refractive index should be calculated from the water-vapor/temperature profile of the atmosphere. However, since the refraction does not have a major effect on the absorption, it was decided to take it into account simply by assuming a standard exponential model of the refractive index, the so-called CRPL Exponential Atmosphere (24) for surface refractivity $N_s = 313$, given by

$$n(h) = 1 + 0.000313\, e^{-kh}, \tag{27}$$

where n is the refractive index and $k = 0.00004385$ for h in feet.

Taking the refraction into account, from Snell's law the derivative in Eq. (26) is given by

$$\frac{dR}{dh} = \frac{n(h)}{\sqrt{1 - \left[\dfrac{n_0 \cos \theta_0}{n(1 - h/r_0)}\right]^2}}, \tag{28}$$

in which n(h) is given by Eq. (27), $n_0 = 0.000313$, $\theta_0$ is the initial elevation angle of the ray (angle at $h = 0$ relative to the horizontal), and $r_0$ is the earth's radius. (The earth's radius for the CRPL Exponential Atmosphere is taken to be 6370 km, or $2.0899 \times 10^7$ ft.)

The cumulative attenuation along this ray path is given by

$$A(R_1) = 2 \int_0^{h_1} \alpha(h) \frac{ds}{dh}\, dh, \tag{29}$$

in which $R_1 = R(h_1)$, $\alpha(h)$ is the absorption coefficient at height h, and

$$\frac{ds}{dh} = \frac{1}{n} \frac{dR}{dh}. \tag{30}$$

That is, ds/dh is given by Eq. (28) with 1 substituted for n(h) in the numerator; R is the distance as measured by a radar, along the ray path, and s is the corresponding geometric distance. The factor 2 in Eq. (29) is used to obtain the radar attenuation, for two-way traversal of the path.

The cumulative absorption is calculated in a Fortran subroutine named ATLOSS, which is listed in the last section of the report. The derivatives ds/dh and dR/dh are computed in the short subroutine named DDH; the derivatives are therein named DSDH3 and DRDH3.

The cumulative integration is performed by a modified Simpson's rule which is described in an NRL Memorandum Report (25). However instead of the actual subroutine described in that report an equivalent procedure is programmed in Subroutine ATLOSS. The method allows the cumulative absorption to be found at each of the 75 ranges (heights) at which $\alpha$ is specified, rather than only at every other one (half as many), as would result if the usual form of Simpson's rule were employed.

This integration cannot be performed however at h = 0 when $\theta_0 = 0$, because then the integrand becomes infinite. A special technique is used to approximate the integral in a small region about h = 0 where $\theta_0 = 0$ (actually, in this case, from h = 0 to h = 200 feet); this technique was described in a paper by the author (26).

Subroutine ALPHA is called by Subroutine ATLOSS for a specified frequency, and the resulting 75 absorption coefficients $\alpha(h)$ are used to calculate the absorption (using Eq. (29)) at 75 corresponding ranges (found from Eq. (26)) along the ray path for the specified elevation angle. These points allow a curve of attenuation in decibels to be plotted as a function of the range in nautical miles, with frequency and elevation angle as parameters. Such curves are given for 38 frequencies in the range 100 MHz to 100 GHz for several elevation angles, as Figs. 7 through 98. Below 1500 MHz only the oxygen attenuation is plotted (Figs. 7 through 17), since water-vapor attenuation is negligible. At 1500 MHz and above plots are given for oxygen and water vapor separately, and for the total attenuation. These curves can be used for estimating tropospheric attenuation for earth-based radars, for targets in the troposphere. They can also be used for estimating attenuation for point-to-point radio communication when one terminal is earth-based and the other is airborne (ground-to-air, ship-to-air, or vice versa), by taking half of the plotted decibel values.

The water-vapor and total-attenuation curves are plotted for the standard water-vapor density (at zero altitude) of $\rho_s = 7.5$ g/m$^3$. The total attenuation for any other value of $\rho_s$ can be obtained by multiplying the decibel value read from the water-vapor curve by $\rho_s/7.5$ and then adding the result to the decibel value read from the corresponding oxygen curve.

Curves of the absorption through the entire troposphere, for oxygen and water vapor separately and for the total, have also been plotted, in Figs. 99 through 101.

## TROPOSPHERIC NOISE TEMPERATURE

The troposphere radiates thermal noise, and the tropospheric noise temperature as seen by an earth-based radar or radio antenna is given by the following equation (27):

$$T_n = 0.2303 \int_0^\infty \alpha(R)\, T_t(R)\, e^{-0.2303 \int_0^R \alpha(r)dr}\, dR, \qquad (31)$$

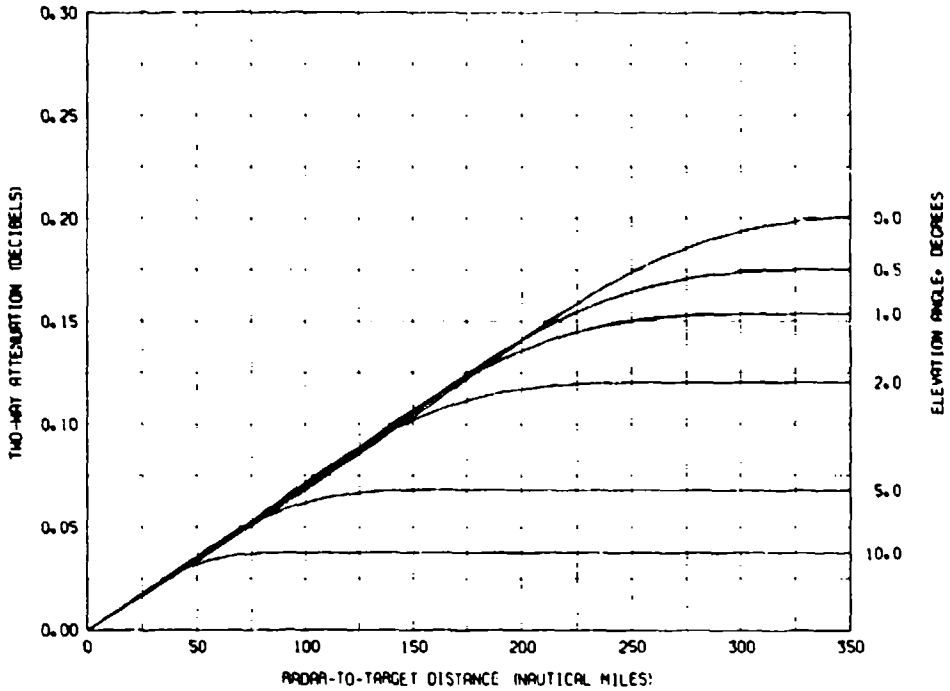


Fig. 7 — Radar absorption loss due to oxygen for ray paths in the standard atmosphere at 100 MHz. Since the loss due to water vapor is negligible up to 1500 MHz, this plot also gives the total absorption loss.

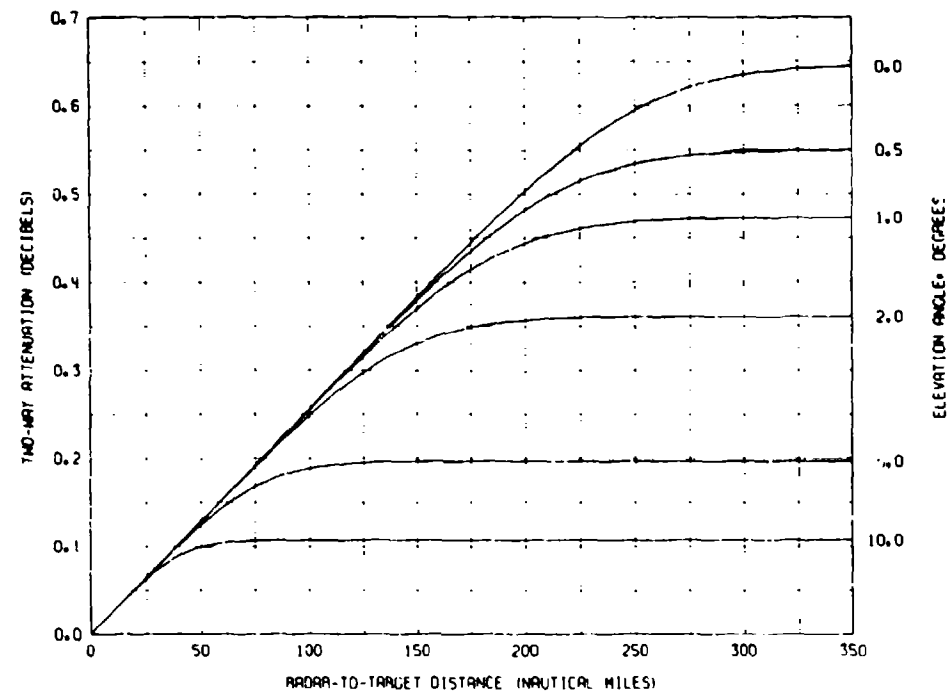


Fig. 8 — Radar absorption loss due to oxygen for ray paths in the standard atmosphere at 200 MHz

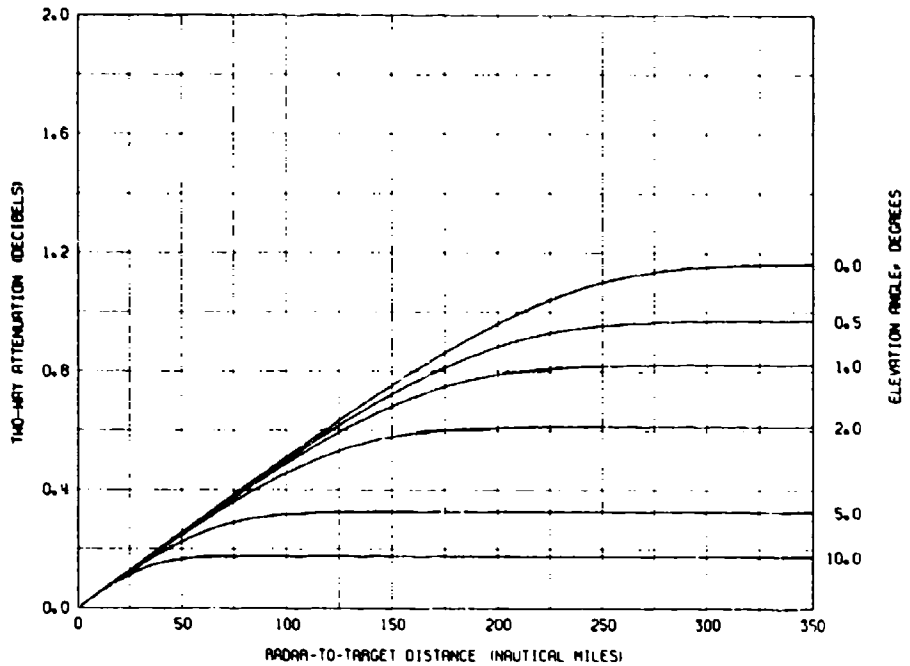


Fig. 9 — Radar absorption loss due to oxygen for ray paths in the standard atmosphere at 300 MHz

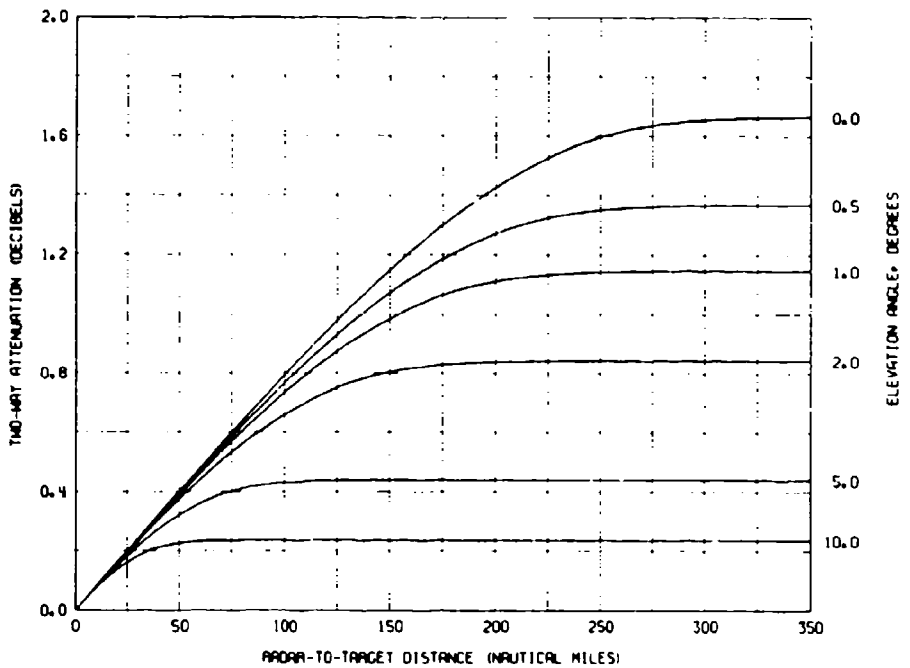


Fig. 10 — Radar absorption loss due to oxygen for ray paths in the standard atmosphere at 400 MHz

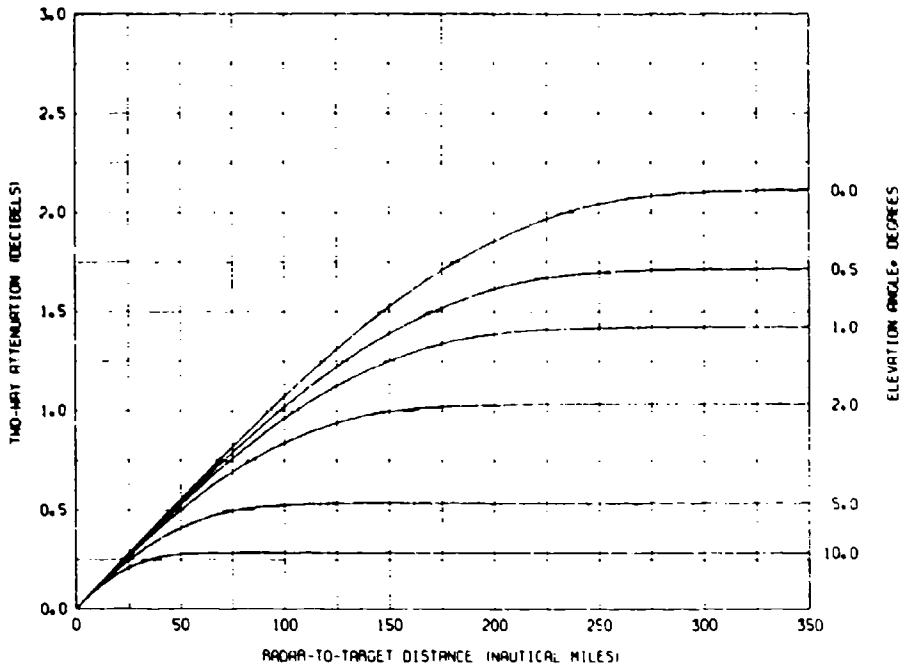


Fig. 11 — Radar absorption loss due to oxygen for ray paths in the standard atmosphere at 500 MHz

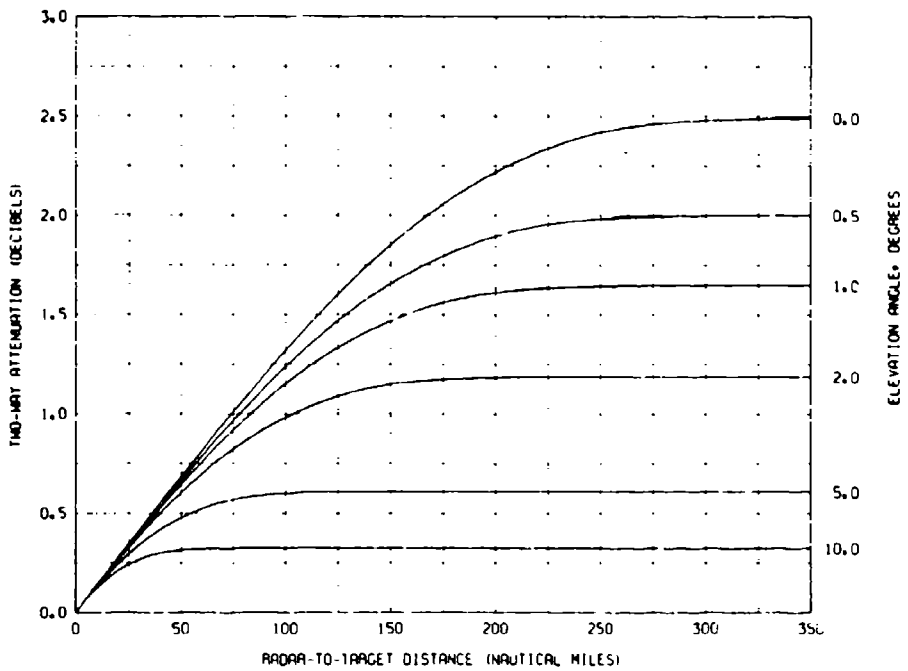


Fig. 12 — Radar absorption loss due to oxygen for ray paths in the standard atmosphere at 600 MHz

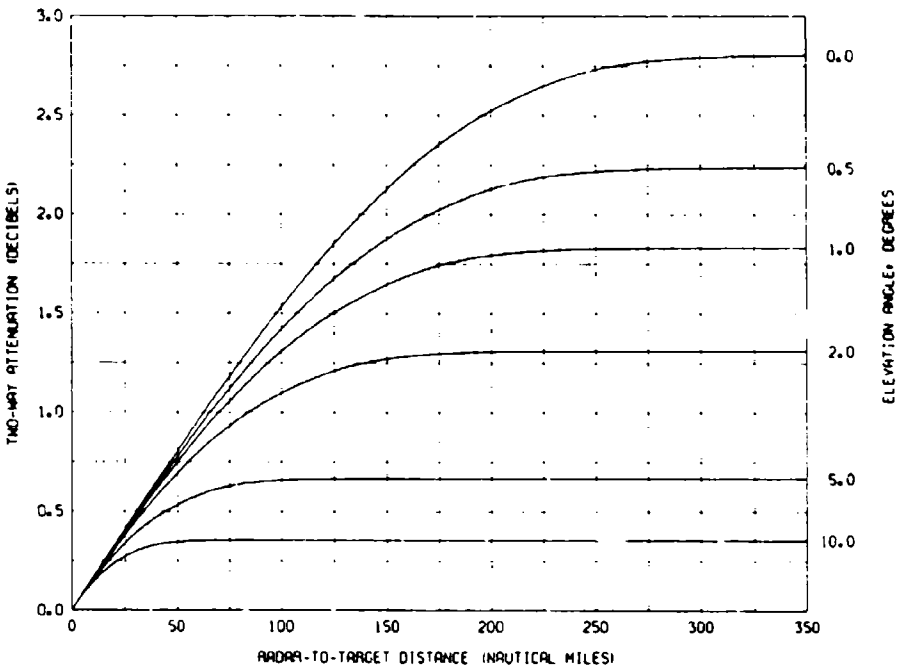


Fig. 13 — Radar absorption loss due to oxygen for ray paths in the standard atmosphere at 700 MHz

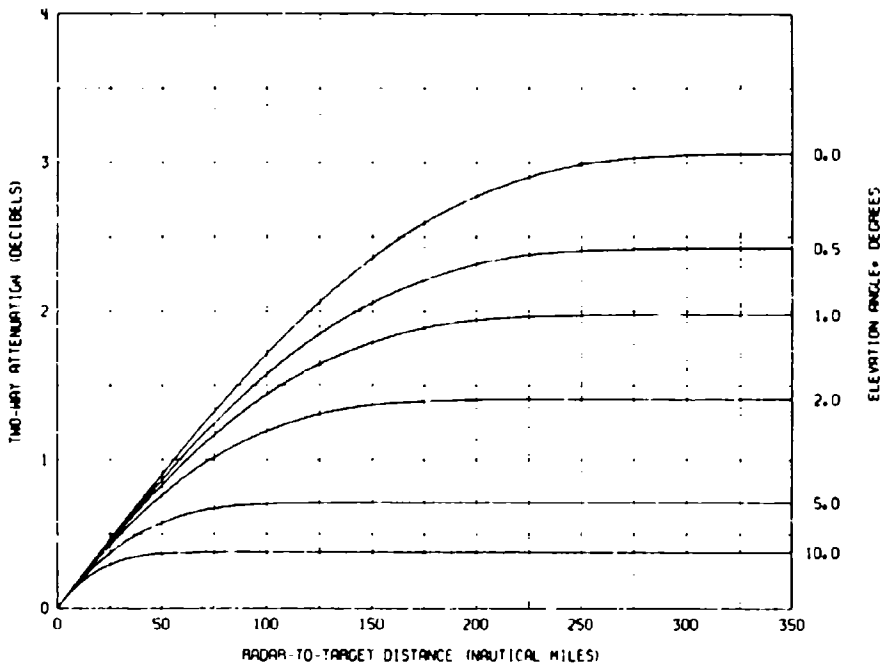


Fig. 14 — Radar absorption loss due to oxygen for ray paths in the standard atmosphere at 800 MHz

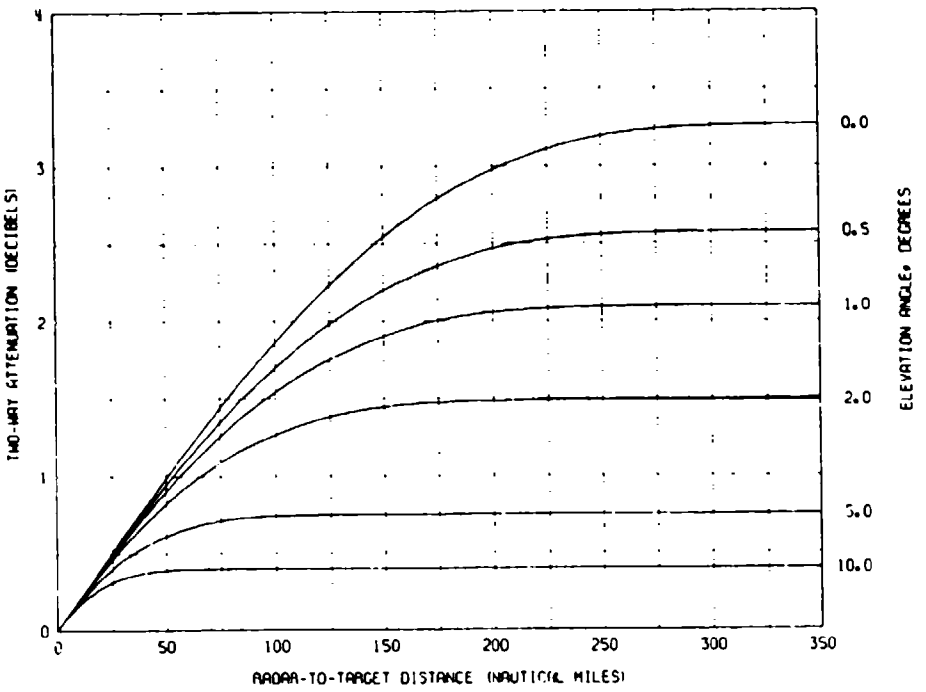


Fig. 15 — Radar absorption loss due to oxygen for ray paths in the standard atmosphere at 900 MHz

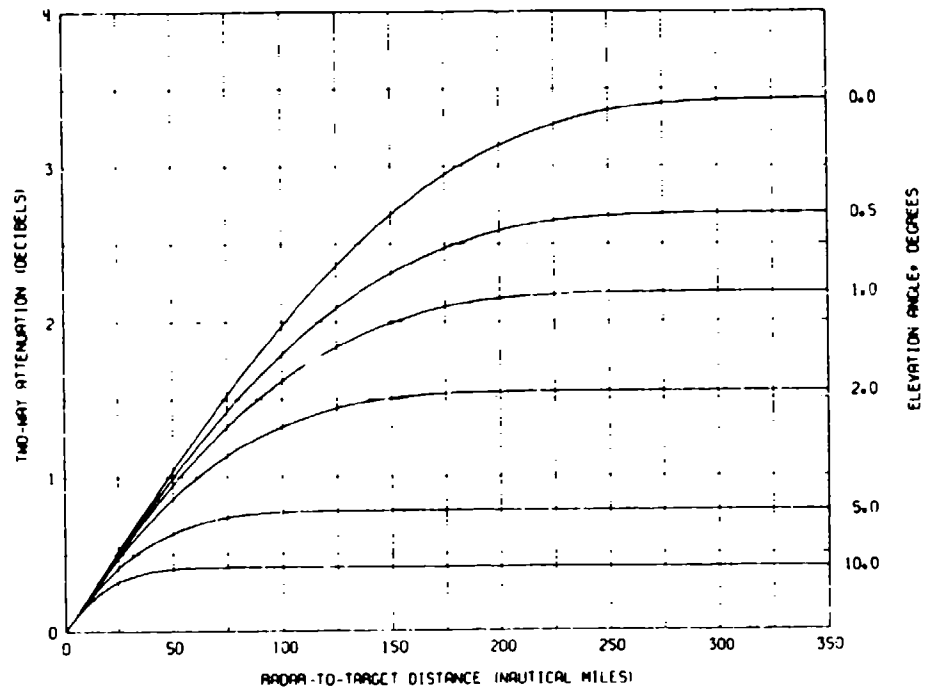


Fig. 16 — Radar absorption loss due to oxygen for ray paths in the standard atmosphere at 1000 MHz

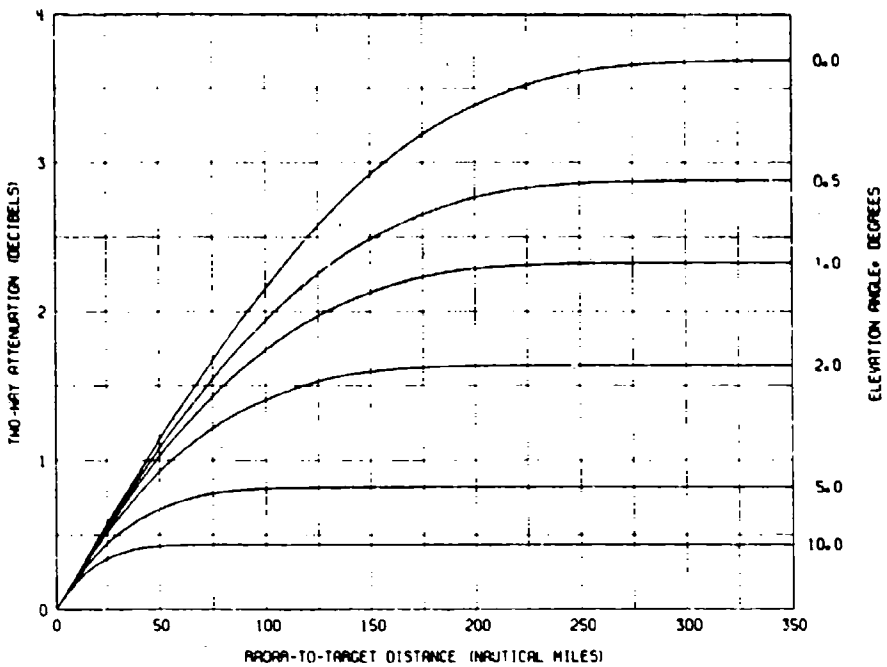


Fig. 17 -- Radar absorption loss due to oxygen for ray paths in the standard atmosphere at 1200 MHz

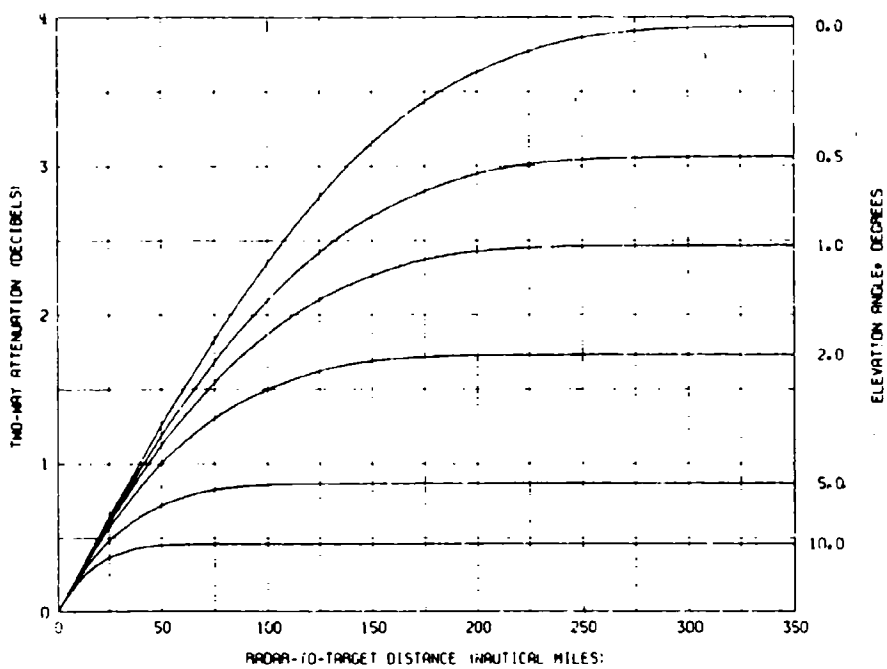


Fig. 18 Oxygen component of the radar absorption loss for ray paths in the standard atmosphere at 1500 MHz

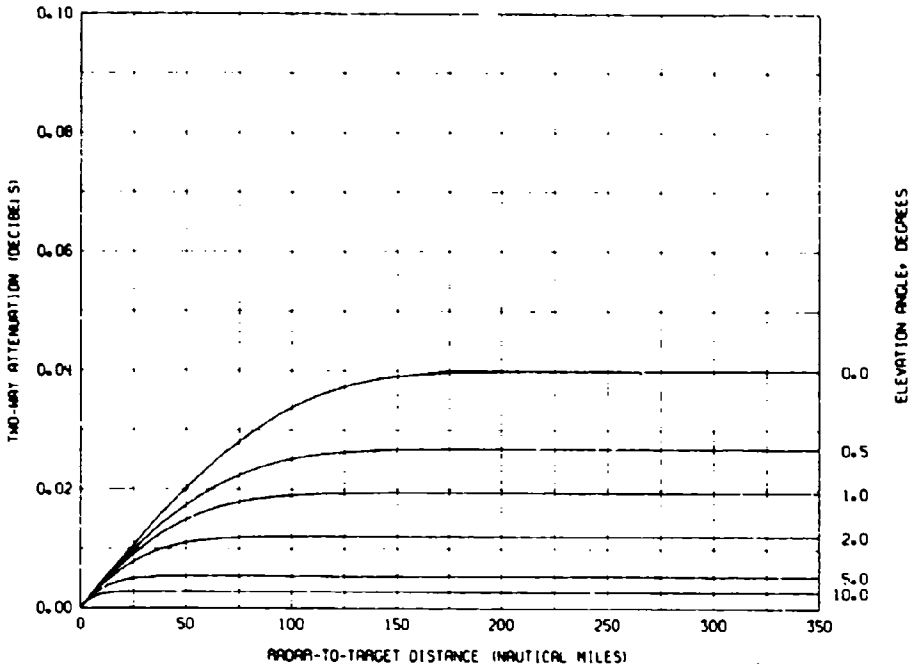


Fig. 19 — Water-vapor component of the radar absorption loss for ray paths in the standard atmosphere at 1500 MHz

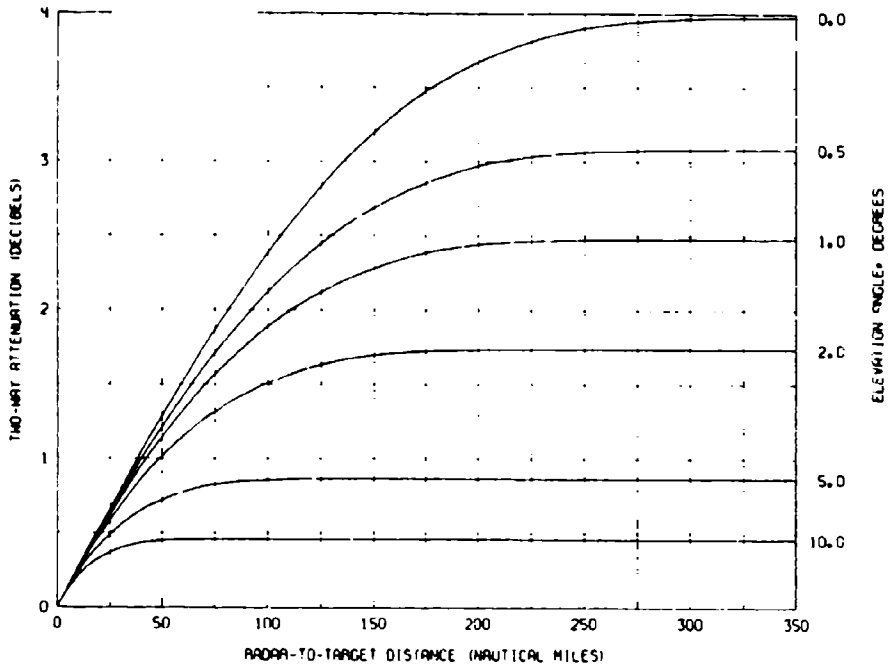


Fig. 20 — Total radar absorption loss for ray paths in the standard atmosphere at 1500 MHz

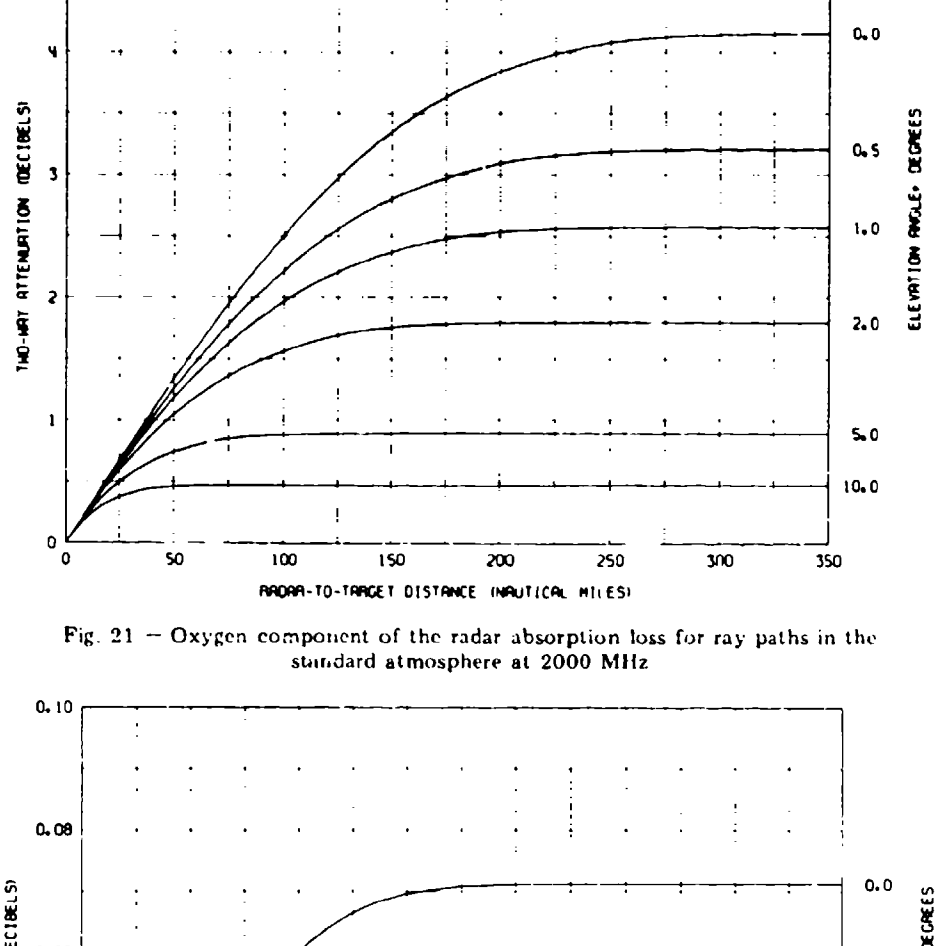


Fig. 21 — Oxygen component of the radar absorption loss for ray paths in the standard atmosphere at 2000 MHz

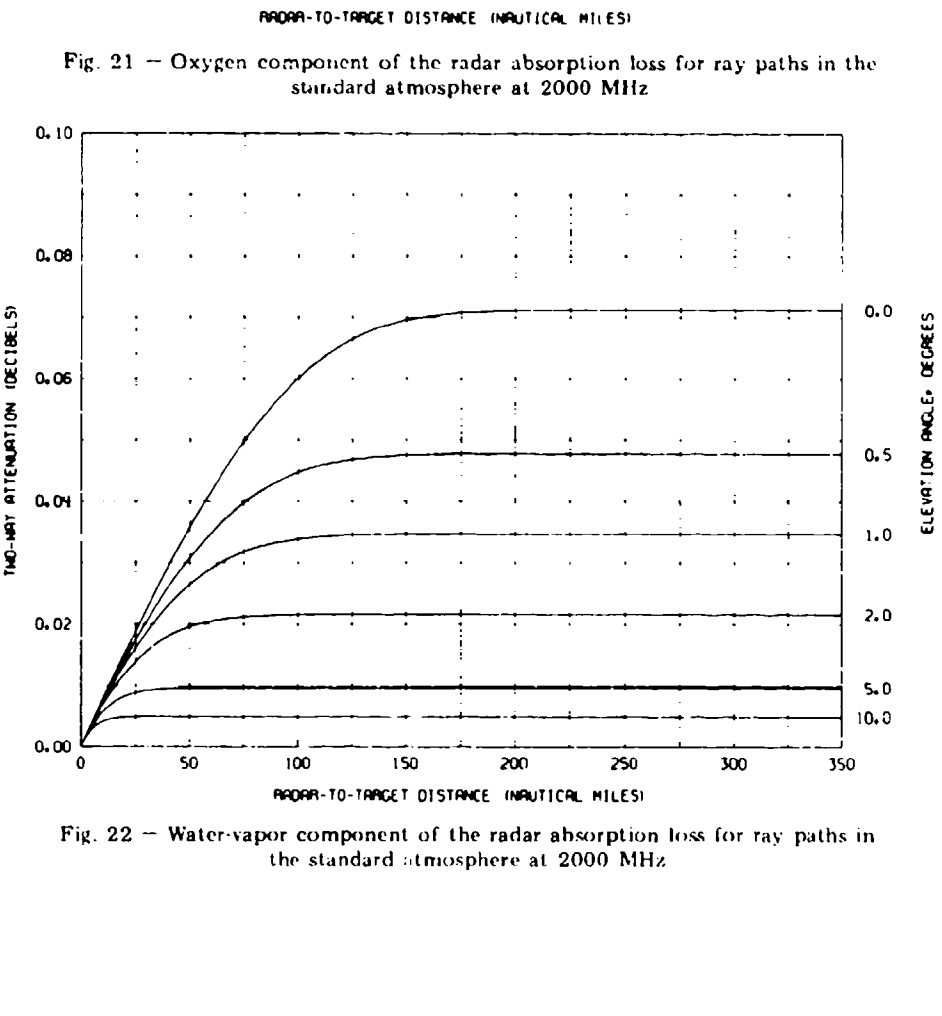


Fig. 22 — Water-vapor component of the radar absorption loss for ray paths in the standard atmosphere at 2000 MHz

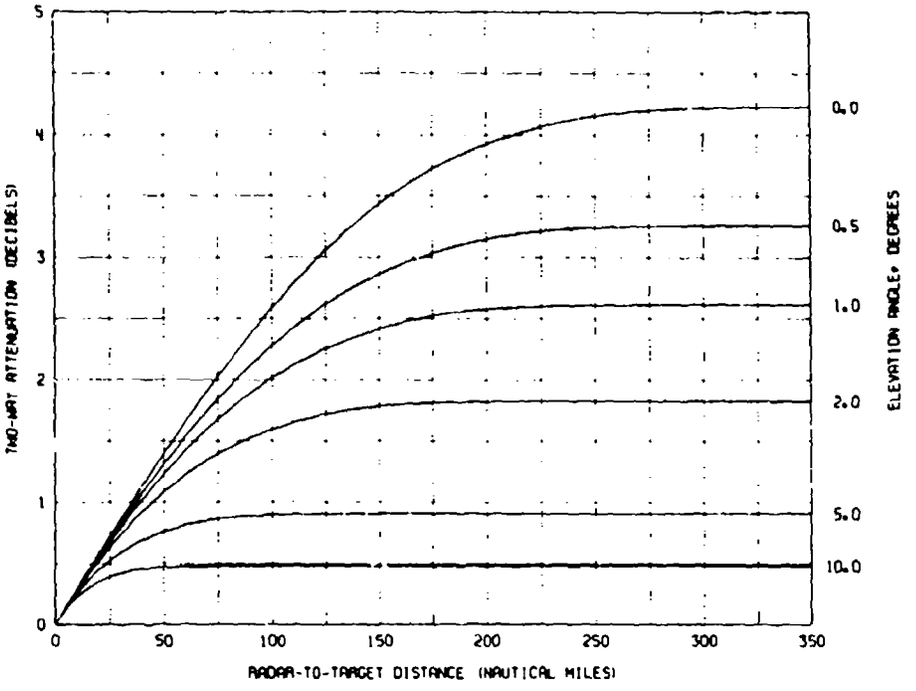


Fig. 23 — Total radar absorption loss for ray paths in the standard atmosphere at 2000 MHz

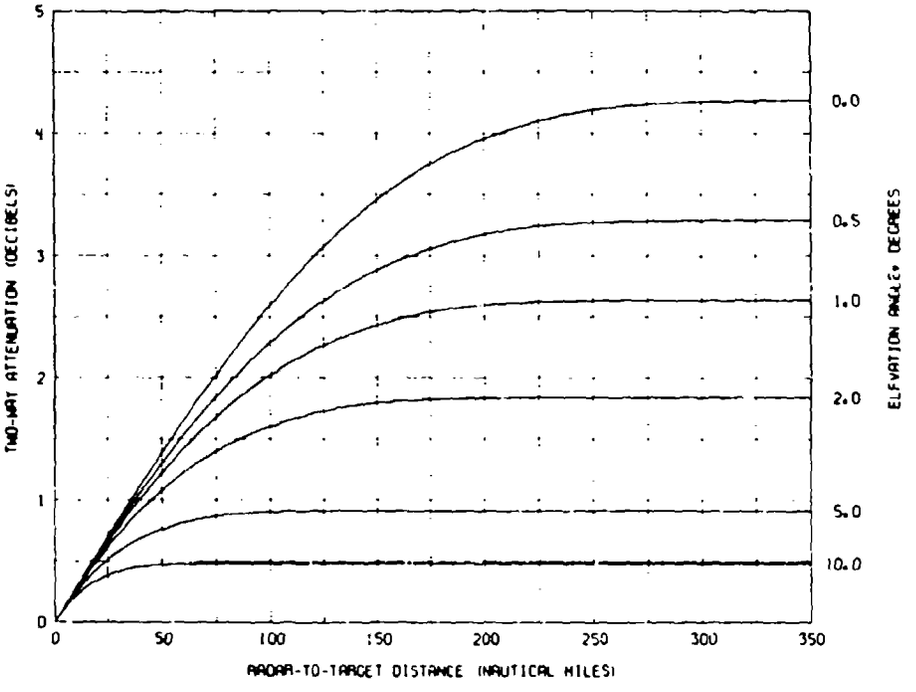


Fig. 24 — Oxygen component of the radar absorption loss for ray paths in the standard atmosphere at 2500 MHz

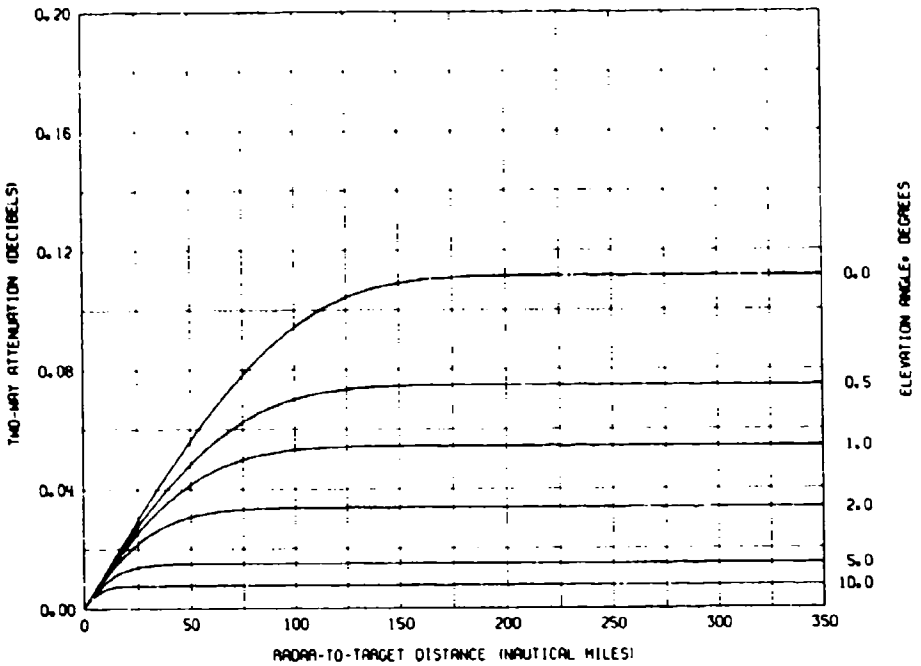


Fig. 25 — Water-vapor component of the radar absorption loss for ray paths in the standard atmosphere at 2500 MHz

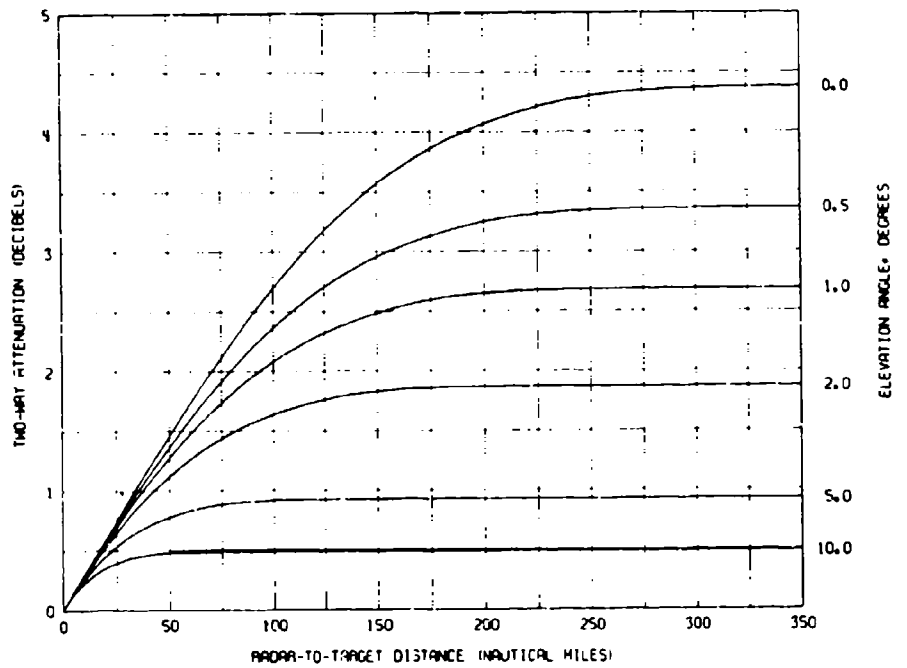


Fig. 26 — Total radar absorption loss for ray paths in the standard atmosphere at 2500 MHz

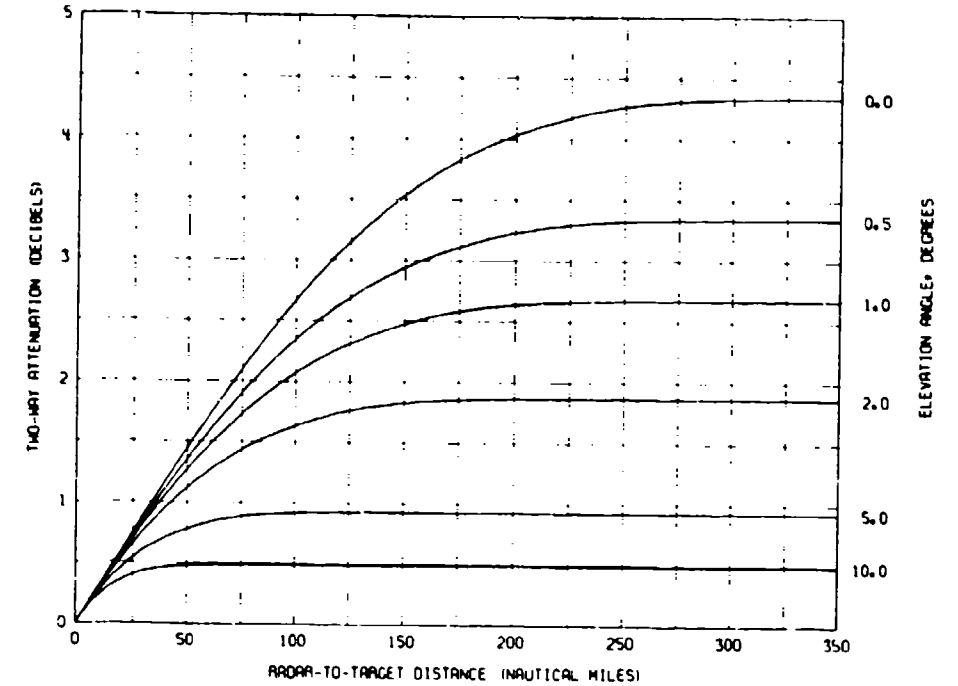


Fig. 27 — Oxygen component of the radar absorption loss for ray paths in the standard atmosphere at 3000 MHz

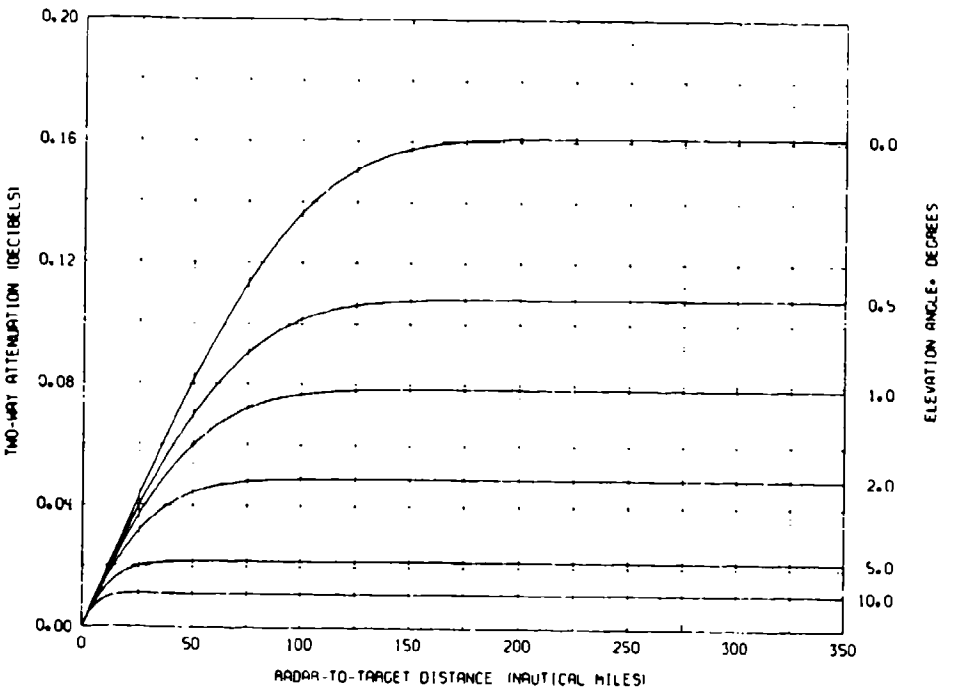


Fig. 28 — Water-vapor component of the radar absorption loss for ray paths in the standard atmosphere at 3000 MHz

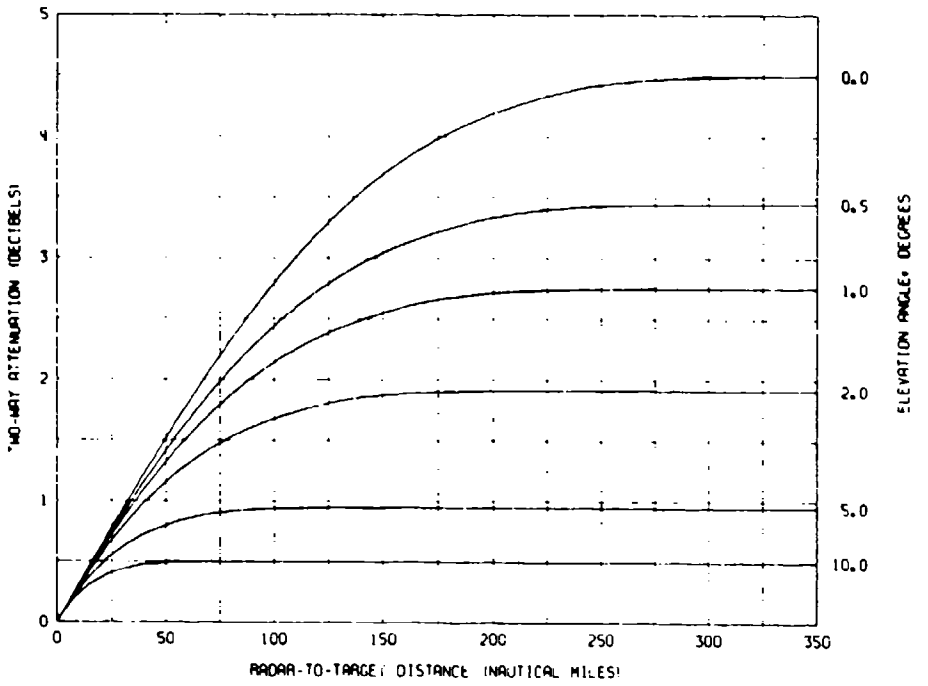


Fig. 29 — Total radar absorption loss for ray paths in the standard atmosphere at 3000 MHz

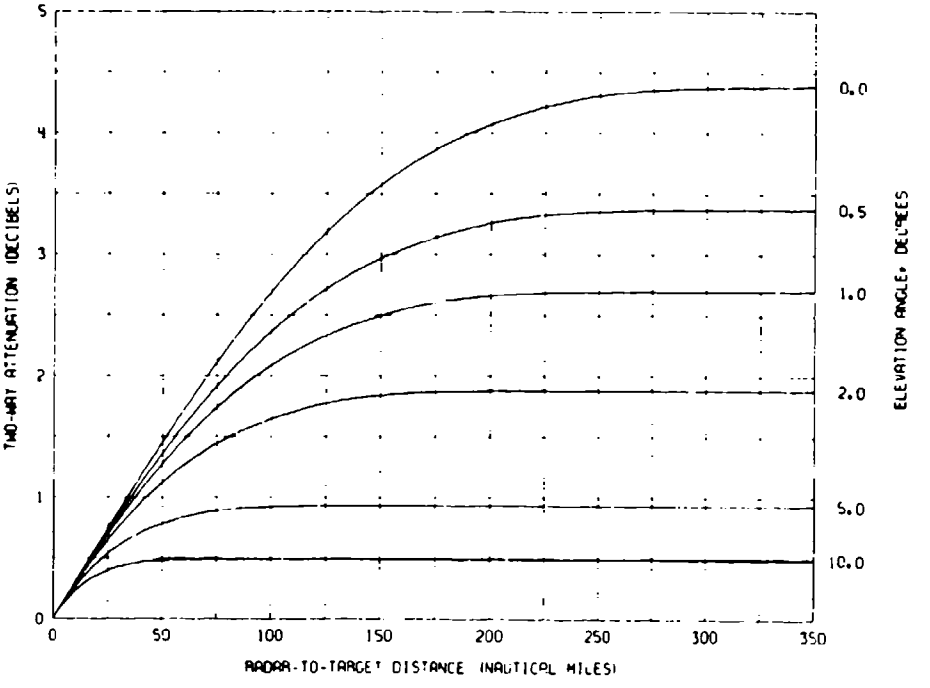


Fig. 30 — Oxygen component of the radar absorption loss for ray paths in the standard atmosphere at 3500 MHz

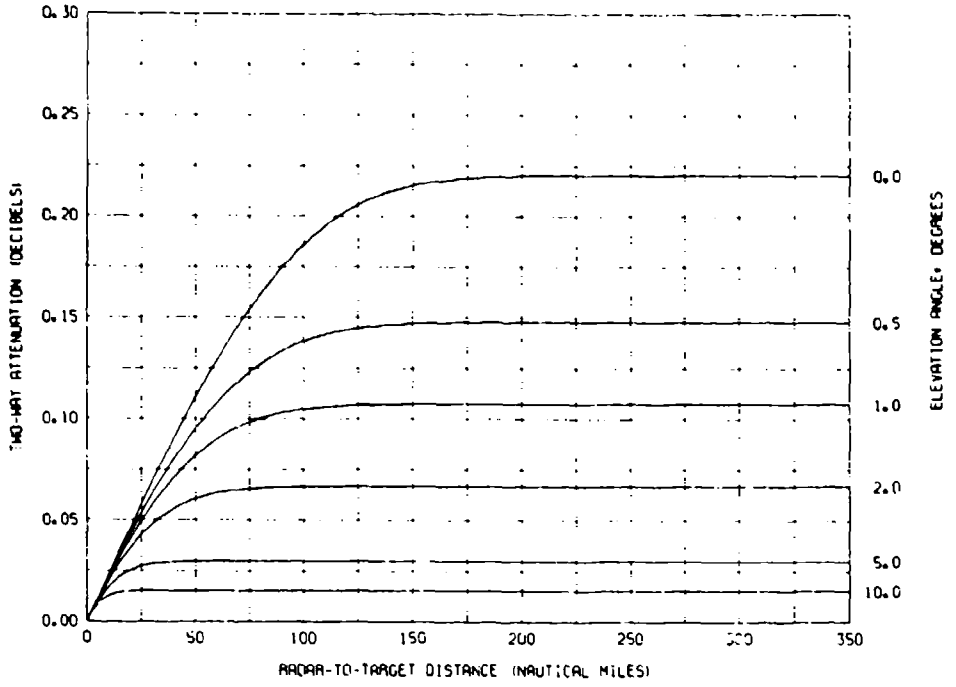


Fig. 31 — Water-vapor component of the radar absorption loss for ray paths in the standard atmosphere at 3500 MHz

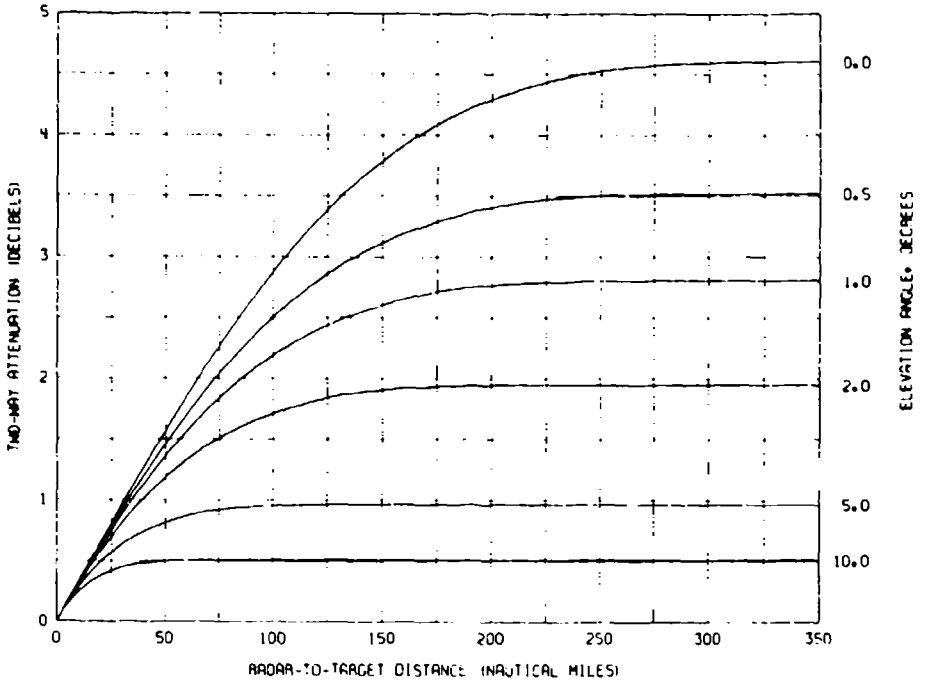


Fig. 32 - Total radar absorption loss for ray paths in the standard atmosphere at 3500 MHz

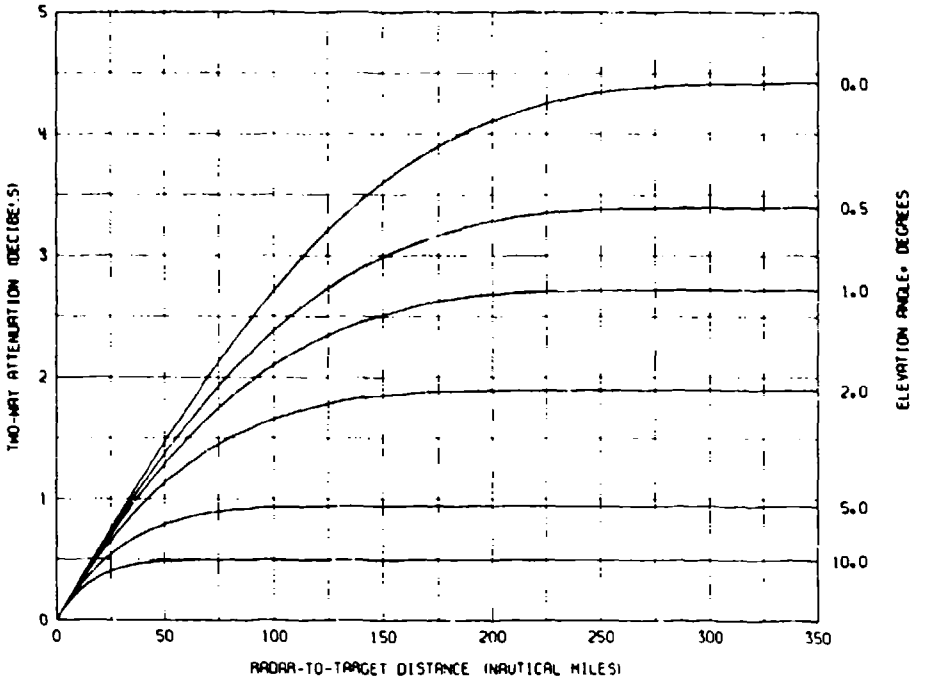


Fig. 33 — Oxygen component of the radar absorption loss for ray paths in the standard atmosphere at 4000 MHz

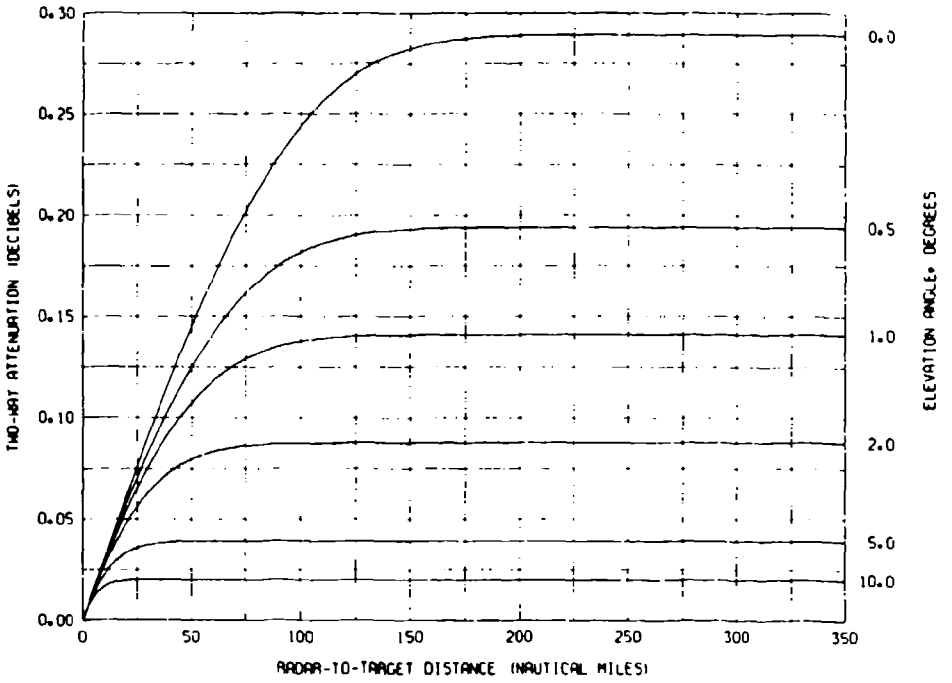


Fig. 34 — Water-vapor component of the radar absorption loss for ray paths in the standard atmosphere at 4000 MHz

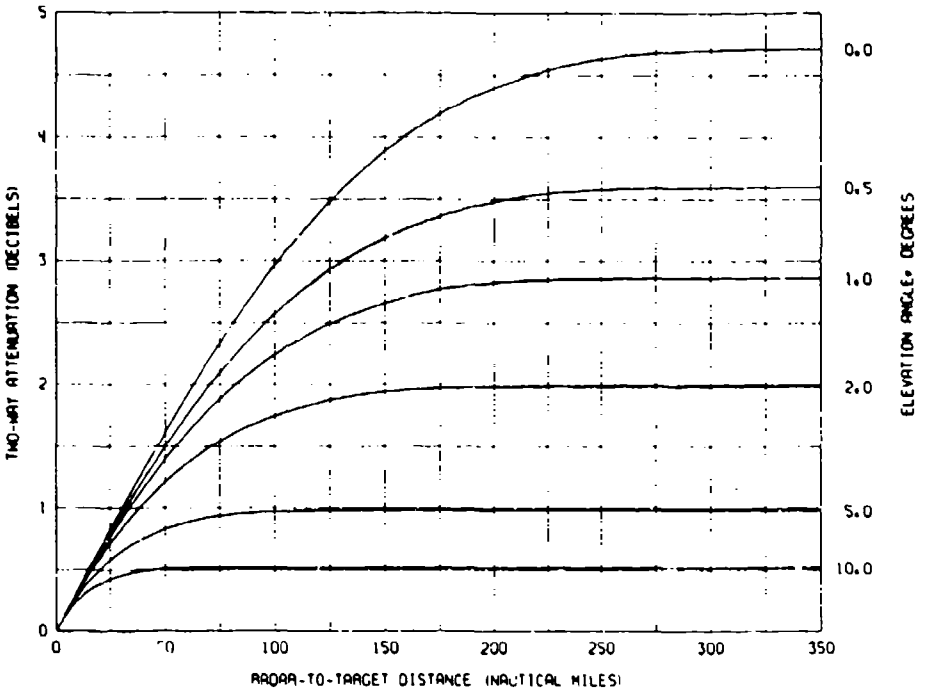


Fig. 35 — Total radar absorption loss for ray paths in the standard atmosphere at 4000 MHz

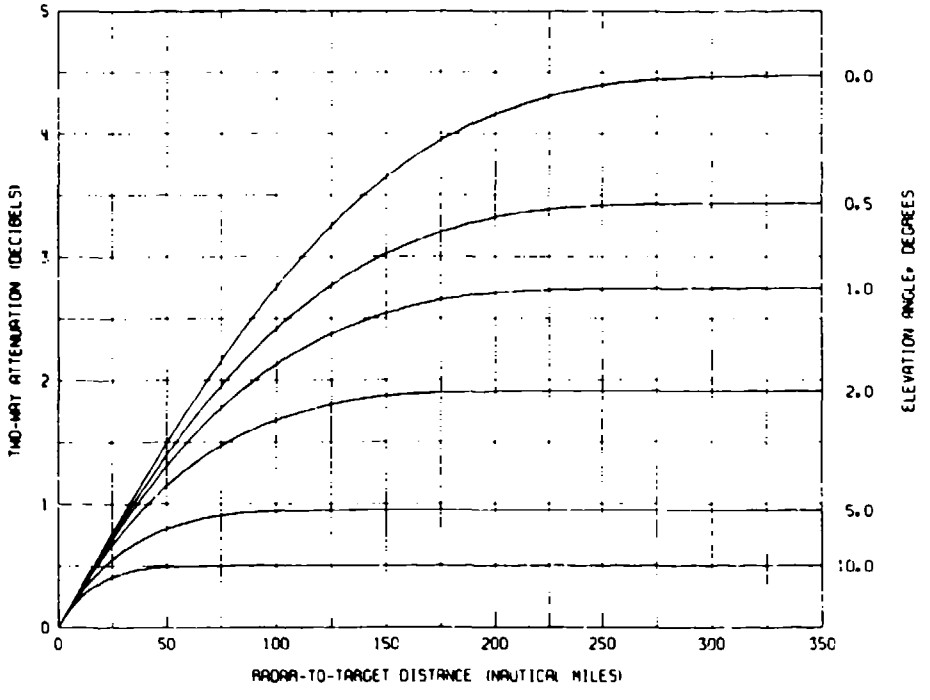


Fig. 36 — Oxygen component of the radar absorption loss for ray paths in the standard atmosphere at 5000 MHz

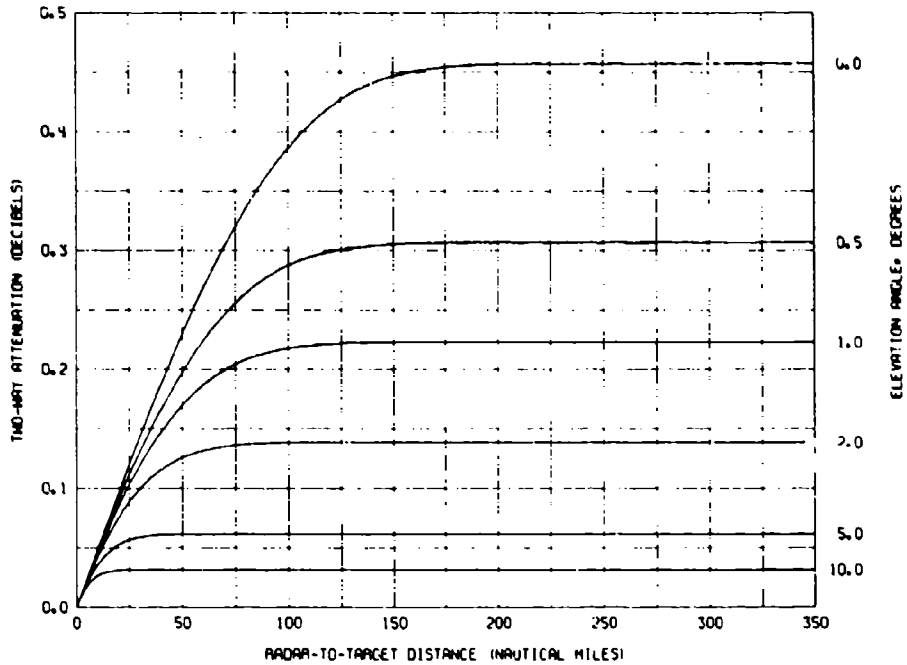


Fig. 37 — Water-vapor component of the radar absorption loss for ray paths in the standard atmosphere at 5000 MHz

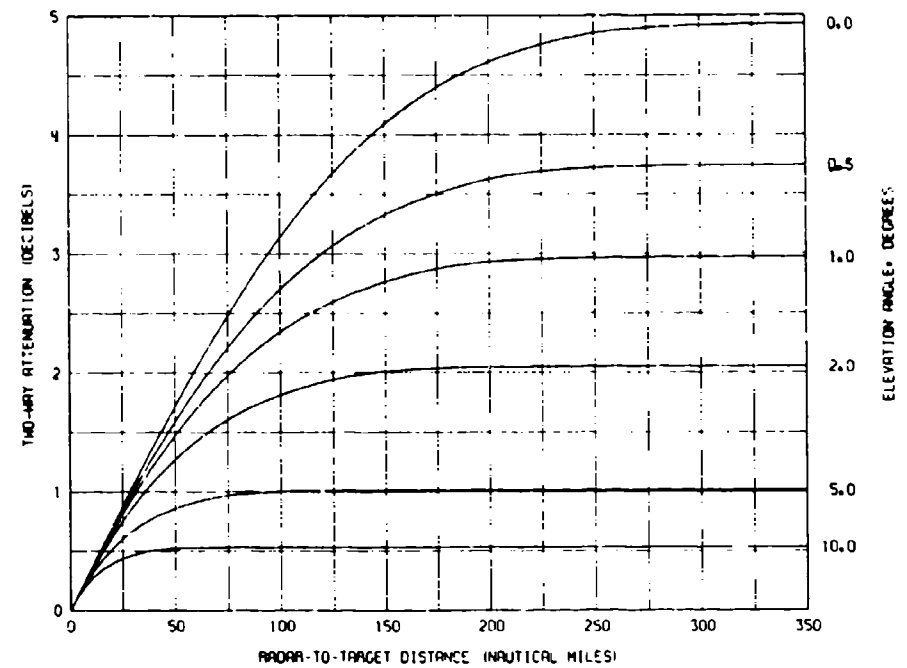


Fig. 38 Total radar absorption loss for ray paths in the standard atmosphere at 5000 MHz

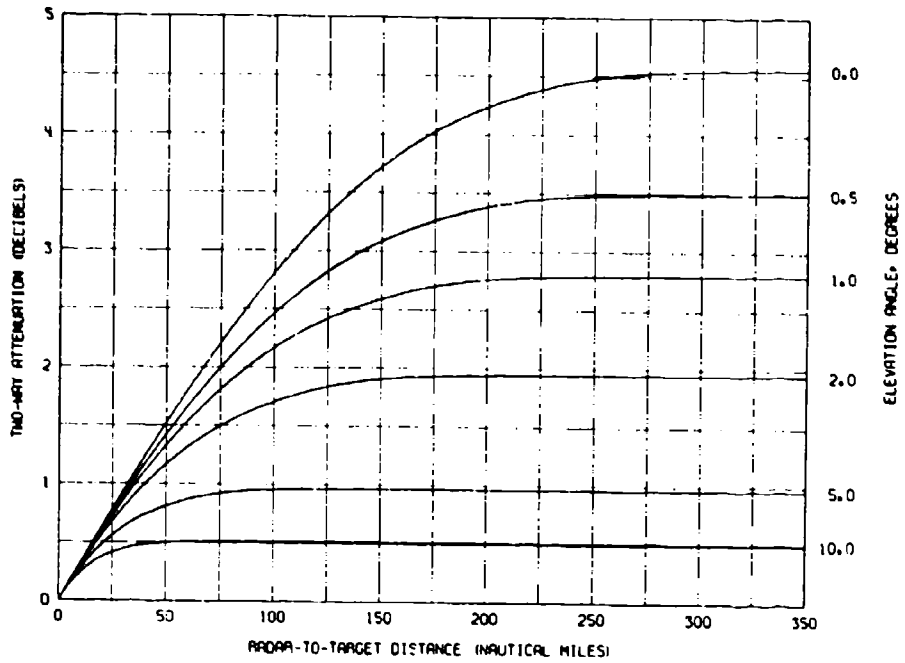


Fig. 39 — Oxygen component of the radar absorption loss for ray paths in the standard atmosphere at 7000 MHz

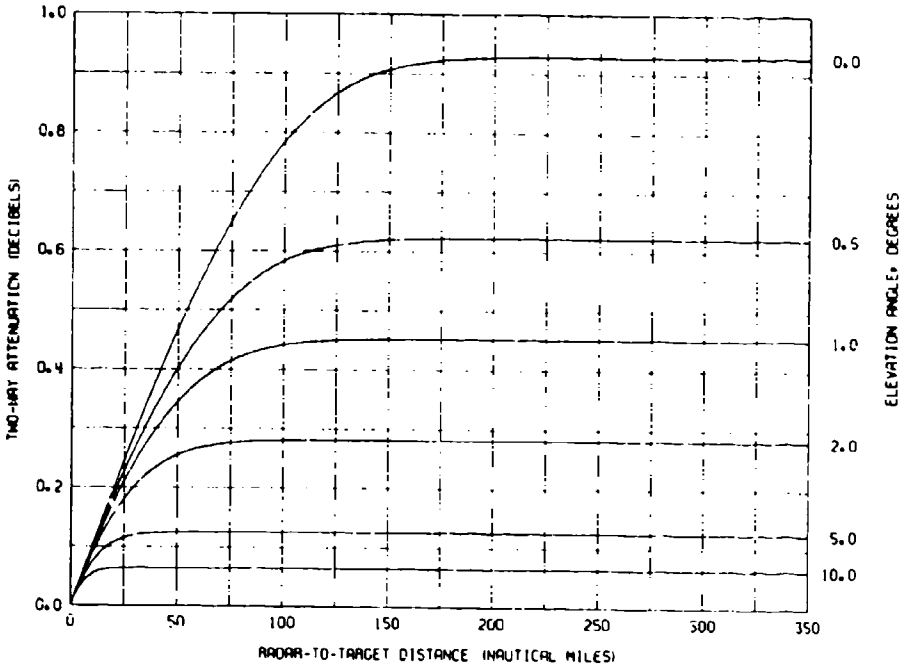


Fig. 40 — Water-vapor component of the radar absorption loss for ray paths in the standard atmosphere at 7000 MHz

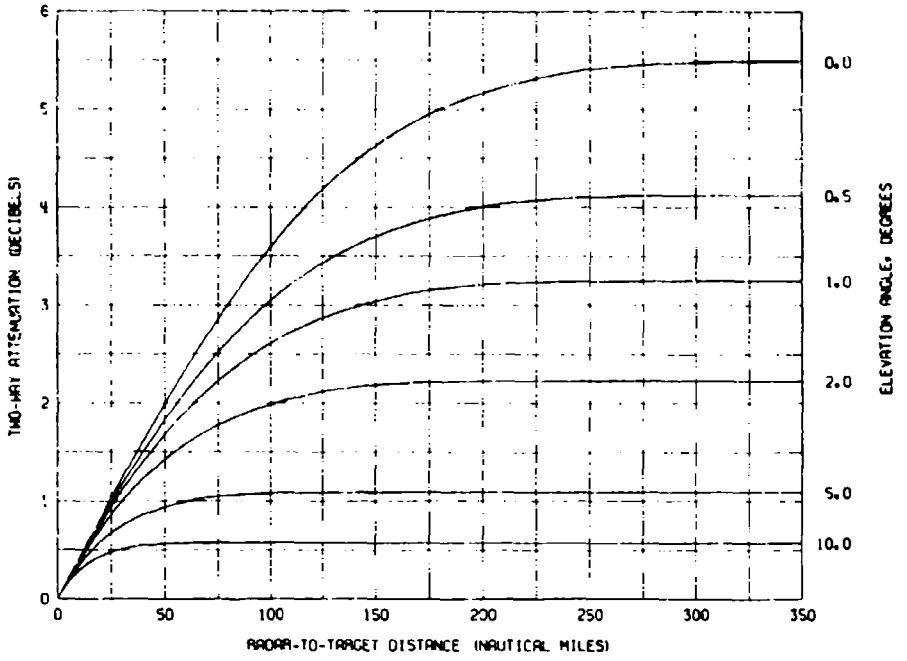


Fig. 41 — Total radar absorption loss for ray paths in the standard atmosphere at 7000 MHz

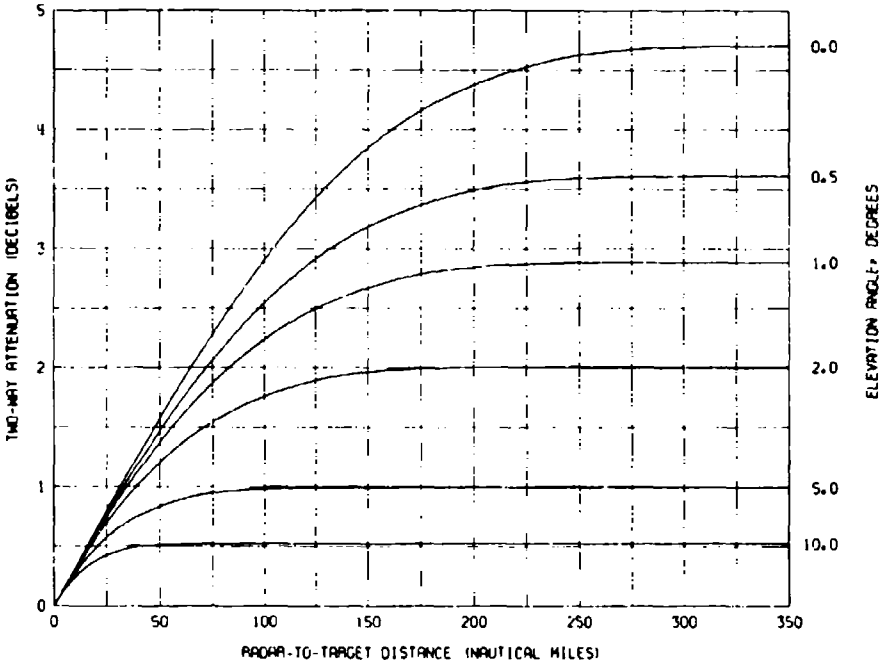


Fig. 42 — Oxygen component of the radar absorption loss for ray paths in the standard atmosphere at 10 GHz

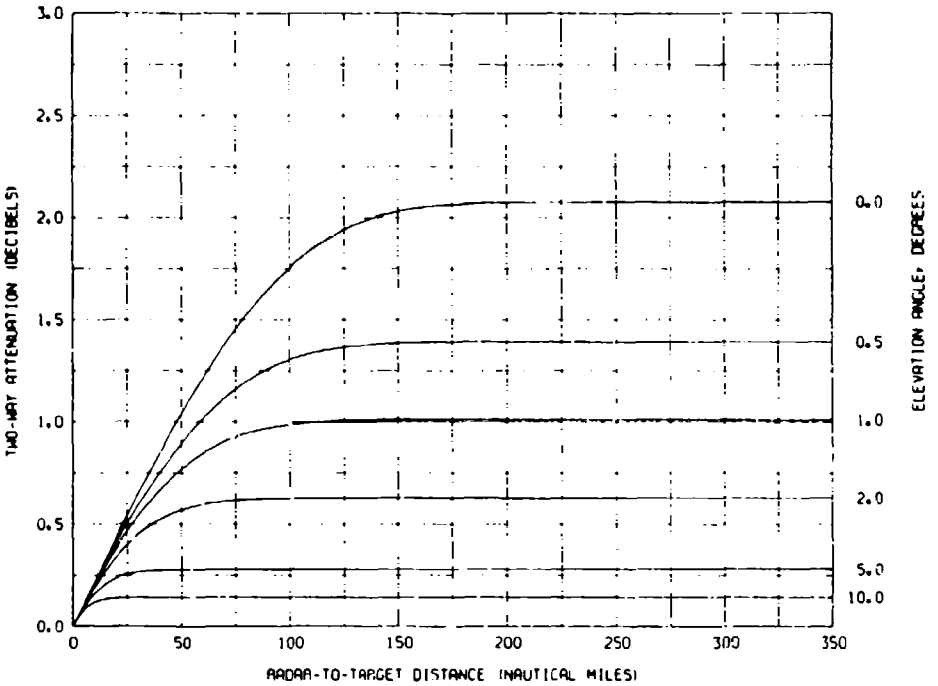


Fig. 43 — Water-vapor component of the radar absorption loss for ray paths in the standard atmosphere at 10 GHz

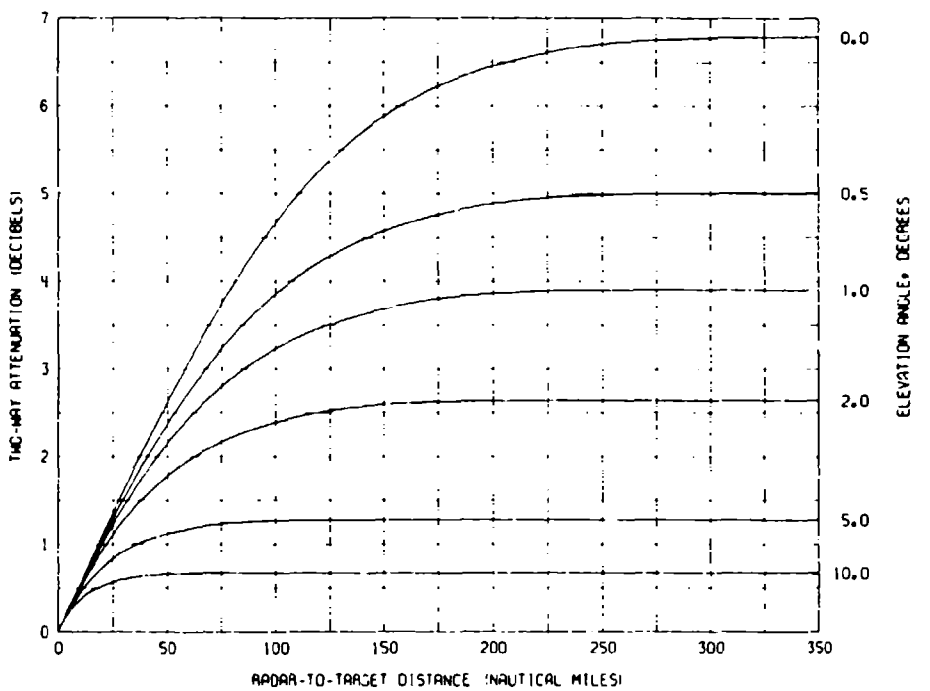


Fig. 44 — Total radar absorption loss for ray paths in the standard atmosphere at 10 GHz

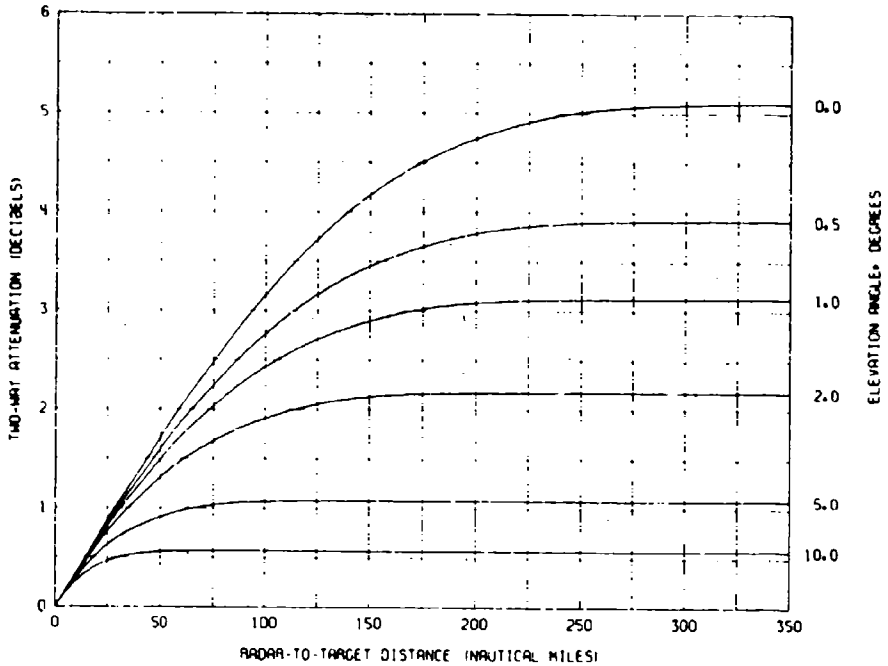


Fig. 45 — Oxygen component of the radar absorption loss for ray paths in the standard atmosphere at 15 GHz

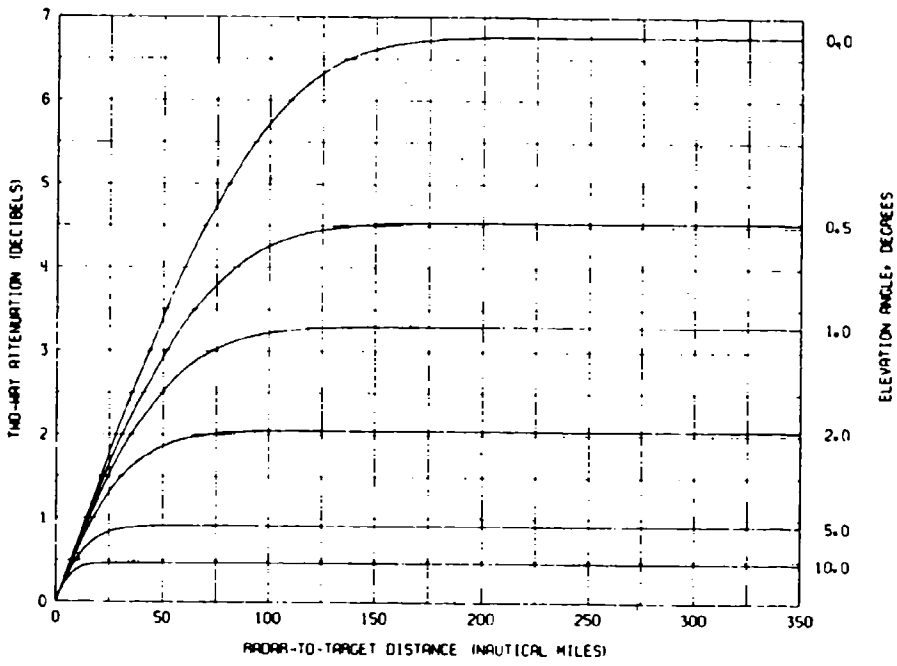


Fig. 46 — Water-vapor component of the radar absorption loss for ray paths in the standard atmosphere at 15 GHz

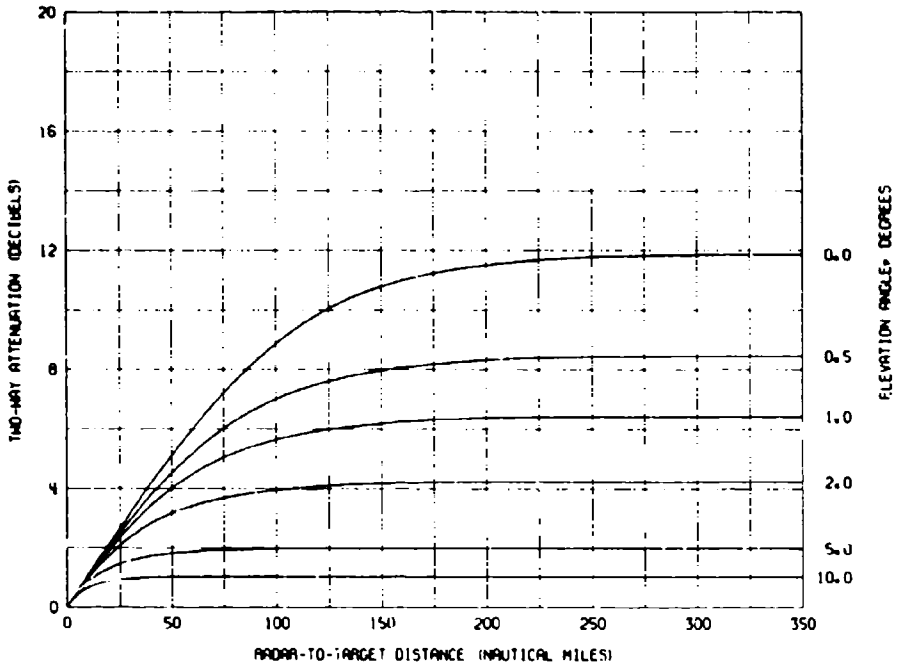


Fig. 47 — Total radar absorption loss for ray paths in the standard atmosphere at 15 GHz

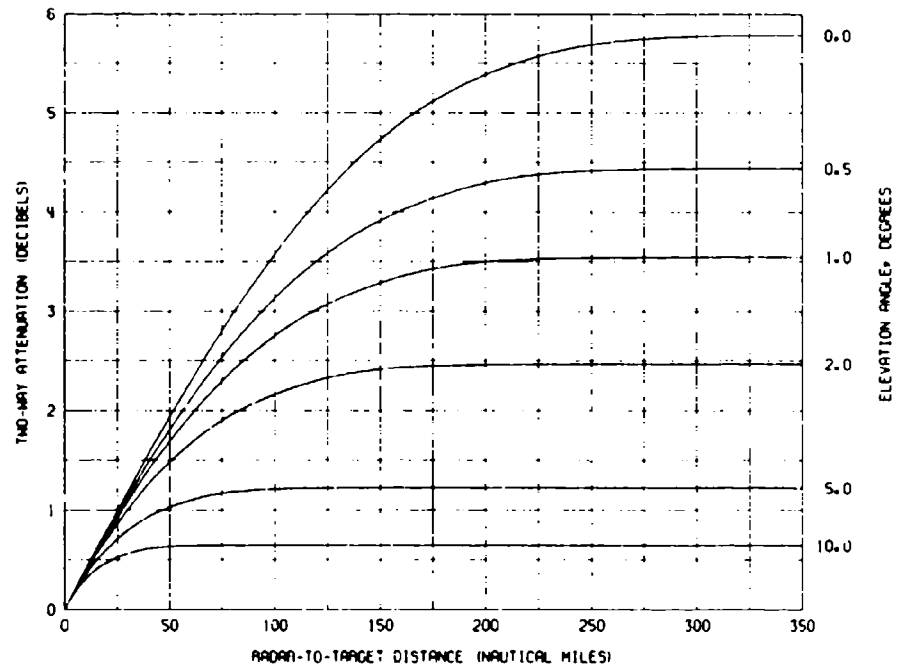


Fig. 48 — Oxygen component of the radar absorption loss for ray paths in the standard atmosphere at 20 GHz

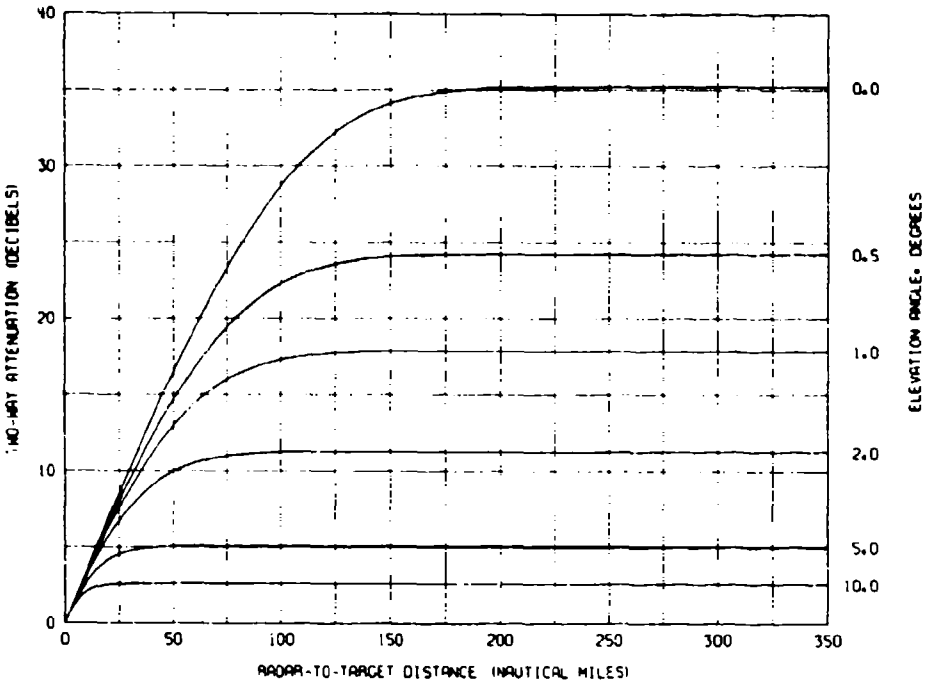


Fig. 49 — Water-vapor component of the radar absorption loss for ray paths in the standard atmosphere at 20 GHz

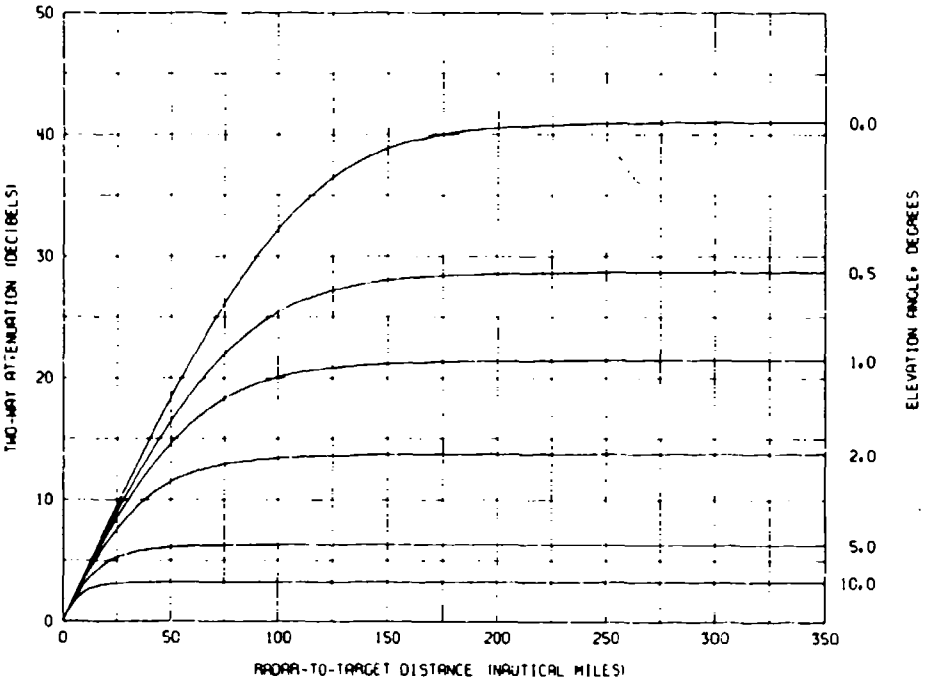


Fig. 50 — Total radar absorption loss for ray paths in the standard atmosphere at 20 GHz

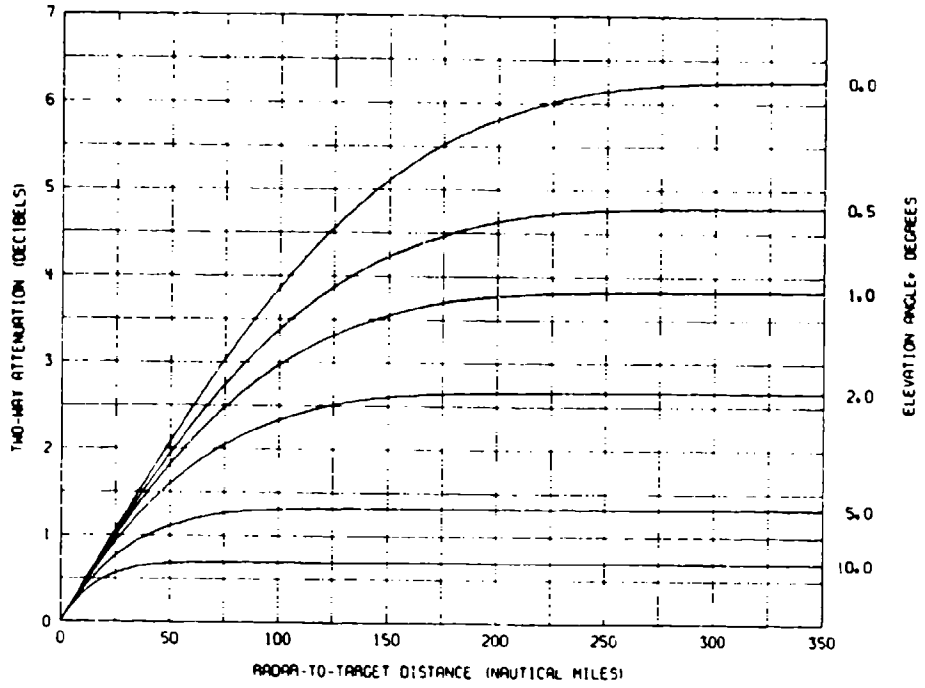


Fig. 51 — Oxygen component of the radar absorption loss for ray paths in the standard atmosphere at 22.235 GHz

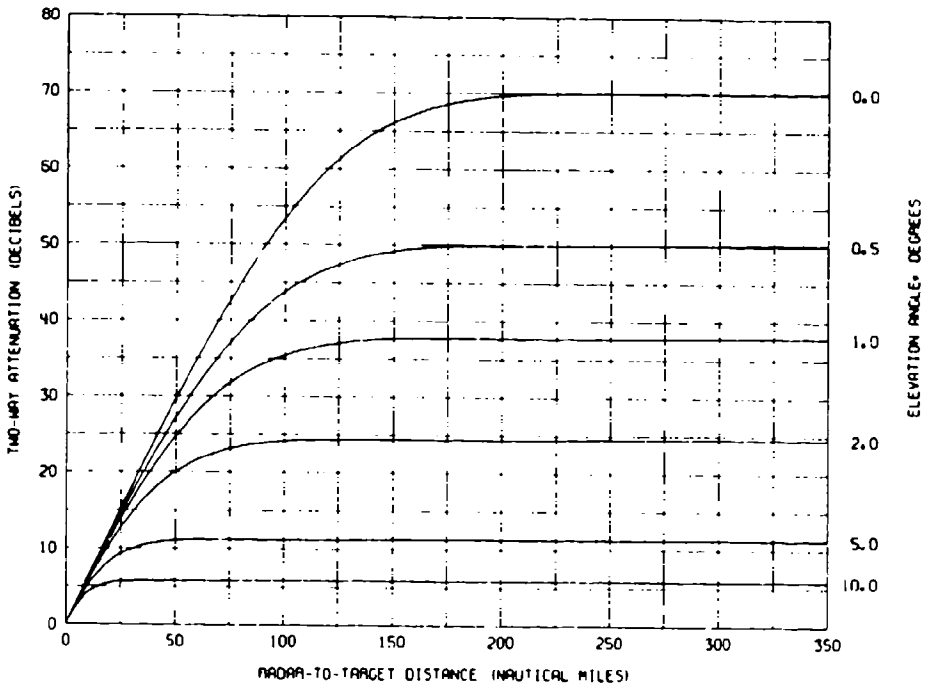


Fig. 52 Water-vapor component of the radar absorption loss for ray paths in the standard atmosphere at 22.235 GHz

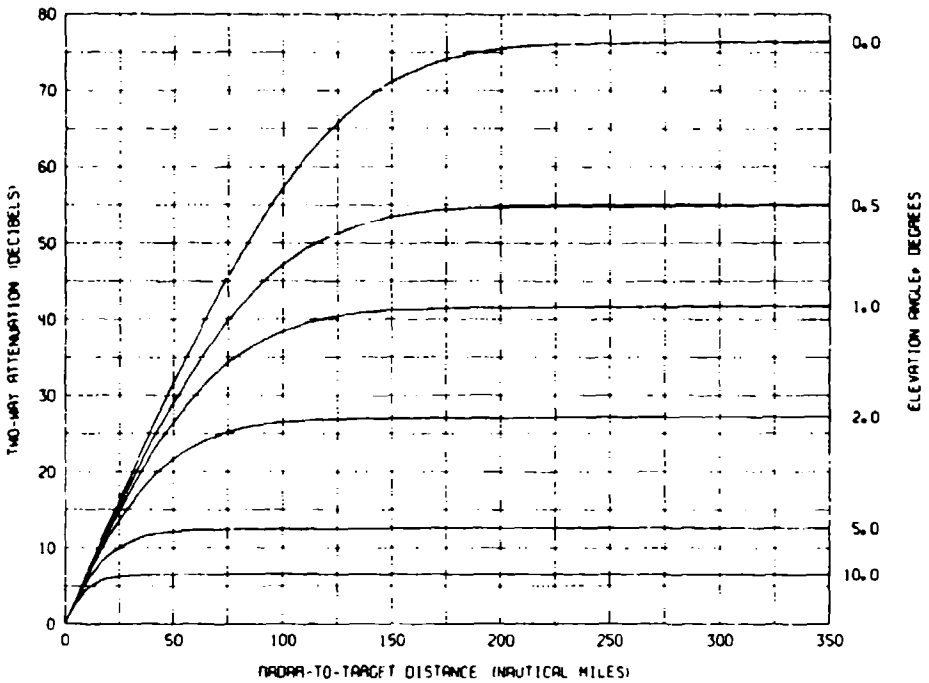


Fig. 53 — Total radar absorption loss for ray paths in the standard atmosphere at 22.235 GHz

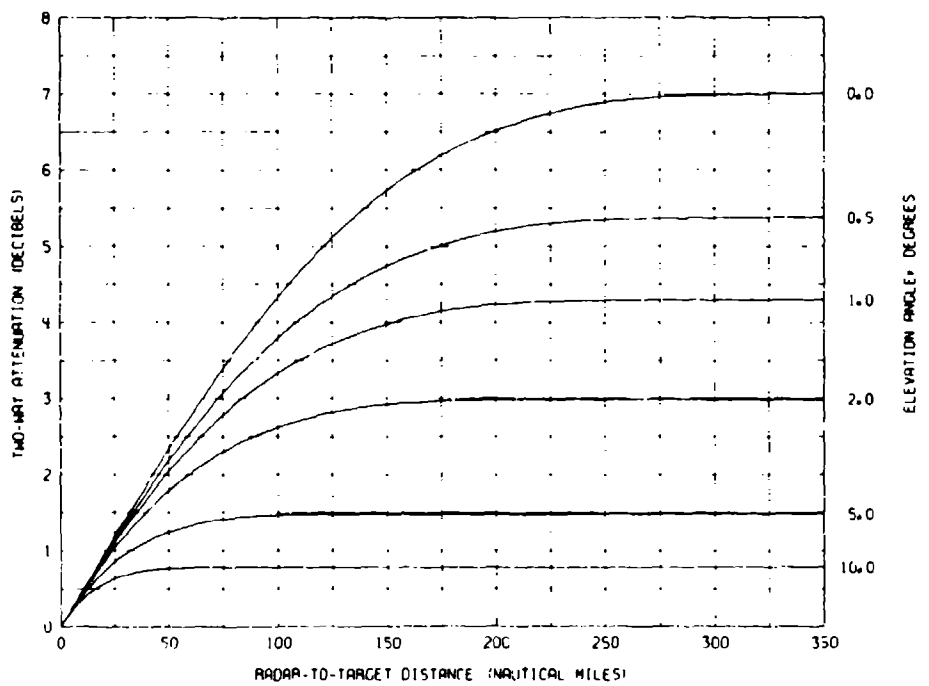


Fig. 54 — Oxygen component of the radar absorption loss for ray paths in the standard atmosphere at 25 GHz

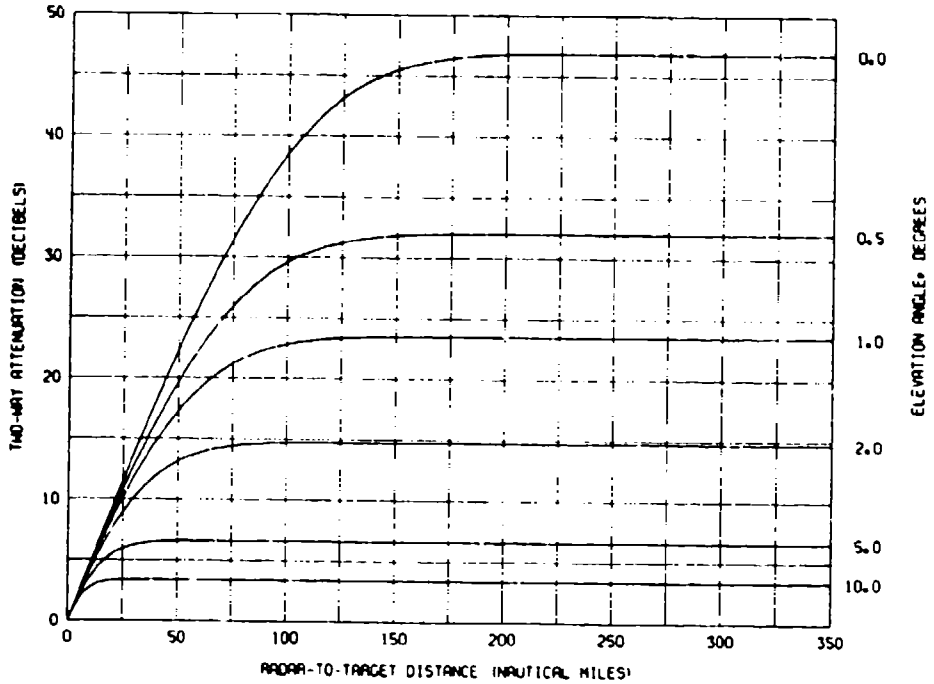


Fig. 55 — Water-vapor component of the radar absorption loss for ray paths in the standard atmosphere at 25 GHz

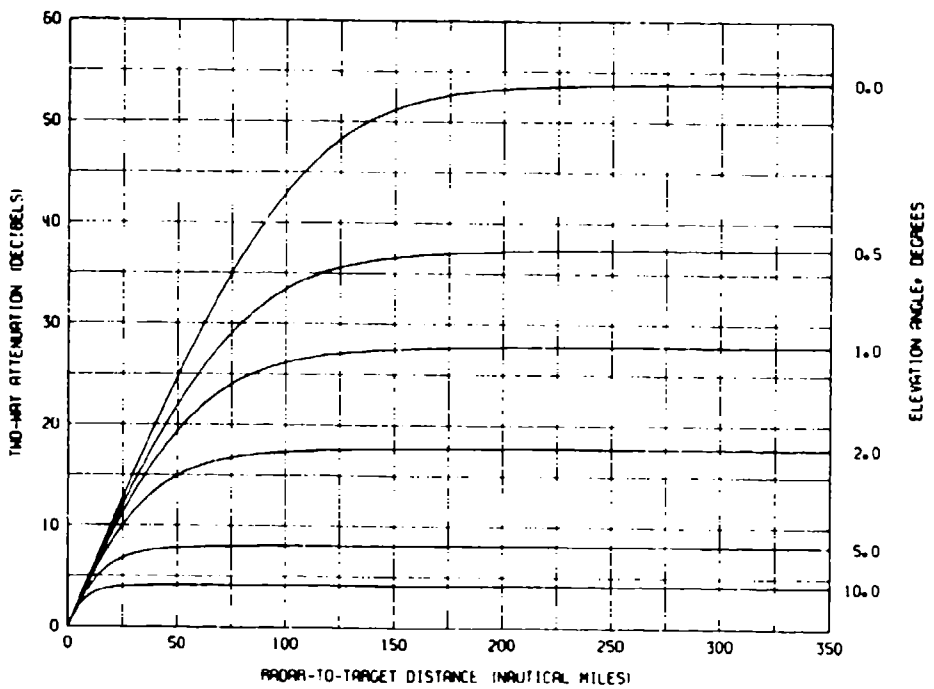


Fig. 56 — Total radar absorption loss for ray paths in the standard atmosphere at 25 GHz

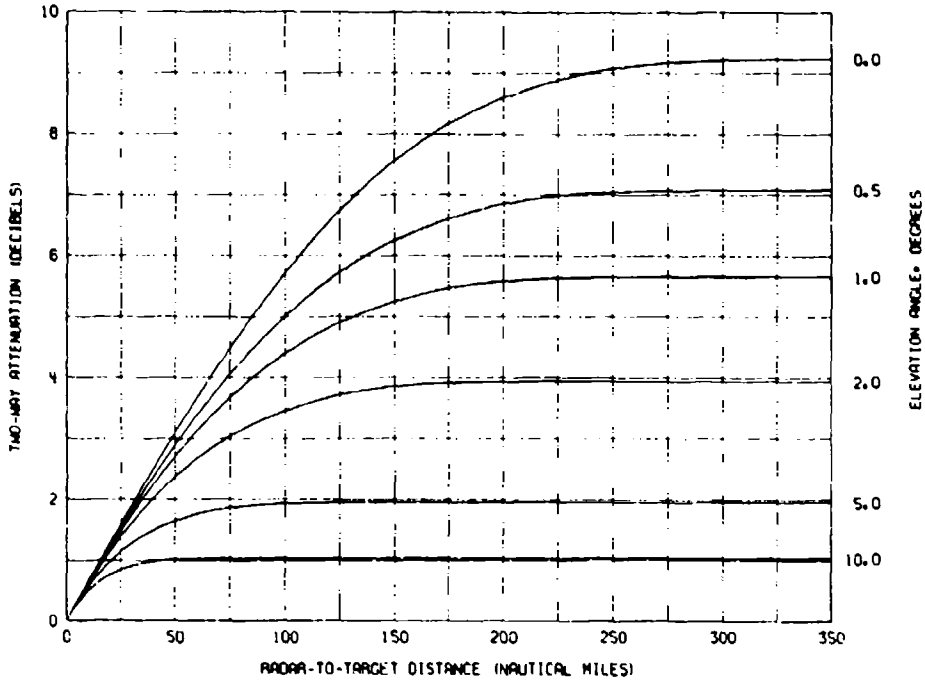


Fig. 57 — Oxygen component of the radar absorption loss for ray paths in the standard atmosphere at 30 GHz

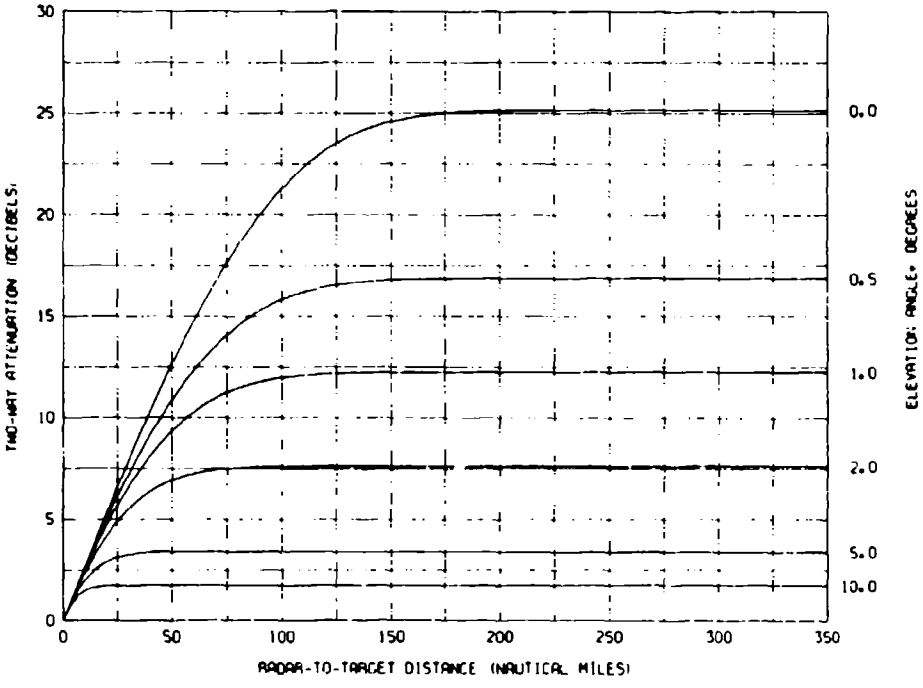


Fig. 58 — Water-vapor component of the radar absorption loss for ray paths in the standard atmosphere at 30 GHz

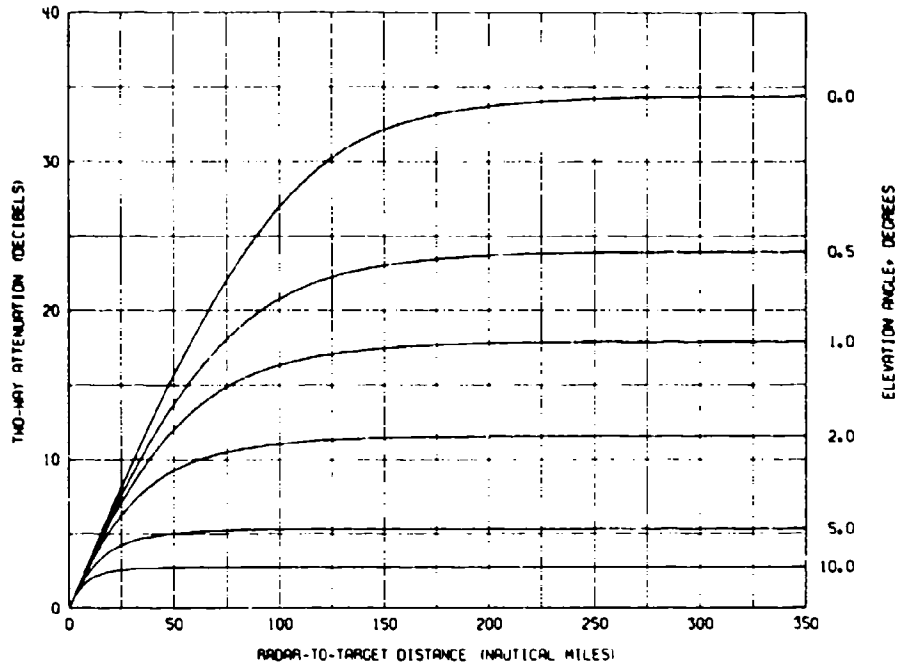


Fig. 59 — Total radar absorption loss for ray paths in the standard atmosphere at 30 GHz

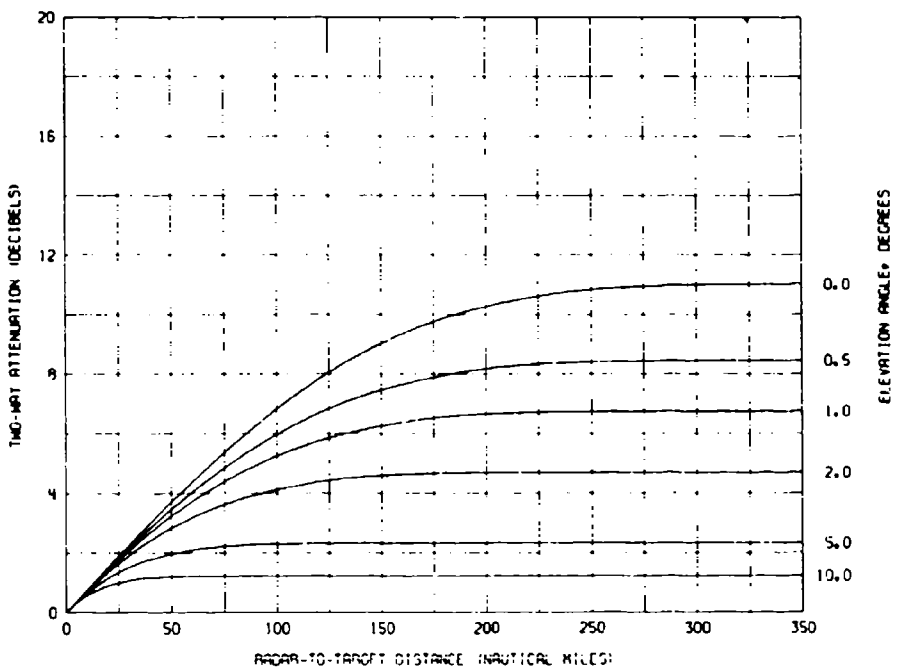


Fig. 60 — Oxygen component of the radar absorption loss for ray paths in standard atmosphere at 32.5 GHz

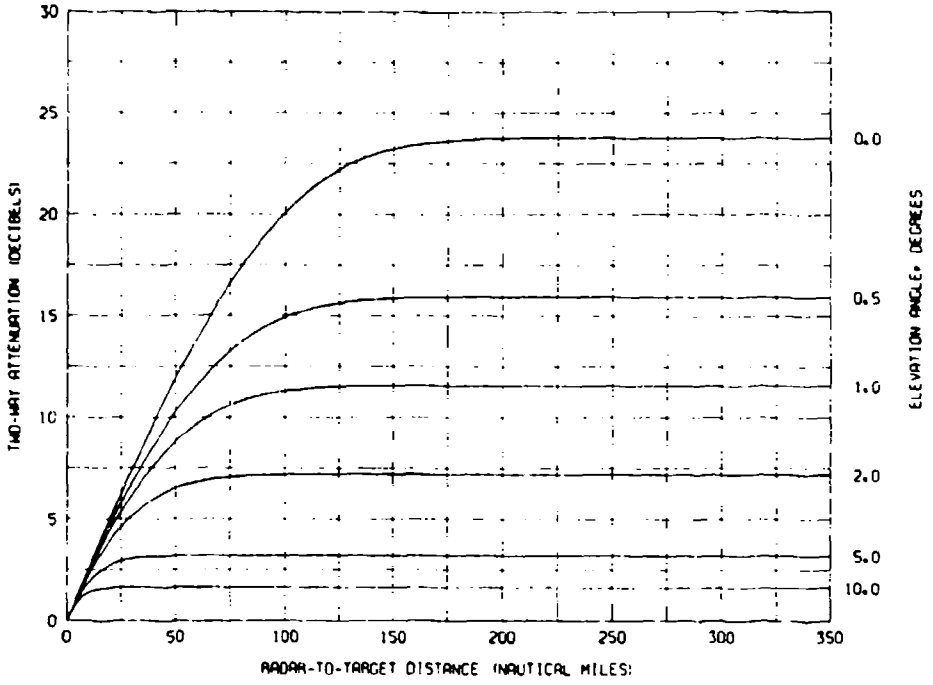


Fig. 61 — Water-vapor component of the radar absorption loss for ray paths in the standard atmosphere at 32.5 GHz

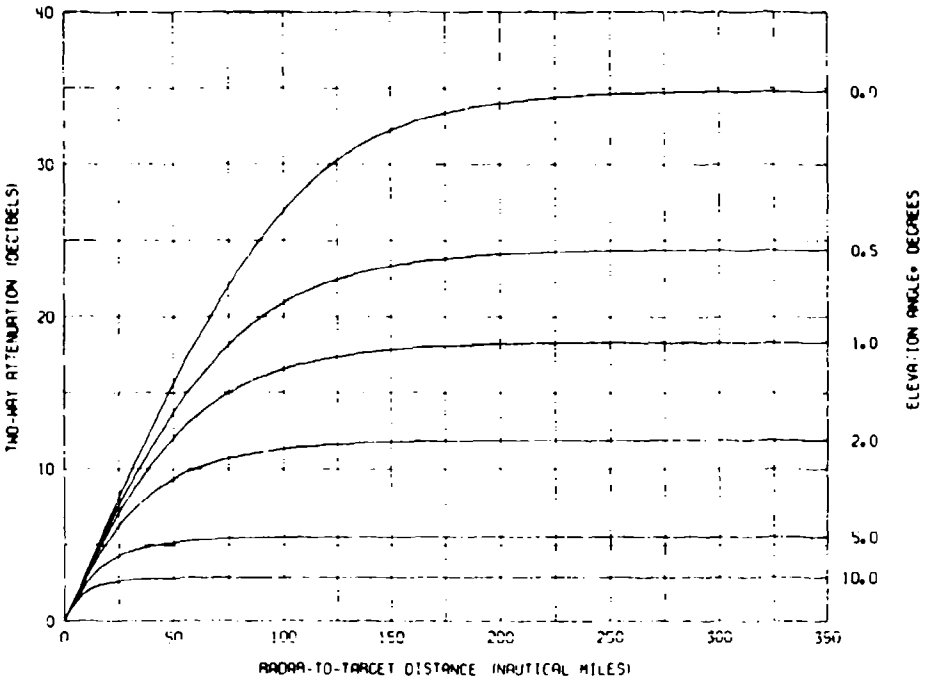


Fig. 62 — Total radar absorption loss for ray paths in the standard atmosphere at 32.5 GHz

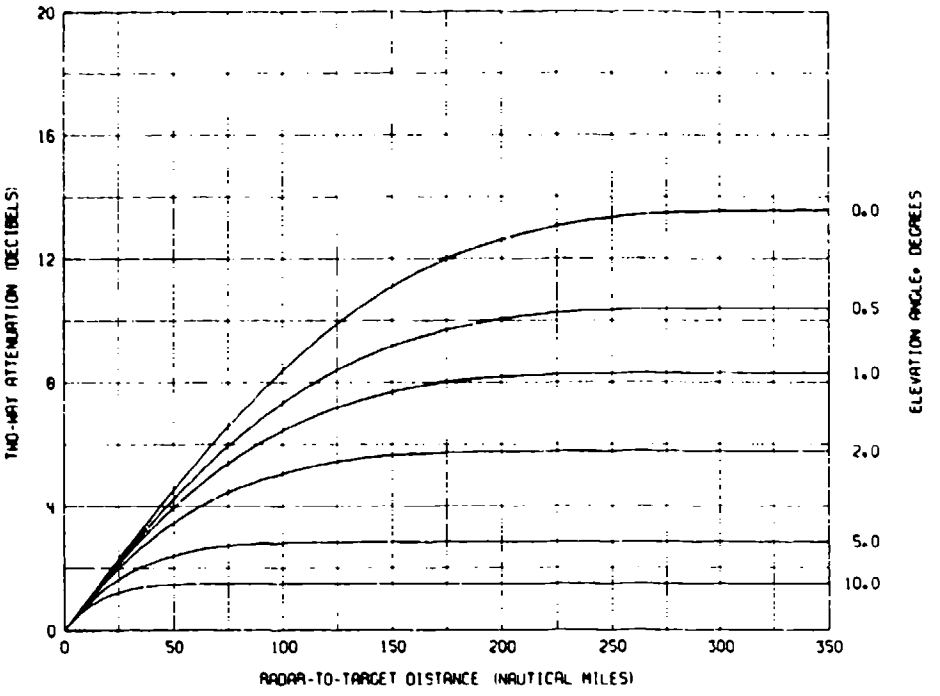


Fig. 63 — Oxygen component of the radar absorption loss for ray paths in the standard atmosphere at 35 GHz

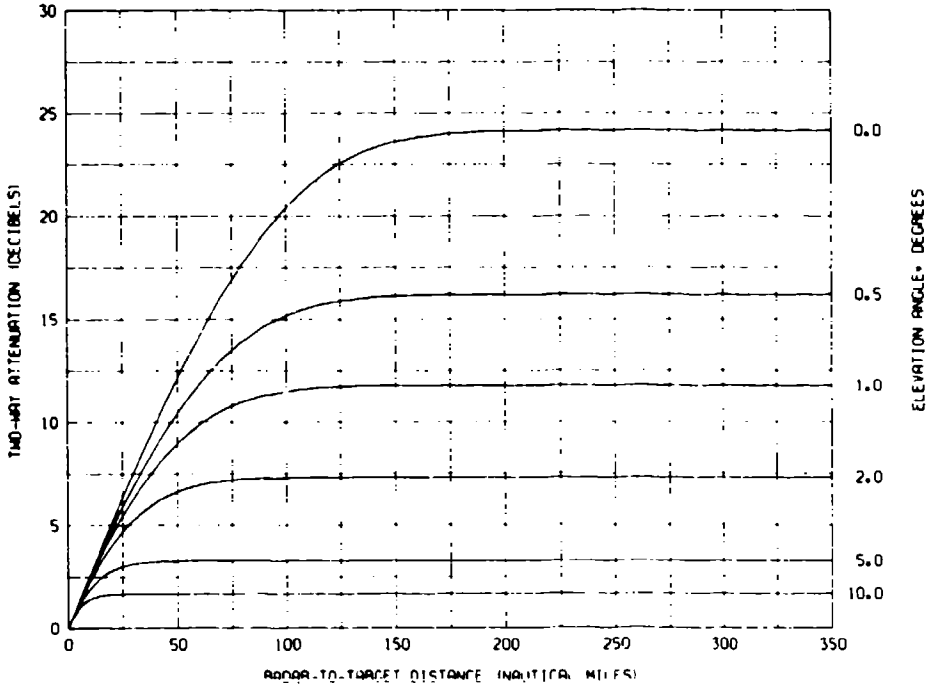


Fig. 64 — Water-vapor component of the radar absorption loss for ray paths in the standard atmosphere at 35 GHz

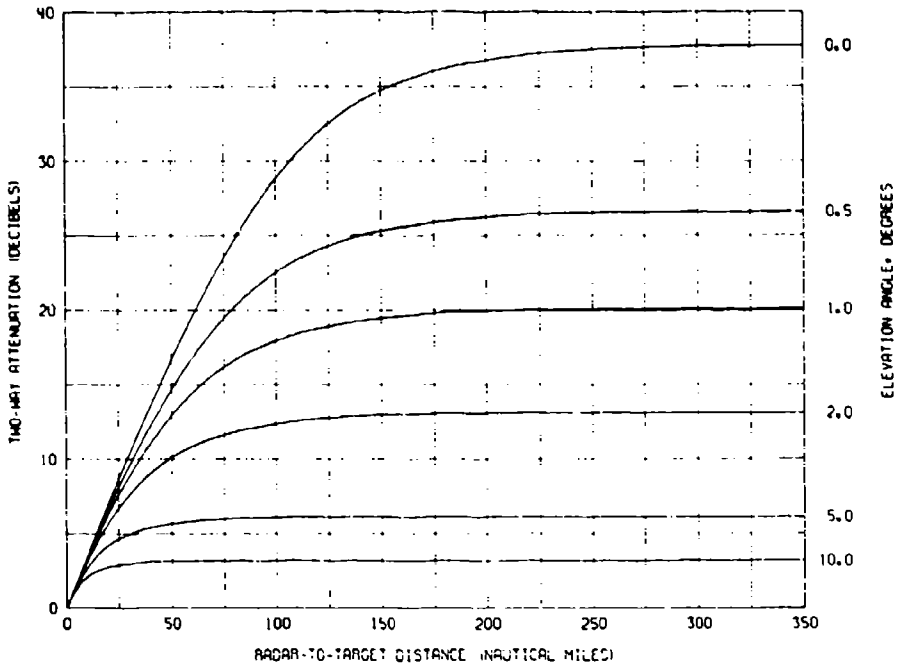


Fig. 65 — Total radar absorption loss for ray paths in the standard atmosphere at 35 GHz

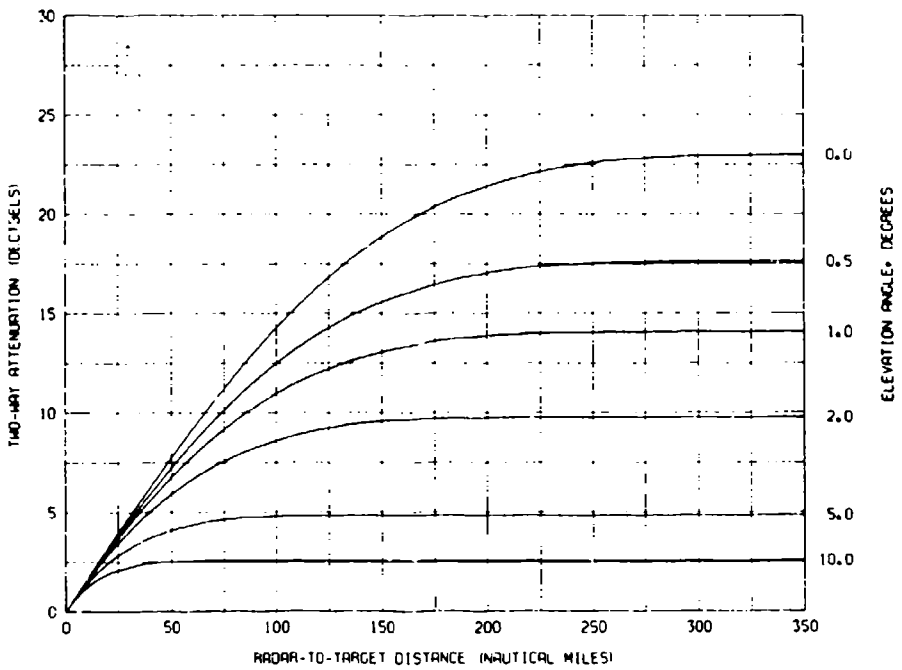


Fig. 66 — Oxygen component of the radar absorption loss for ray paths in the standard atmosphere at 40 GHz

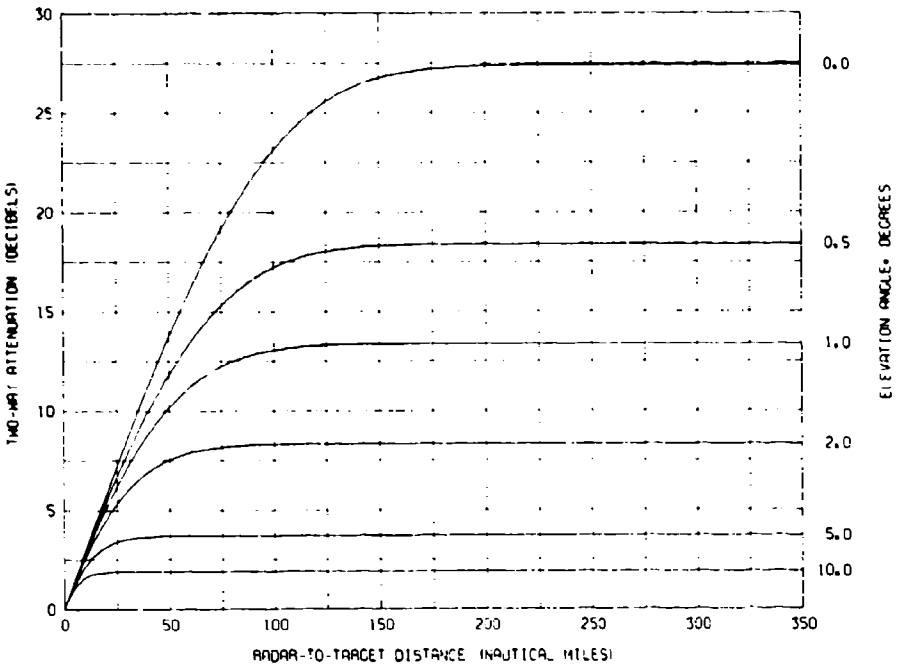


Fig. 67 — Water-vapor component of the radar absorption loss for ray paths in the standard atmosphere at 40 GHz

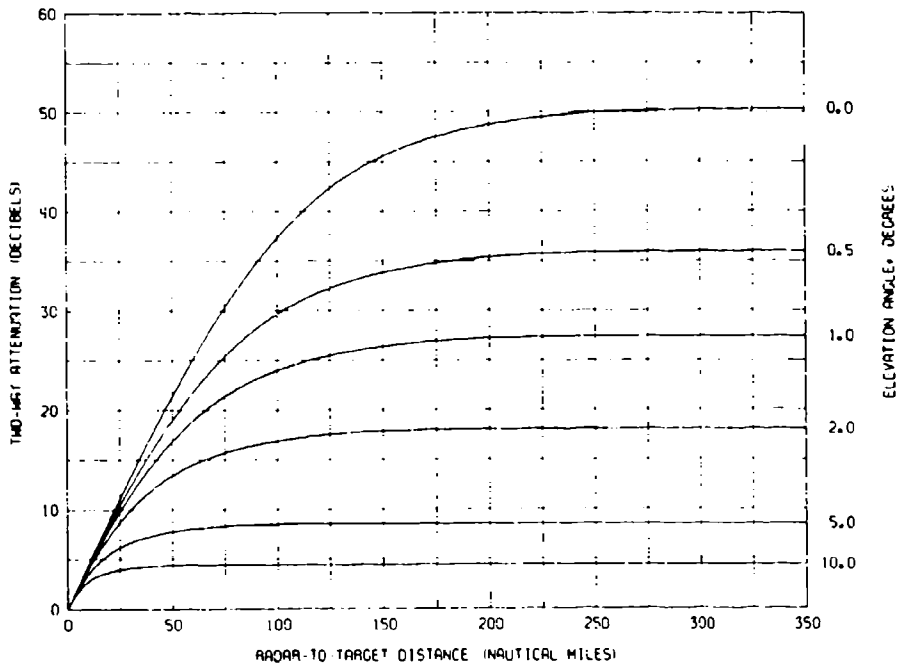


Fig. 68 — Total radar absorption loss for ray paths in the standard atmosphere at 40 GHz

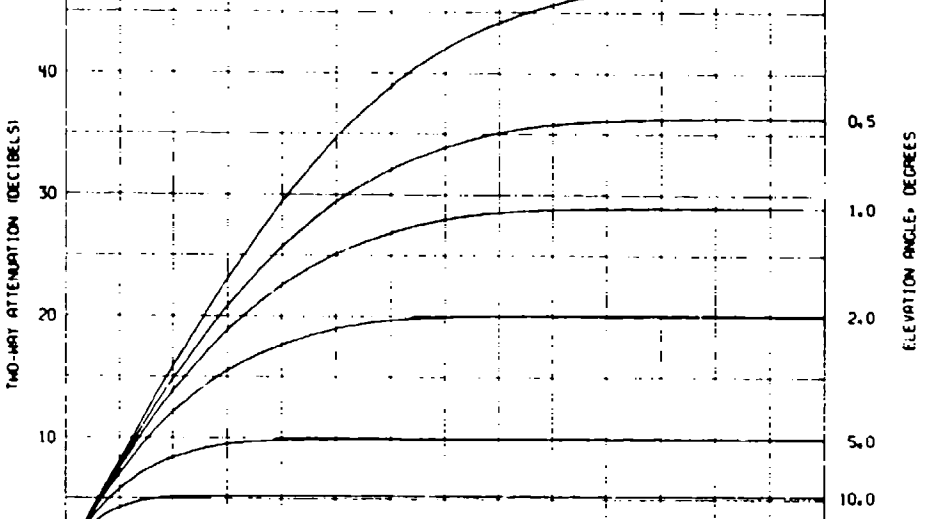


Fig. 69 — Oxygen component of the radar absorption loss for ray paths in the standard atmosphere at 45 GHz

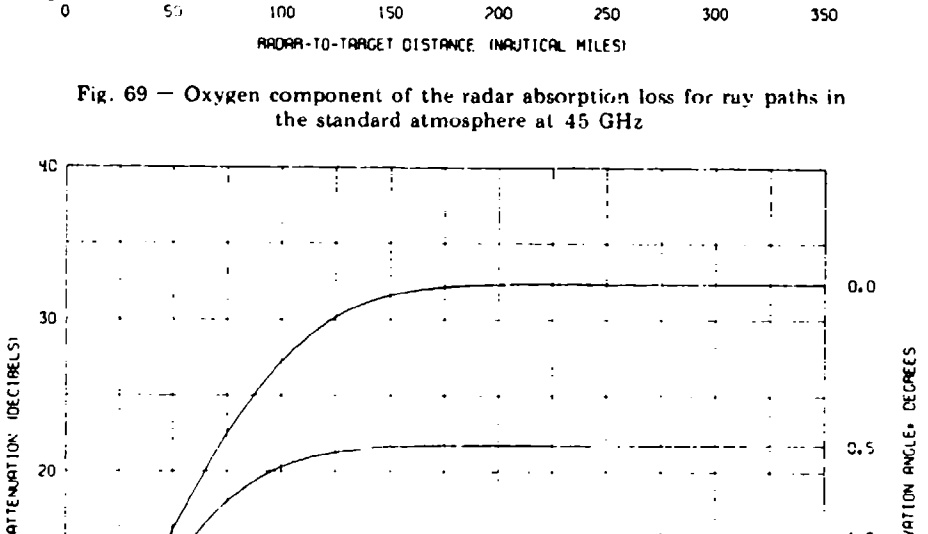


Fig. 70 — Water-vapor component of the radar absorption loss for ray paths in the standard atmosphere at 45 GHz

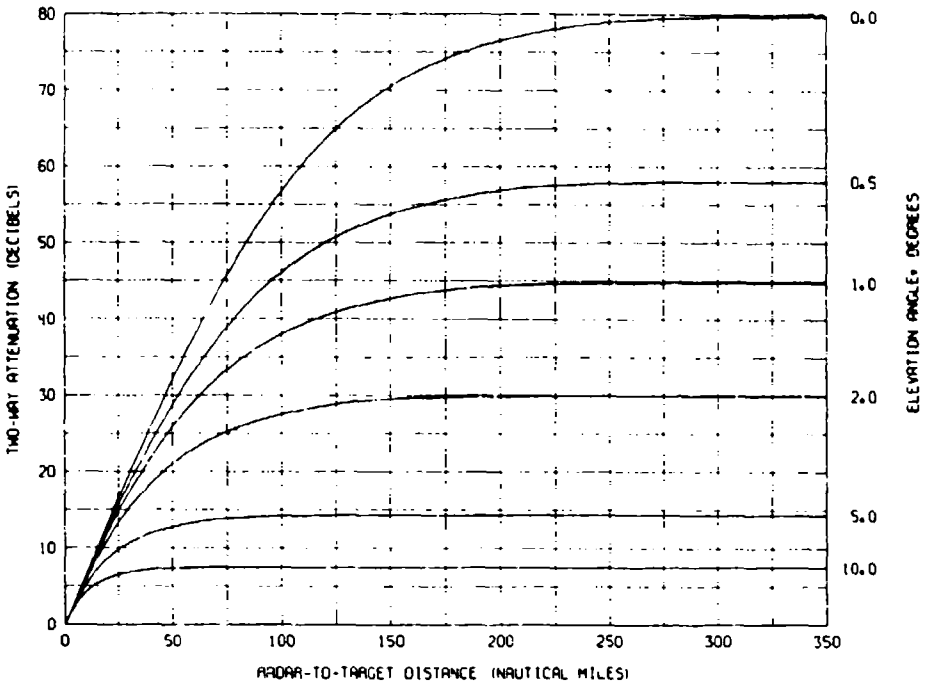


Fig. 71 — Total radar absorption loss for ray paths in the standard atmosphere at 45 GHz

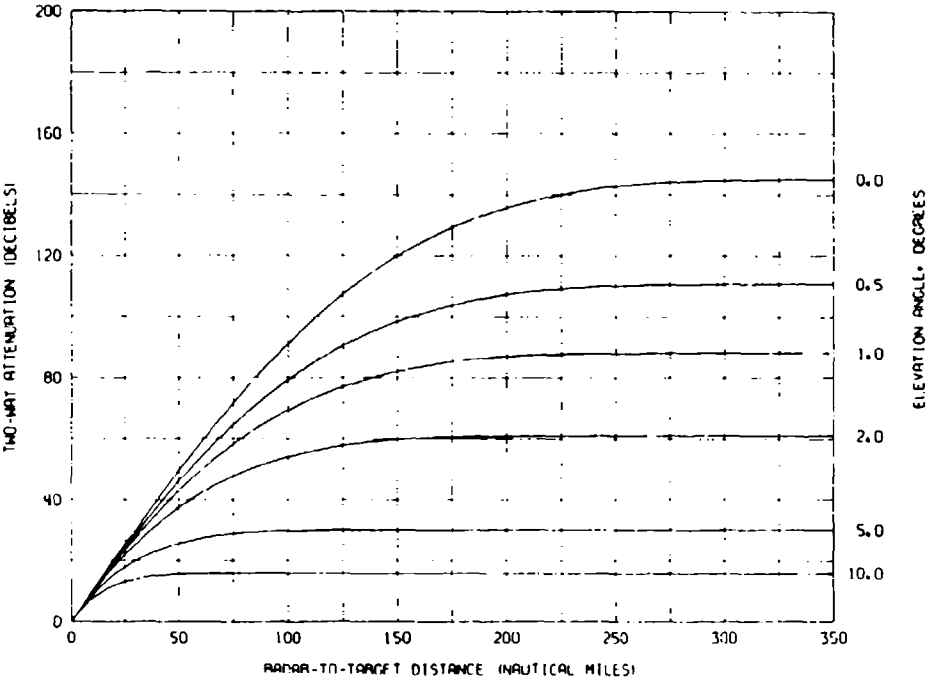


Fig. 72 — Oxygen component of the radar absorption loss for ray paths in the standard atmosphere at 50 GHz

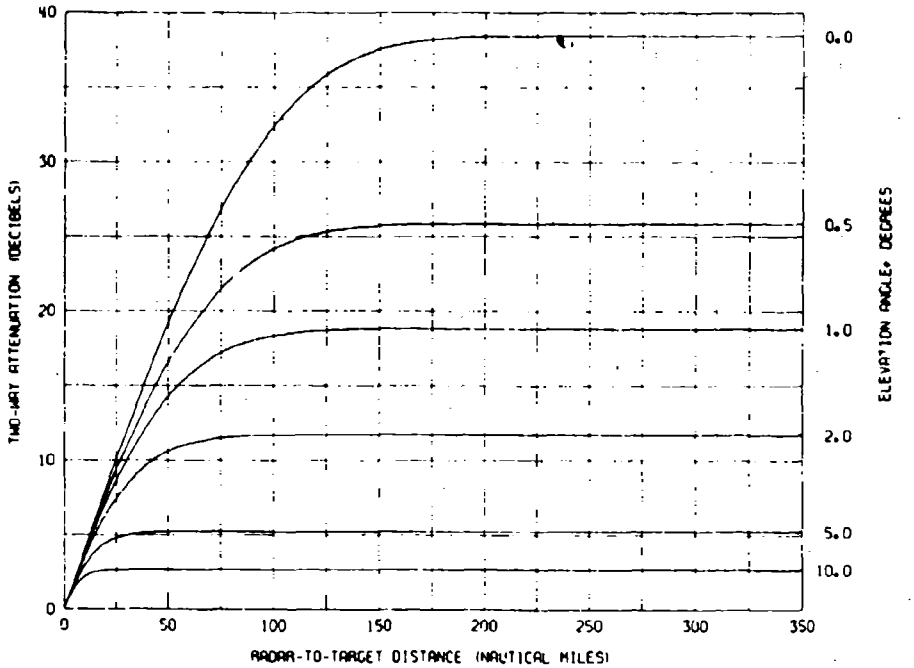


Fig. 73 — Water-vapor component of the radar absorption loss for ray paths in the standard atmosphere at 50 GHz

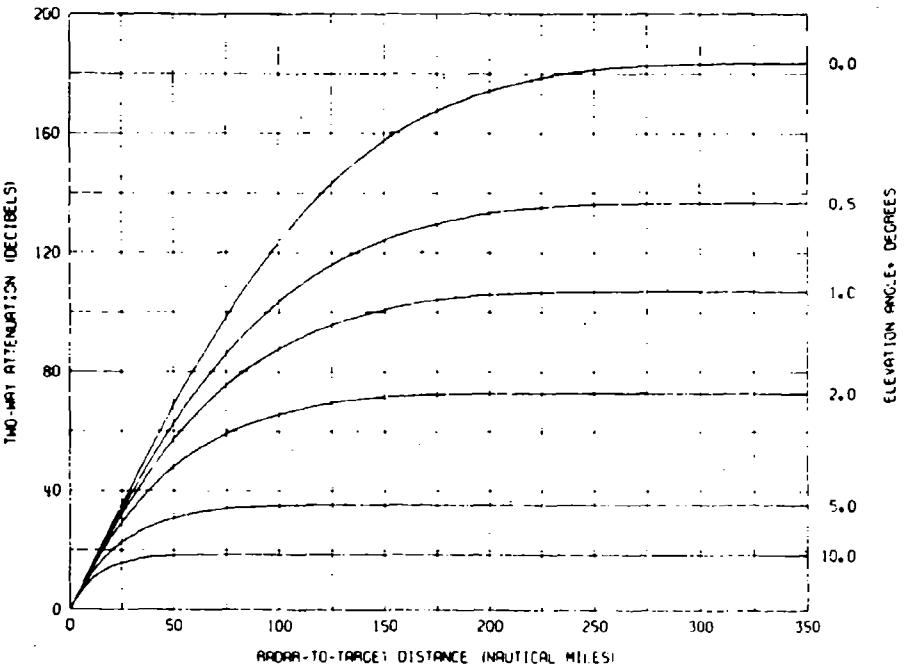


Fig. 74 — Total radar absorption loss for ray paths in the standard atmosphere at 50 GHz

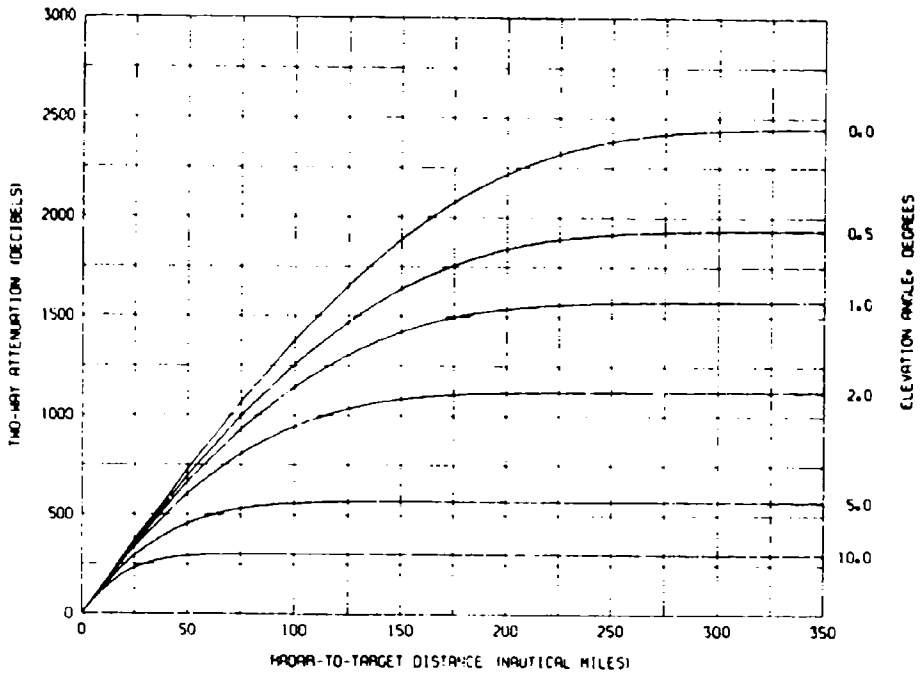


Fig. 75 — Oxygen component of the radar absorption loss for ray paths in the standard atmosphere at 55 GHz

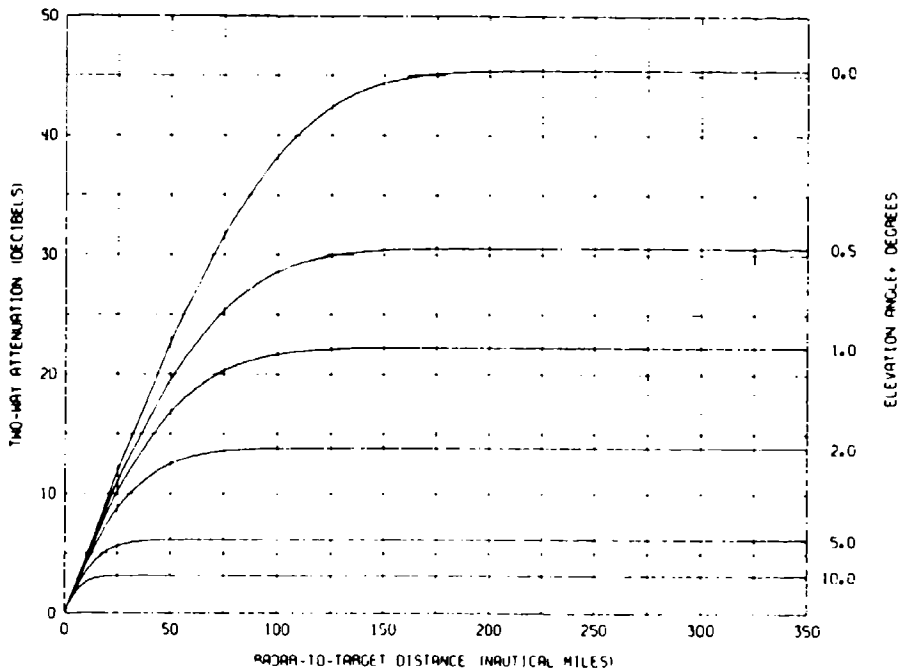


Fig. 6 — Water-vapor component of the radar absorption loss for ray paths in the standard atmosphere at 55 GHz

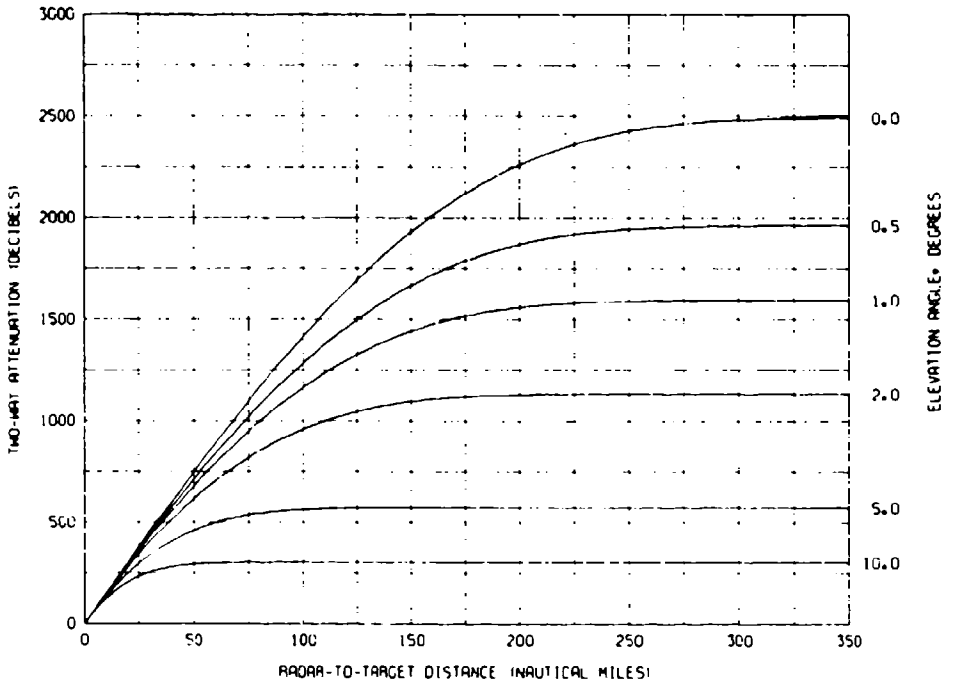


Fig. 77 — Total radar absorption loss for ray paths in the standard atmosphere at 55 GHz

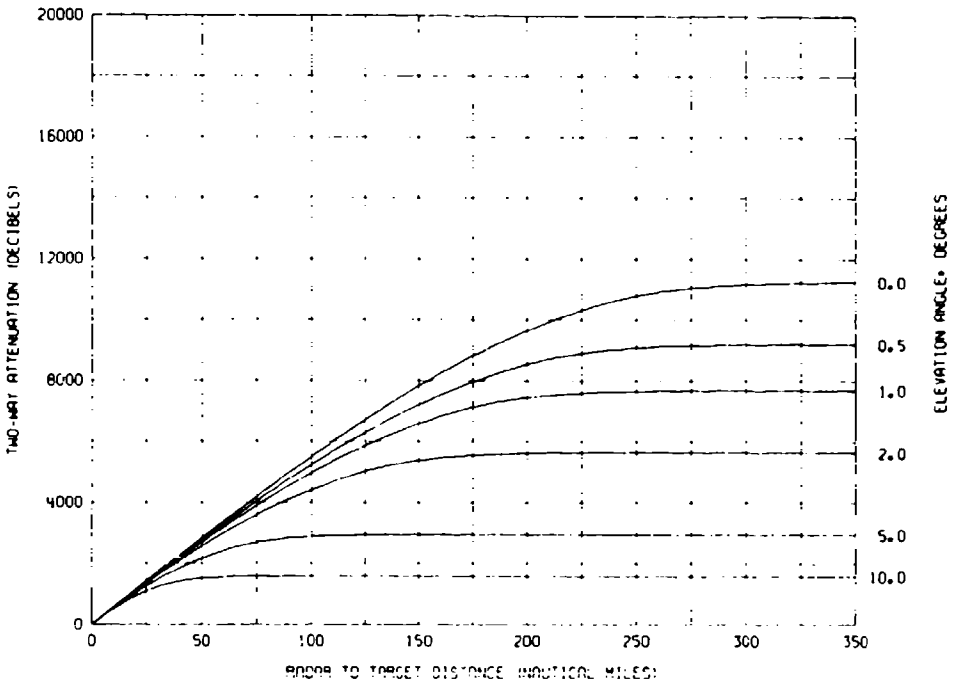


Fig. 78 — Oxygen component of the radar absorption loss for ray paths in the standard atmosphere at 60 GHz

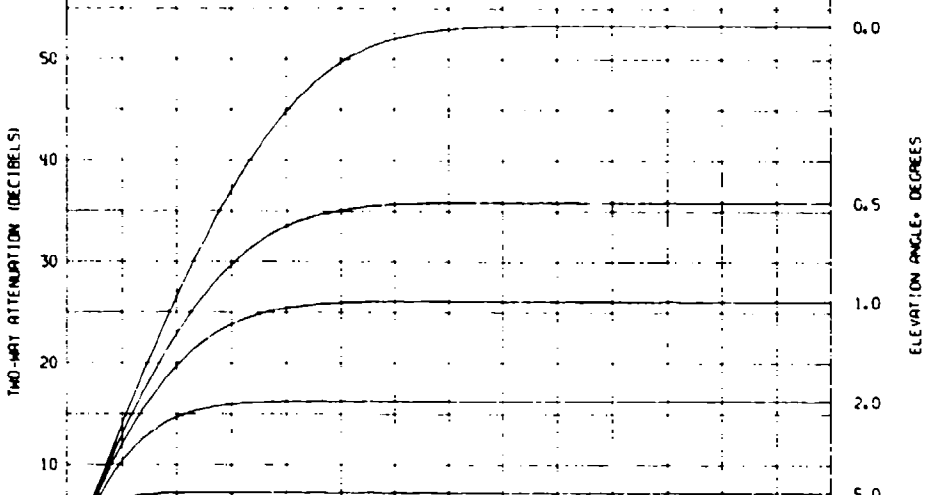


Fig. 79 — Water-vapor component of the radar absorption loss for ray paths in the standard atmosphere at 60 GHz

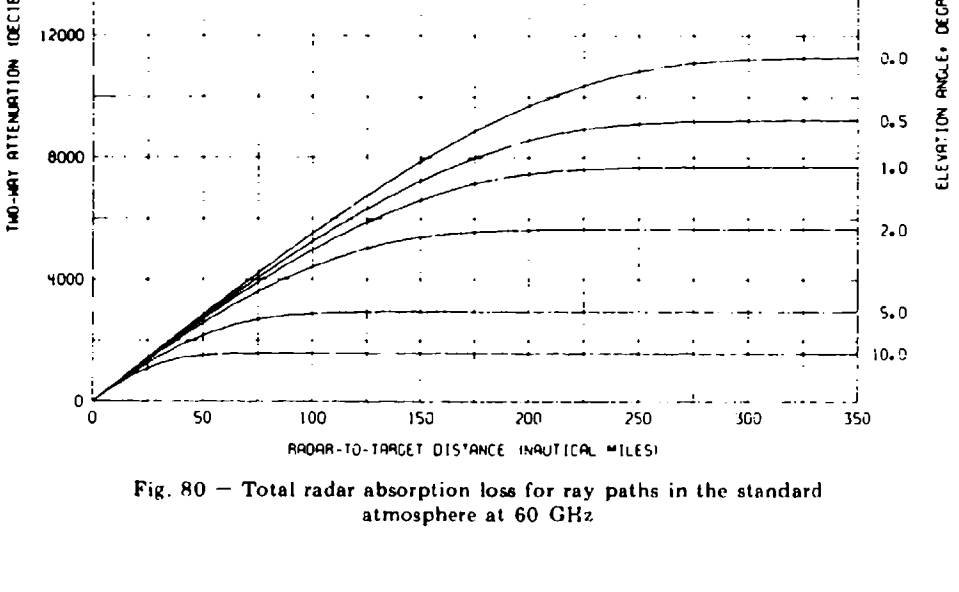


Fig. 80 — Total radar absorption loss for ray paths in the standard atmosphere at 60 GHz

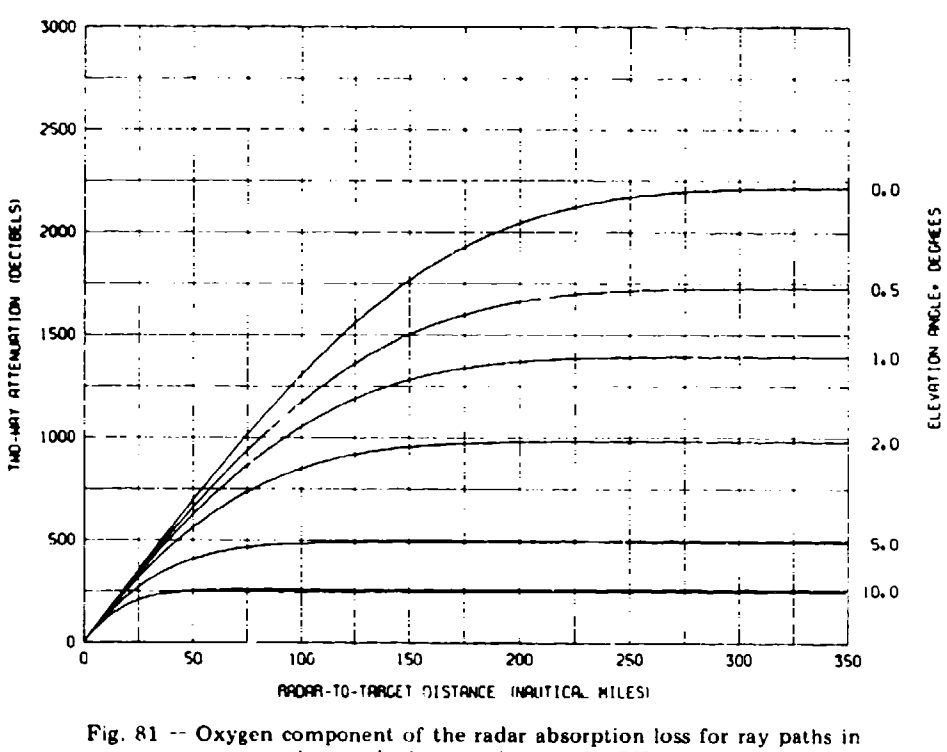


Fig. 81 -- Oxygen component of the radar absorption loss for ray paths in the standard atmosphere at 65 GHz

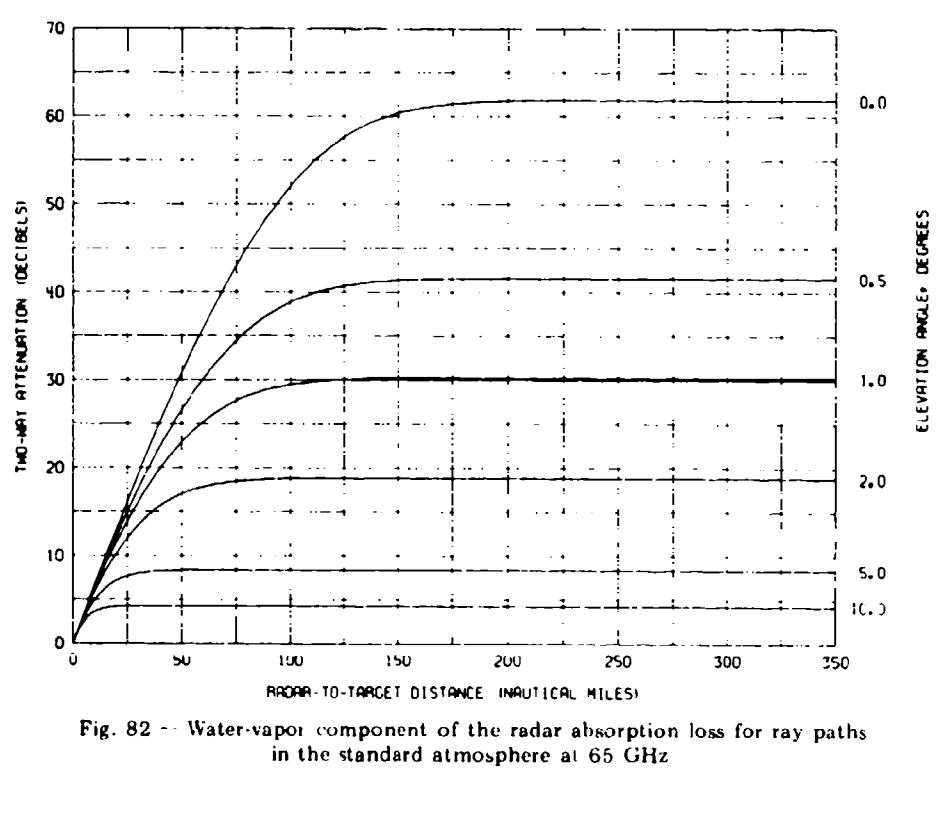


Fig. 82 -- Water-vapor component of the radar absorption loss for ray paths in the standard atmosphere at 65 GHz

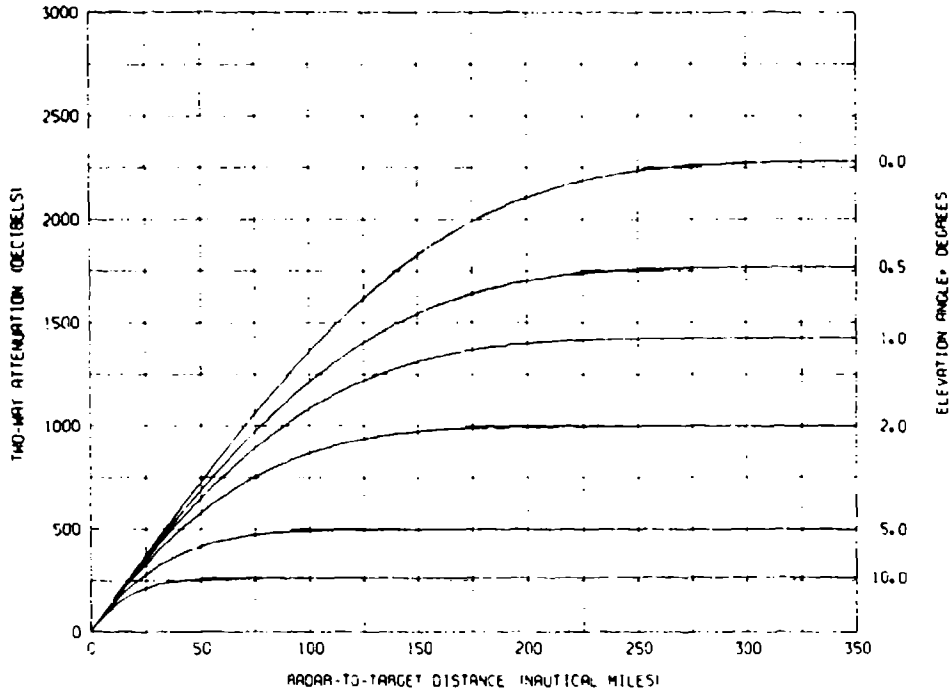


Fig. 83 — Total radar absorption loss for ray paths in the standard atmosphere at 65 GHz

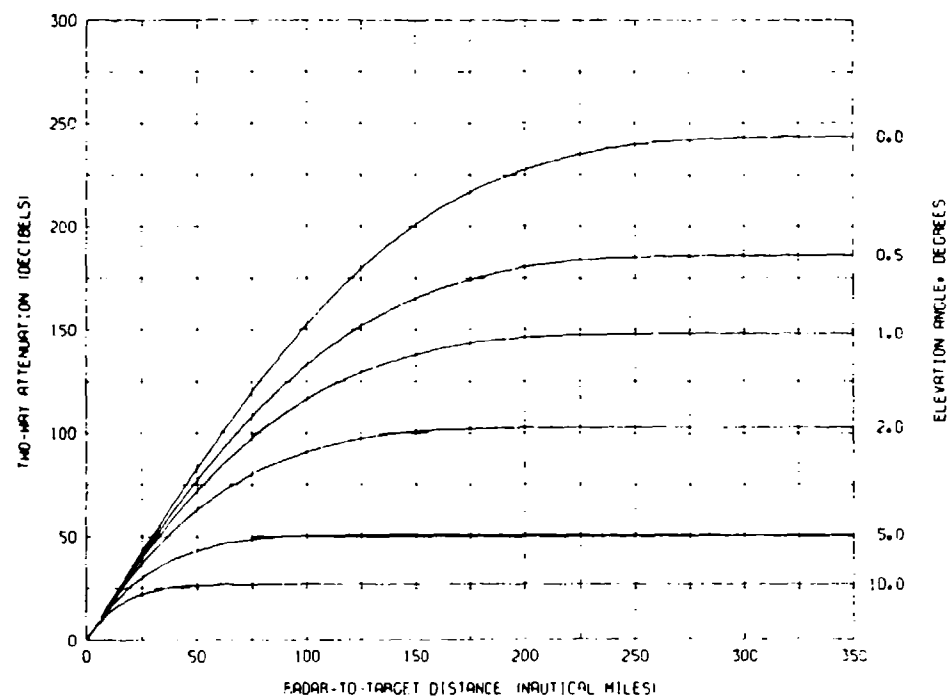


Fig. 84 — Oxygen component of the radar absorption loss for ray paths in the standard atmosphere at 70 GHz

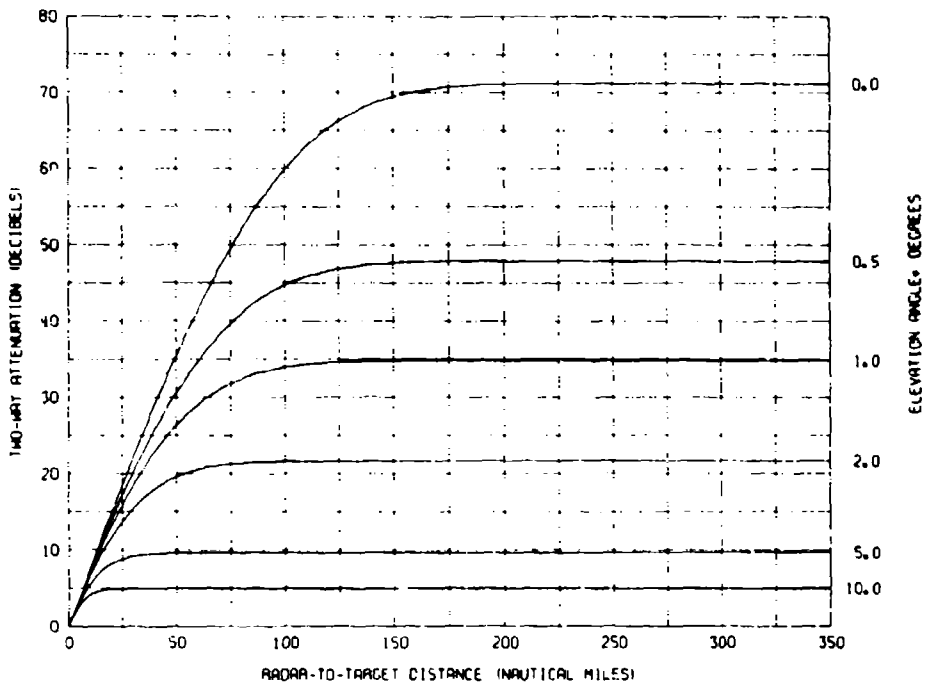


Fig. 85 — Water-vapor component of the radar absorption loss for ray paths in the standard atmosphere at 70 GHz

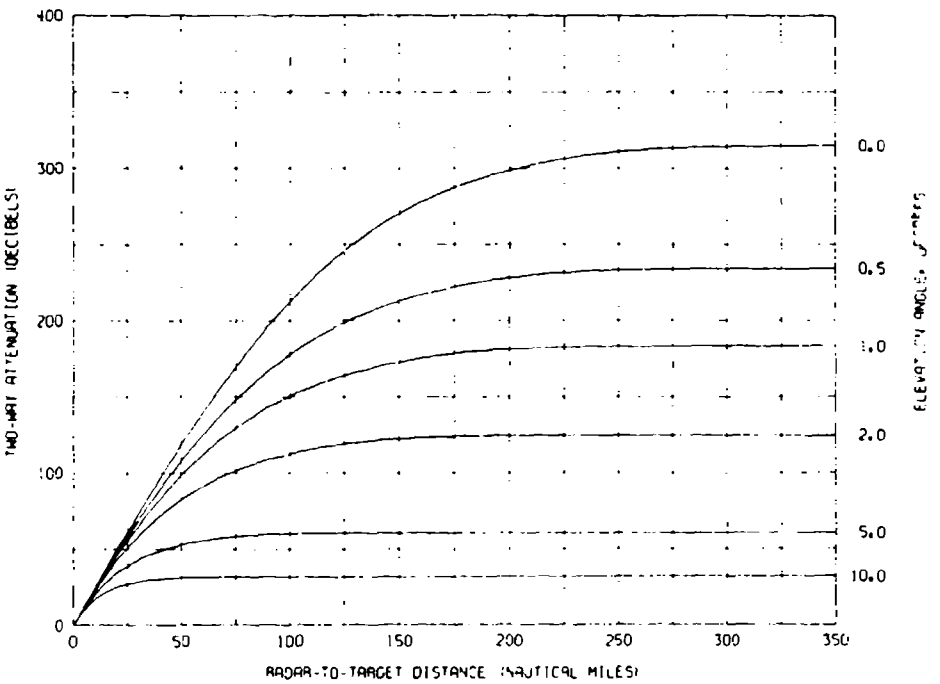


Fig. 86 — Total radar absorption loss for ray paths in the standard atmosphere at 70 GHz

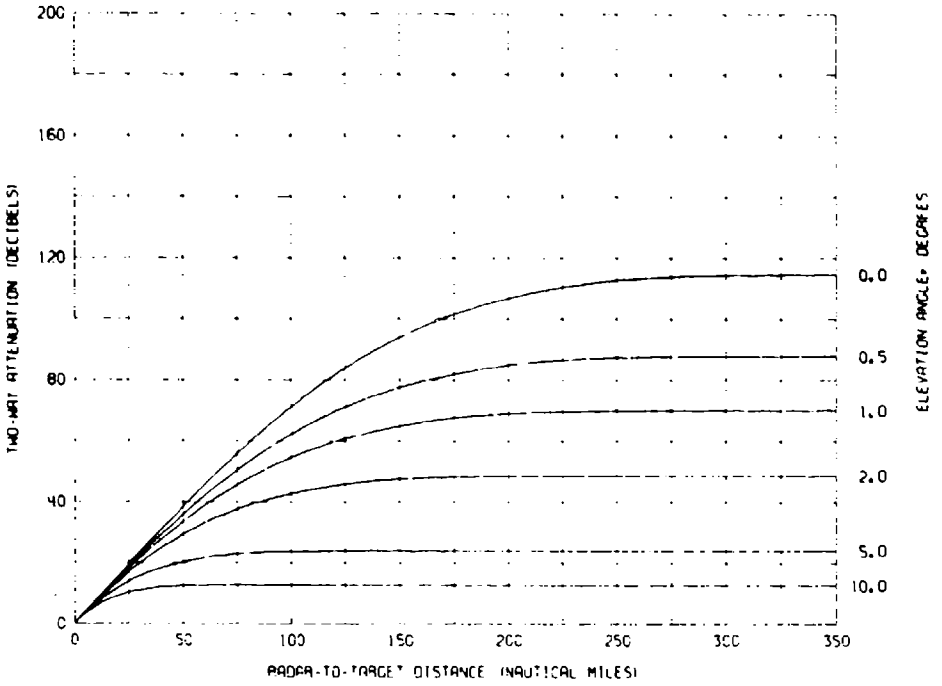


Fig. 87 — Oxygen component of the radar absorption loss for ray paths in the standard atmosphere at 75 GHz

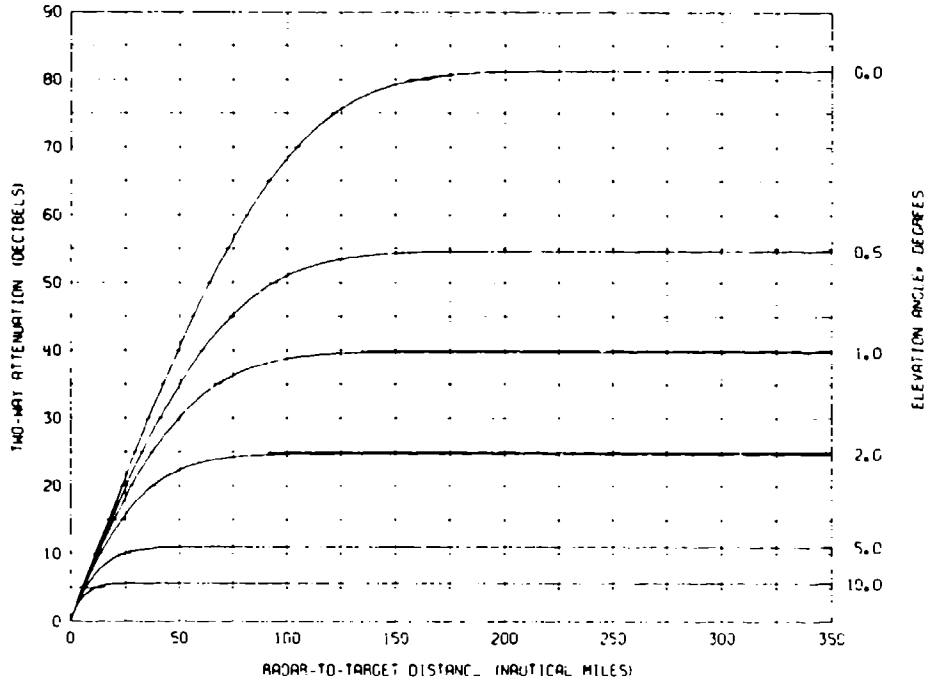


Fig. 88 — Water-vapor component of the radar absorption loss for ray paths in the standard atmosphere at 75 GHz

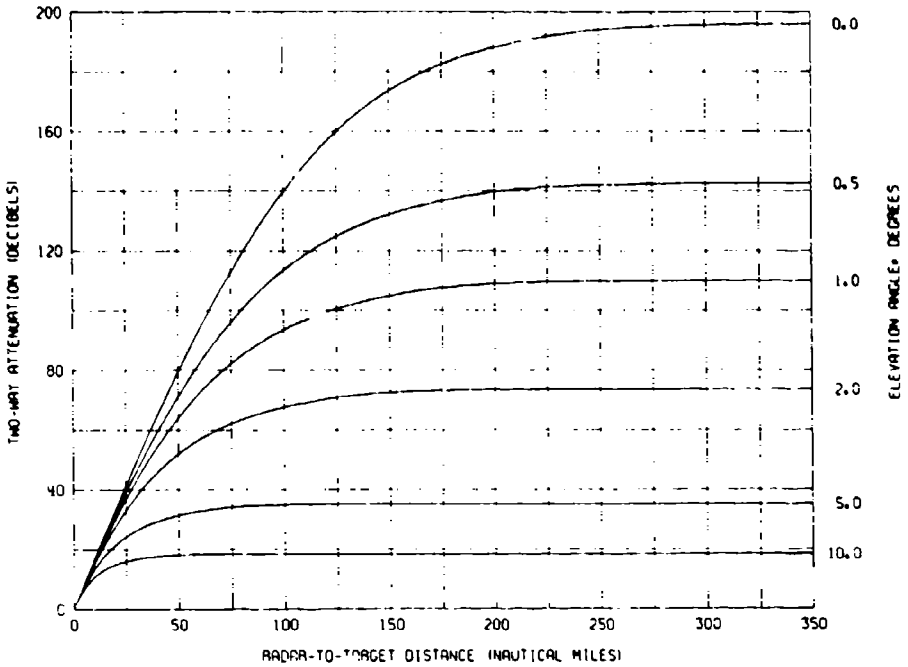


Fig. 89 — Total radar absorption loss for ray paths in the standard atmosphere at 75 GHz

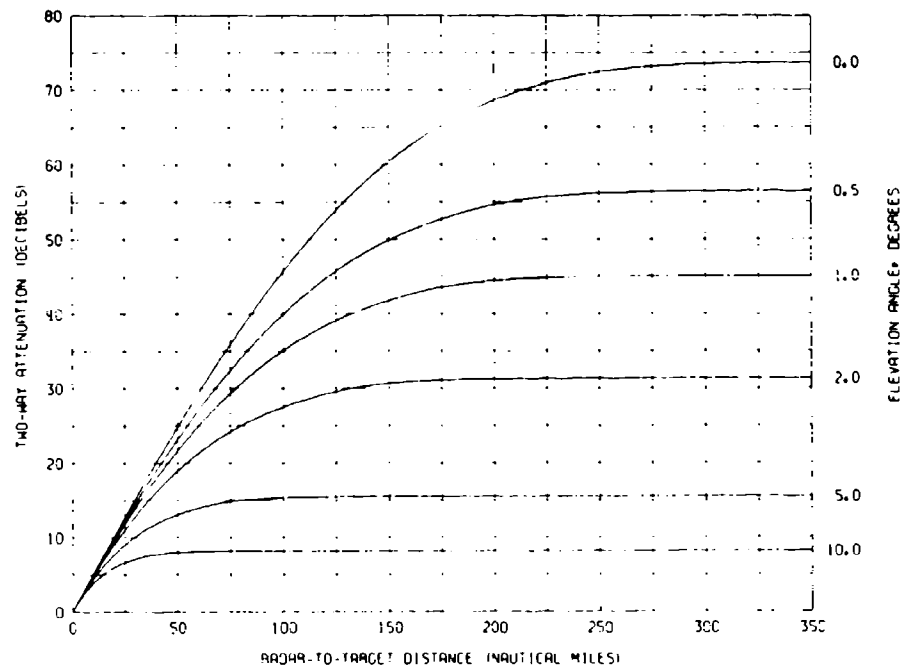


Fig. 90 — Oxygen component of the radar absorption loss for ray paths in the standard atmosphere at 80 GHz

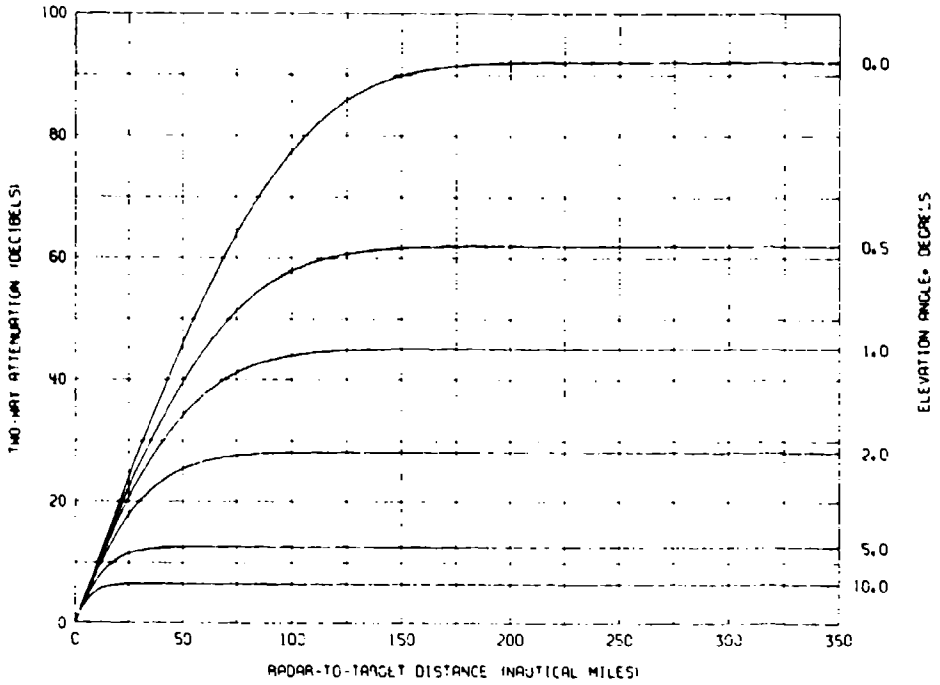


Fig. 91 — Water-vapor component of the radar absorption loss for ray paths in the standard atmosphere at 80 GHz

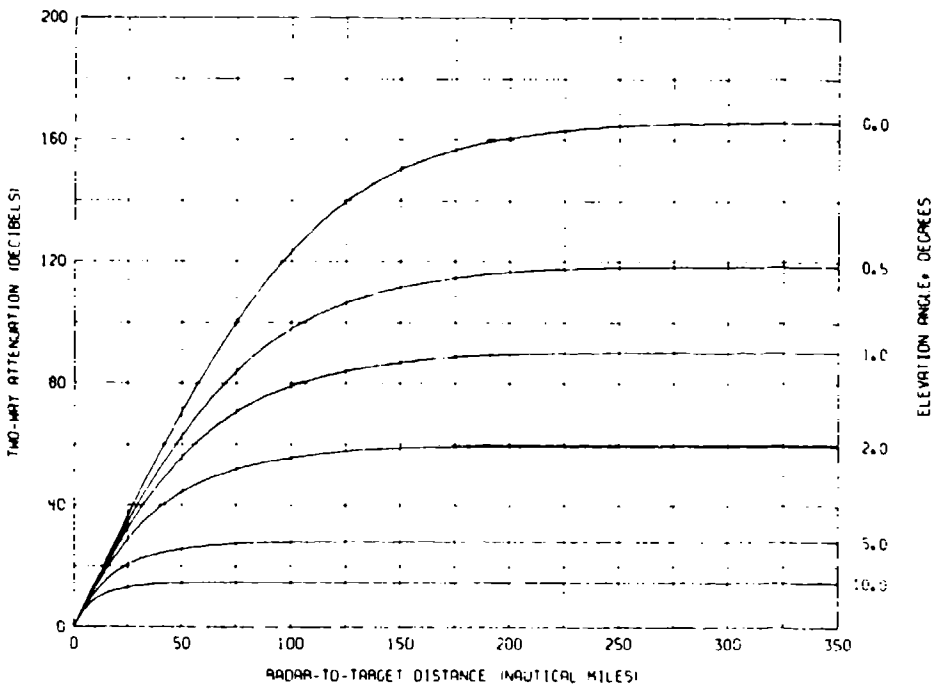


Fig. 92 — Total radar absorption loss for ray paths in the standard atmosphere at 80 GHz

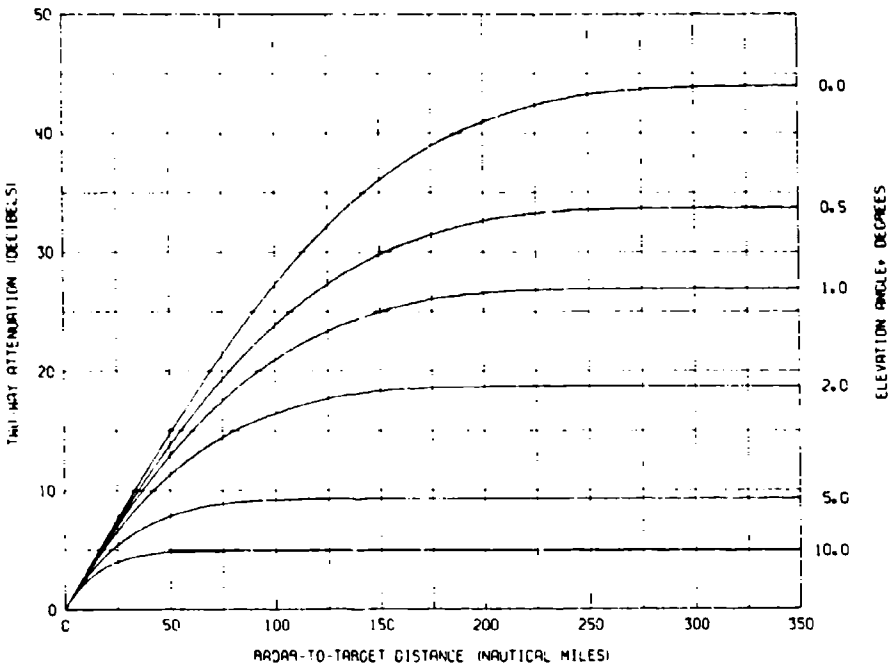


Fig. 93 — Oxygen component of the radar absorption loss for ray paths in the standard atmosphere at 90 GHz

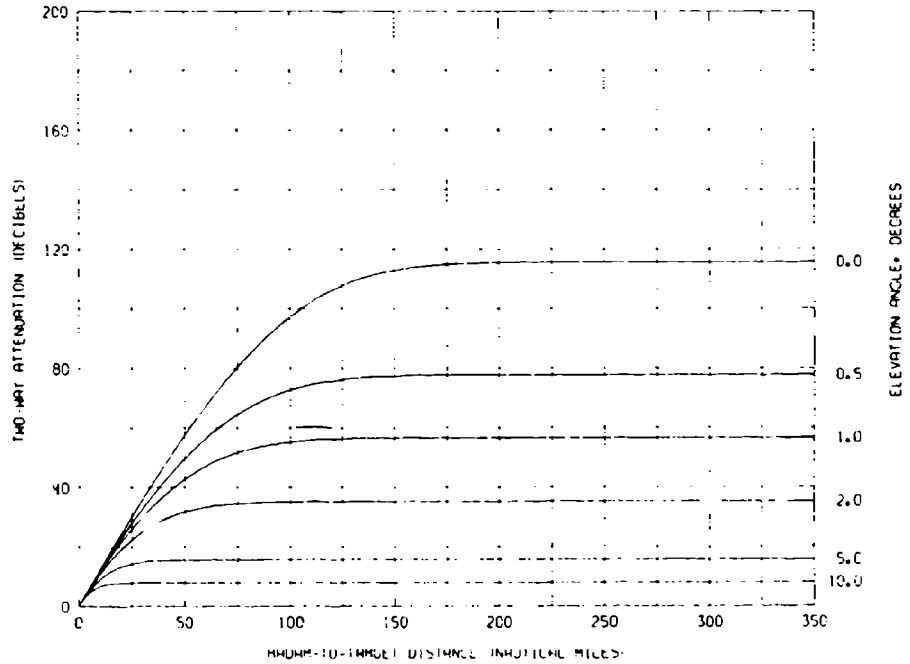


Fig. 94 — Water-vapor component of the radar absorption loss for ray paths in the standard atmosphere at 90 GHz

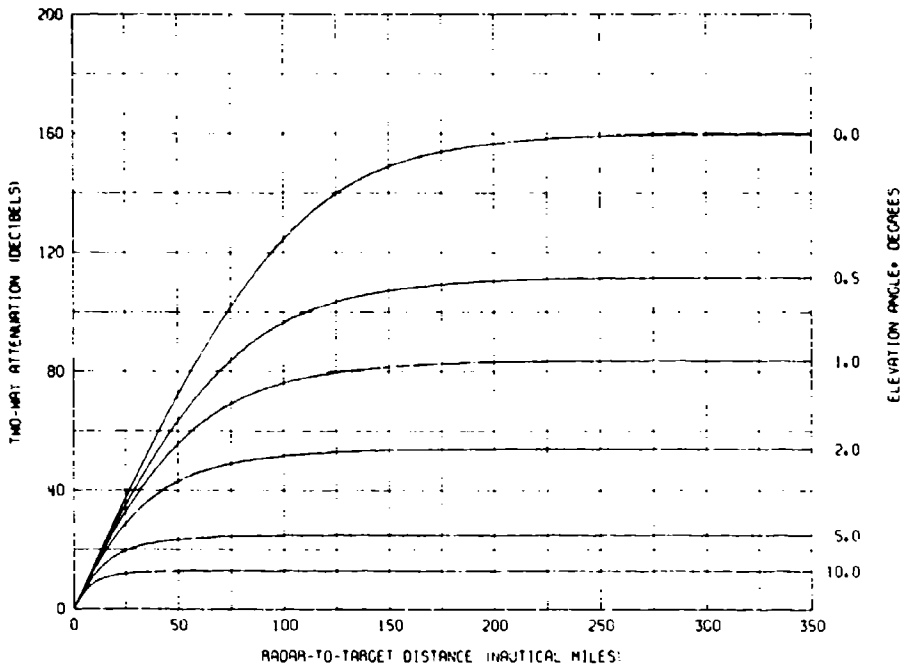


Fig. 95 — Total radar absorption loss for ray paths in the standard atmosphere at 90 GHz

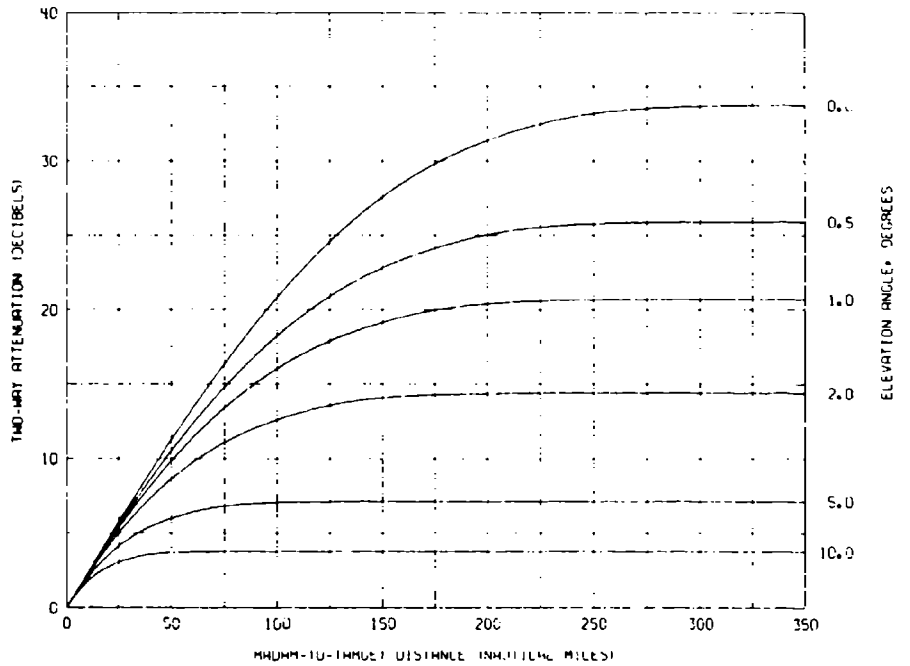


Fig. 96 — Oxygen component of the radar absorption loss for ray paths in the standard atmosphere at 100 GHz

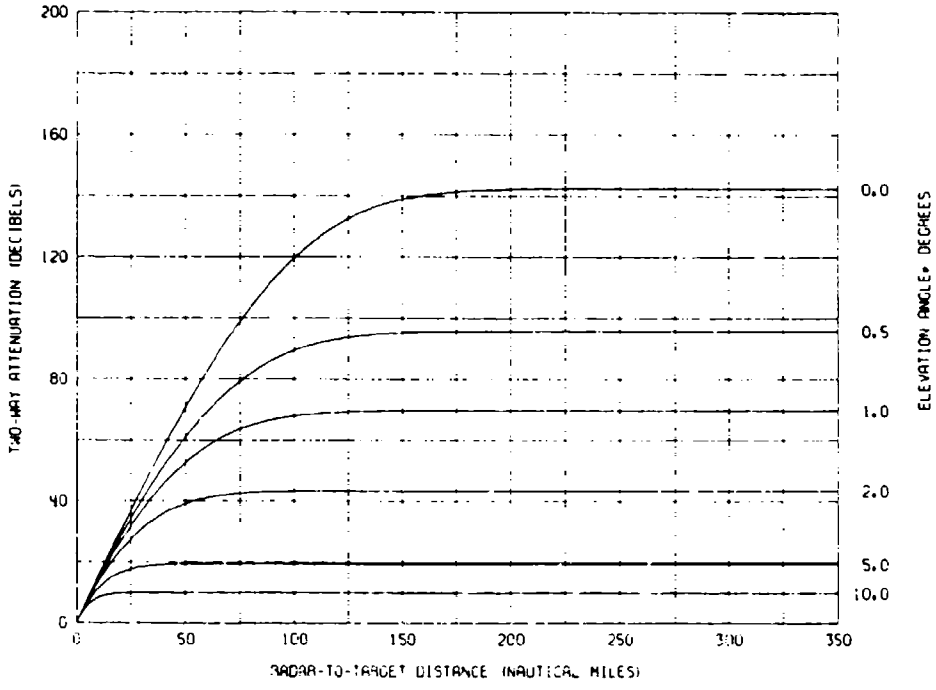


Fig. 97 — Water-vapor component of the radar absorption loss for ray paths in the standard atmosphere at 100 GHz

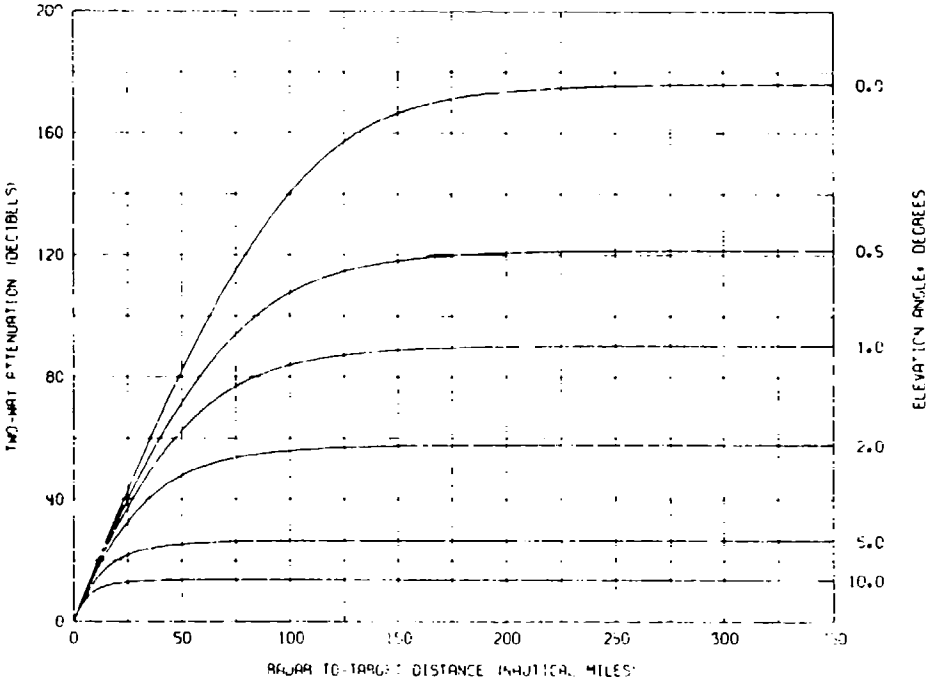


Fig. 98 — Total radar absorption loss for ray paths in the standard atmosphere at 100 GHz

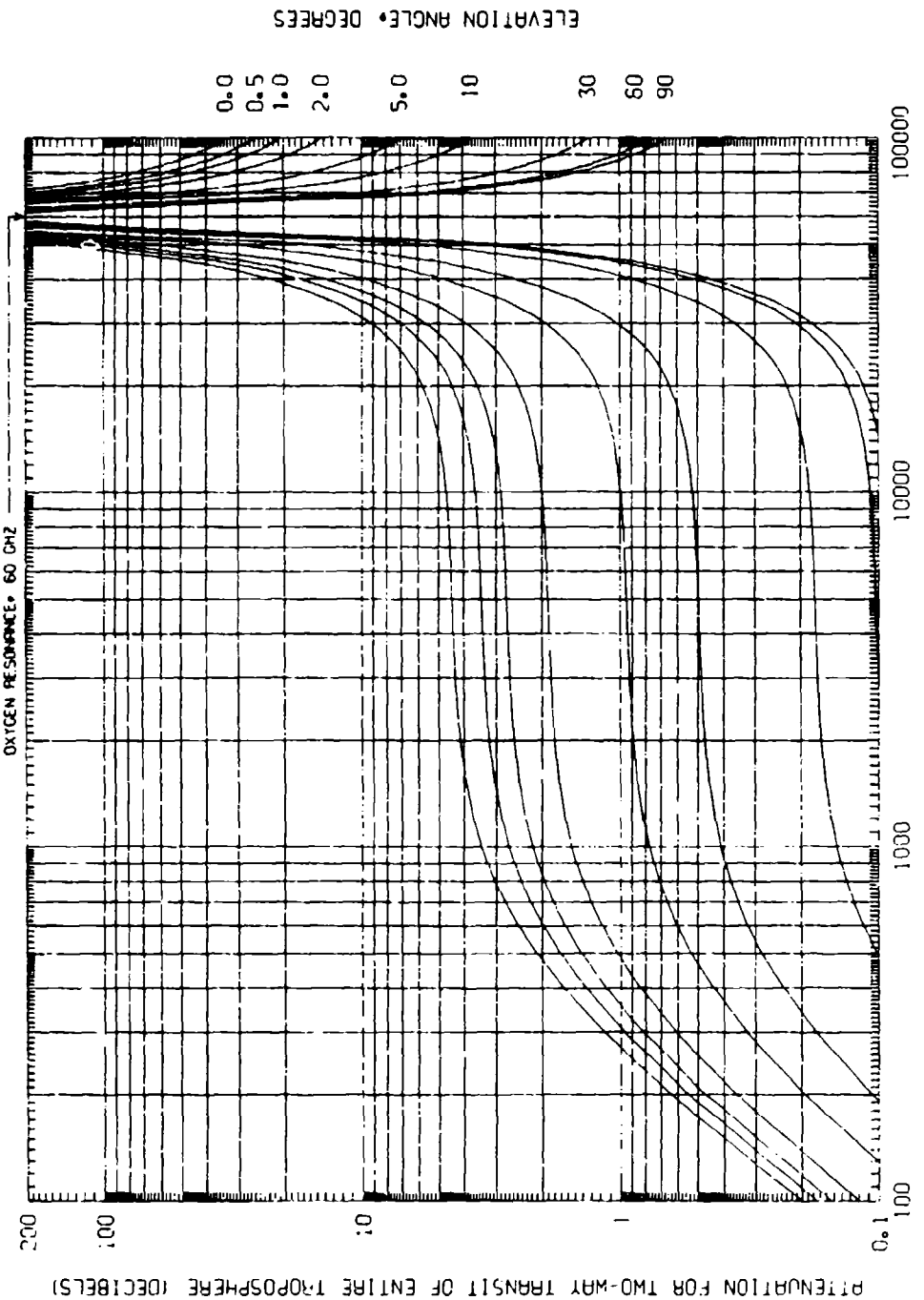


Fig. 99 — Oxygen component of the earth-based-radar absorption loss for a target outside the troposphere (above 100,000 feet in altitude) for several elevation angles and the standard atmosphere

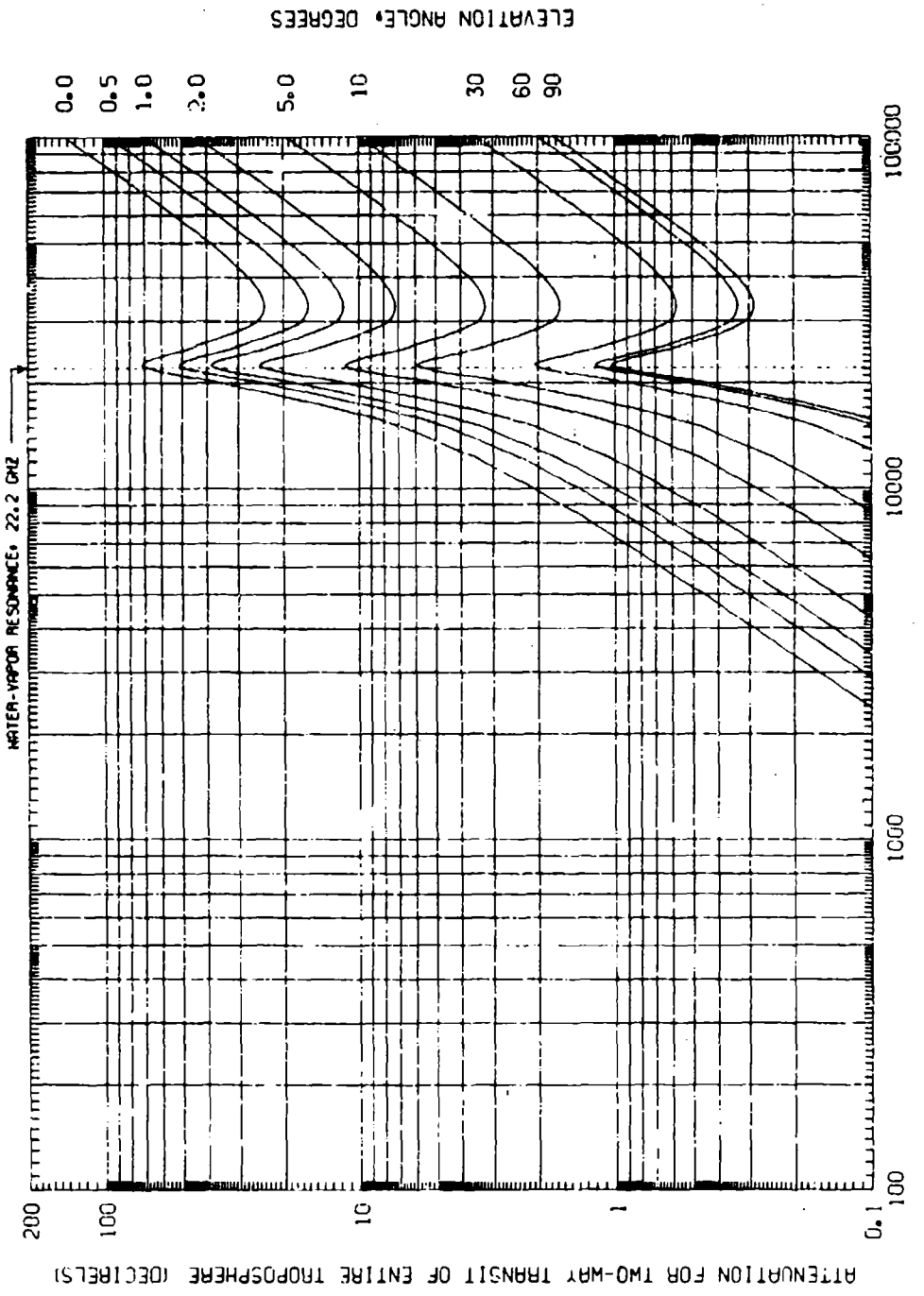


Fig. 100 — Water-vapor component of the earth-based-radar absorption loss for a target outside the troposphere (above 100,000 feet in altitude) for several elevation angles and the standard atmosphere

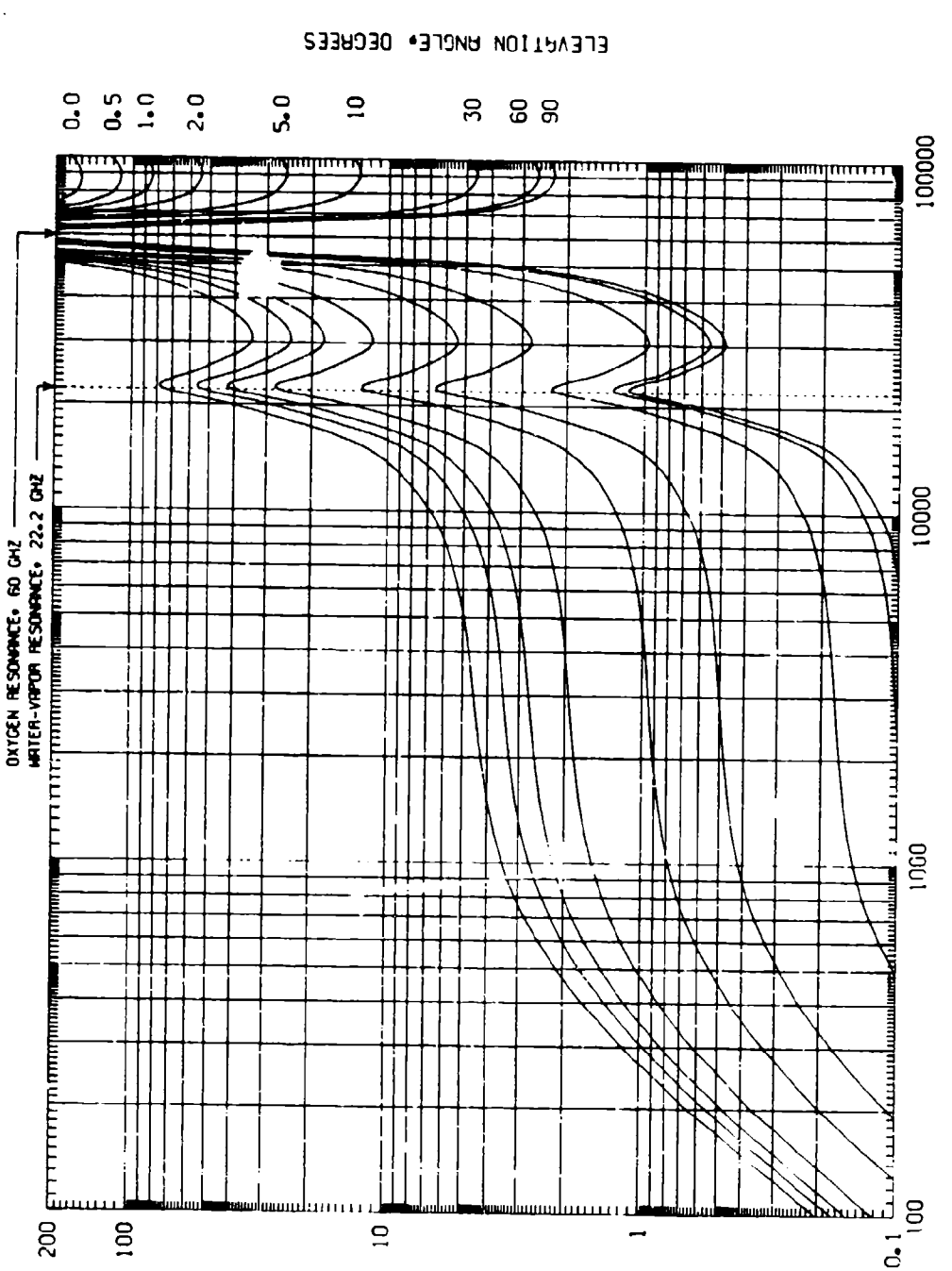


Fig. 101 – Total earth-based-radar absorption loss for a target outside the troposphere (above 100,000 feet in altitude) for several elevation angles and the standard atmosphere

where dR is measured along the ray path ($T_n$, in degrees Kelvin, is a function of the ray elevation angle), $T_t$ is the thermal temperature of the troposphere, defined by the standard atmosphere of Subroutine ALPHA, and $\alpha$ is the absorption coefficient. (The factors 0.2303 are needed in this equation because $\alpha$ is here assumed to be in decibels per unit distance.)

The previously described modification of Simpson's rule cannot be used for this integration, because it is an integration with respect to range (R) rather than height (h). The height intervals are (within each of the four height regions defined in Subroutine ALPHA) uniformly spaced, as required by Simpson's rule; but the corresponding range intervals are not uniformly spaced, because of the nonlinear relationship between range and height in the space above a spherical earth and in a refracting atmosphere (for all elevation angles except 90 degrees). Therefore another special modification of Simpson's rule was devised to fit this situation; it is Fortran-coded in Subroutine INTGRT.

When the absorption loss is great, as it is at the oxygen resonance frequency for example, most of the tropospheric noise seen by a ground-based antenna comes from the lowest layer of the atmosphere; that is, the integrand of Eq. (31) is large at R = 0 and decreases steeply beyond R = 0, going quickly to virtually zero. Because of the extreme departure of the integrand from a parabolic curve in this circumstance, the Simpson's rule integration is not accurate. An analytic approximation to the integral in this region is numerically more accurate than numerical integration of the "exact" expression. Therefore such an approximation is used for the integration over the first two height (range) intervals, corresponding to the first 200 feet of atmospheric altitude. The approximation is derived by assuming that both $\alpha$ and $T_t$, Eq. (31), are constants within those intervals. If $R_1$ and $R_2$ are the ranges at h = 100 and h = 200 feet, then Eq. (31) for these intervals may be written

$$\Delta T_n = \bar{T}_{t_2} \int_0^{R_1} k_1 e^{-k_1 R}\, dR + \bar{T}_{t_2} \int_{R_1}^{R_2} k_2 e^{-k_2 R}\, dR, \tag{32}$$

where $k_1 = 0.2303\bar{\alpha}_1$, $k_2 = 0.2303\bar{\alpha}_2$, $\bar{T}_{t_1}$ is the average tropospheric temperature in the range interval 0 to $R_1$, $\bar{T}_{t_2}$ is the average temperature in the interval $R_1$ to $R_2$, and $\bar{\alpha}_1$ and $\bar{\alpha}_2$ are the corresponding average absorption coefficients. Integrating this expression gives

$$\Delta T_n = \bar{T}_{t_1}(1 - e^{-k_1 R_1}) + \bar{T}_{t_2}\,(e^{-k_2 R_1} - e^{-k_2 R_2}). \tag{33}$$

This is the approximation employed in Subroutine ATLØSS for the first two range intervals. (The approximation is used whether the attenuation is large or not, because it is equally accurate when the attenuation is not large.)

The noise temperature is calculated in Subroutine ATLØSS, since it is efficient to calculate it concomitantly with the absorption. The result is reported as the output parameter ATMP. A plot of the resulting values for several elevation angles in the frequency range 100 MHz to 100 GHz is given in Fig. 102. This quantity is not computed and plotted separately for the oxygen and water-vapor contributions, because they are not linearly additive as are the absorption values.

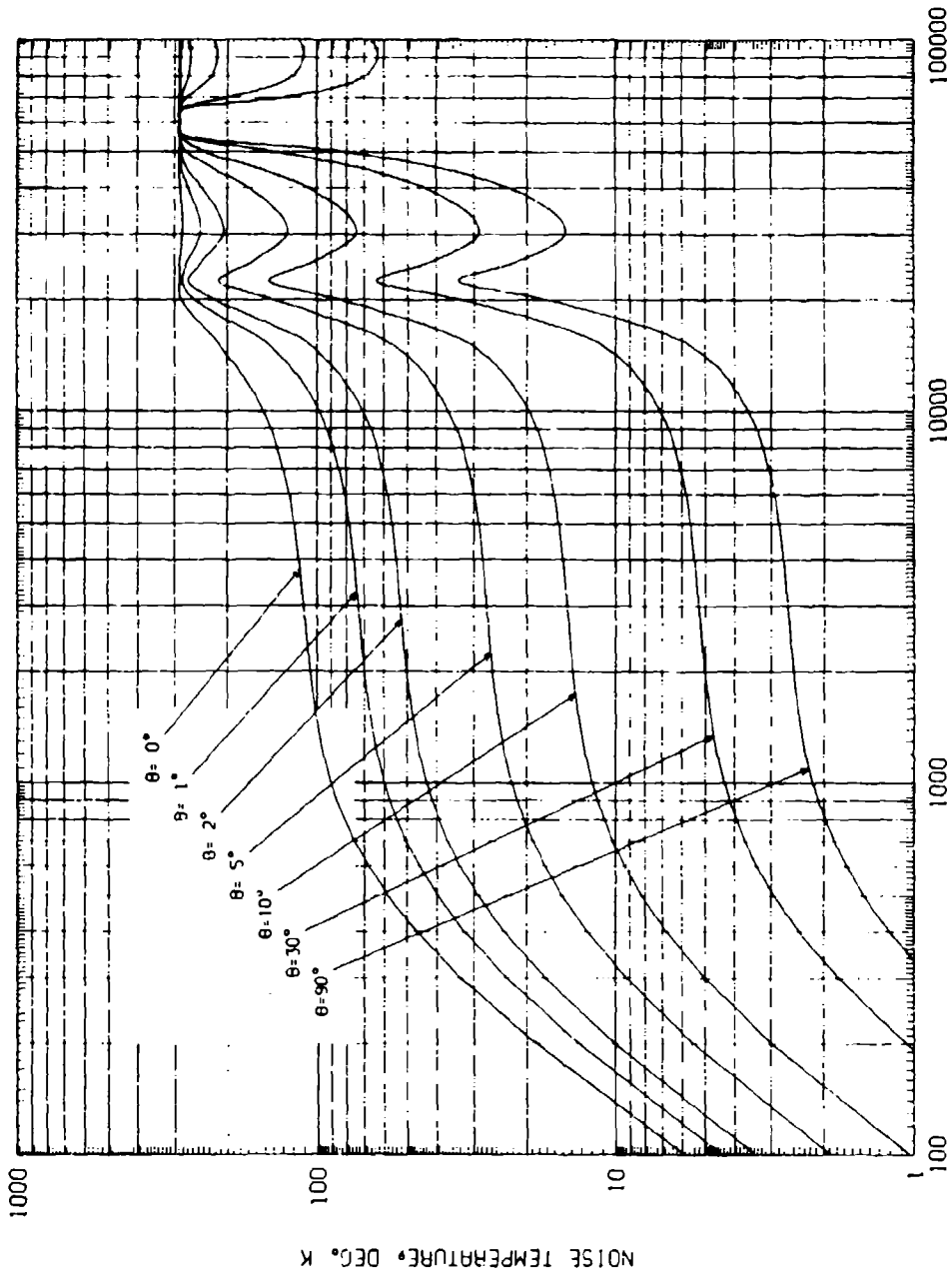


Fig. 102 — Tropospheric noise temperature computed for the standard atmosphere at several elevation angles

## COMPUTER ROUTINES

The Fortran subroutines ATLØSS, ALPHA, DDH, and INTGRT, which have been discussed in the preceding sections of this report, are listed on the following pages. Their calling sequences, pertinent CØMMØN blocks, and definitions of the parameters are as follows:

SUBRØUTINE ATLØSS (FMHZ, ELEV, ATMP)

CØMMØN/RGA/RG(75), ATTN(3,75)

FMHZ — radio frequency, megahertz (input)

ELEV — initial ray elevation angle, degrees (input)

ATMP — tropospheric noise temperature, degrees Kelvin (output)

RG — 75 monotonically increasing values of range, nautical miles, along the ray path from h = 0 to h = 100,000 ft (output)

ATTN — 75 corresponding decibel radar attenuation values (output) for oxygen (1), water vapor (2), and oxygen plus water vapor (3)

SUBRØUTINE ALPHA (FMHZ)

CØMMØN/PTR/PP(75), TT(75), RR(75), ALPH(3,75)

CØMMØN/H2Ø/RHØFAC

FMHZ — frequency, megahertz (input)

PP, TT, RR — standard atmosphere values, specified in DATA statements (available as output via the CØMMØN block if desired)

RHØFAC — A numerical factor by which the water-vapor-density values of the standard atmosphere are multiplied. If RHØFAC is not set to some other value by the user, the value RHØFAC = 1, set by a DATA statement, will apply.

ALPH(I,J) — the 3-by-75 output array of absorption coefficients. The I subscripts have the meanings I = 1, oxygen; I = 2, water vapor; I = 3, oxygen plus water vapor. The subscripts J = 1 through 75 correspond to the 75 altitudes to which the RG values of Subroutine ATLØSS also correspond.

SUBRØUTINE DDH(H)

CØMMØN/RRG/REF0, RAD, GRAD, U

CØMMØN/DRS/DSDH3, DRDH3, AN

H — altitude, feet (input)

REFO, RAD, GRAD, U — refractive-index profile parameters transmitted from ATLØSS

DSDH3, DRDH3 — ds/dh and dR/dh corresponding to H (output)

AN — refractive index n(h) at H (output)

SUBRØUTINE INTGRT (H1, H2, Y1, Y2, Y3, AREA)

If X1, X2, and X3 are successive points on the x axis of a cartesian coordinate system and Y1, Y2 and Y3 are the corresponding y values, then

H1 = X2 − X1 and H2 = X3 − X2. AREA (output parameter) is the value of the integral:

$$\int_{X1}^{X3} y(x)\,dx, \tag{34}$$

where y(x) is the second-degree polynomial that passes through the points Y1, Y2, and Y3. It is not necessary that H1 = H2.

The subroutine listings follow. (Slightly different but essentially the same subroutines are used in a computer program that calculates the maximum range of a radar; this program is described Ref. 1.) The lengths of these subroutines (number of memory locations required) are as follows:

| Subroutine Name | Octal Length | Decimal Length |
|---|---|---|
| ATLØSS | 756 | 494 |
| ALPHA | 520 | 336 |
| DDH | 211 | 137 |
| INTGRT | 112 | 74 |
| Totals | 2021 | 1041 |

06/23/72

```
      SUBROUTINE ATLOSS(FMHZ,ELEV,ATMP)
      COMMON /PTR/ PP(75), TT(75), HR(75),ALPH(3,75)
      COMMON/RGA/ RG(75),ATTN(3,75)
      DIMENSION I66(4), DELH(4)
      COMMON /RHG/REFQ,RAD,GRAD,J
      COMMON/DRS/ DSDH3,DRDH3,AN
      DATA(RG(1)=0.),(ATTN(1,1)=0.),(ATTN(2,1)=0.),(ATTN(3,1)=0.)
      DATA (REFQ=,000313),(RAD=20998959.13),(GRAD=,00004385)
      DATA(FLAST=0.),(ELAST=100.),(CONST=.2002585)
      DATA (I66=10,14,10,3),(DELH=100.,1000.,2000.,5000.)
      ATT1(YY)=FAC2*(1.25*Y1+2.*Y2-.25*YY)
      ATT2(YY)=FAC2*(-.25*Y1+2.*Y2+1.25*YY)
      RG1(DR)=FAC1*(1.25*DRDH1+2.*DRDH2-.25*DR)
      RG2(DR)=FAC1*(-.25*DRDH1+2.*DRDH2+1.25*DR)
      IF (FMHZ.EQ.FLAST.AND.ELEV.EQ.ELAST) RETURN
      ELAST = ELEV
      IS1G=1
      THETA=ELEV/57.295795
      SN=SIN(THETA)
      CS=COS(THETA)
      SS=SN*SN
      RP1=1.+REFQ
      U=(RP1*SN)**2 - 2.*REFQ - REFQ*REFQ
      IF (FMHZ.EQ. FLAST) GO TO 55
      CALL ALPHA(FMHZ)
      FLAST=FMHZ
    5 H=0.
      RNG=0.
      ATTEN1=ATTEN2=0.
      K=-1
      HMIN =0.
      IF (ELEV.EQ.0.) HMIN=1.E-9
      CALL DDH(HMIN)
      DRDH1=DRDH3
      DSDH1=DSDH3
      AN1=AN
      TH1=ALPH(3,1)*TT(1)
      TEMP = 0.
      Y1=ALPH(1,1)*DSDH1
      Y11=Y1
      Y12=ALPH(2,1)*DSDH1
      DO 60 J=1,4
      FAC1=DELH(J)/(3.*6078.1155)
      FAC2=2.*FAC1
      IMAX= I66(J)
      DO 61 I=1,IMAX
      K=K+2
      H=H+DELH(J)
      H1=H
      CALL DDH(H)
      DRDH2=DRDH3
      DSDH2=DSDH3
      AN2=AN
      H=H+DELH(J)
      CALL DDH(H)
      Y2=ALPH(1,K+1)*DSDH2
```

06/23/72

```
      Y21=Y2
      Y22=ALPH(2,K+1)*DSDH2
      Y3=ALPH(1,K+2)*DSDH3
      Y32=ALPH(2,K+2)*DSDH3
      AN3=AN
      IF (ELEV .LT. 1. .AND. H .LT. 201.) 5, 6
    5 CC=CS*CS*(1./RAD-REF0*GRAD/RP1)
      CC1=1./(CC*60/6.1155)
      PR0D=2.*CC*H1
C     FOLLOWING IS APPROXIMATION REQUIRED NEAR THETA=0 AND H=0 FOR RANGE
C     CALCULATION,  RANGE IS CALCULATED THUS FOR H = 100 AND H= 200 WHEN
C     ELEVATION ANGLE IS LESS THAN 1 DEGREE.
      RNG=CC1*PR0D/(SQRTF(PR0D+SS)+SN)
      DS1=RNG
C     APPROXIMATE ATTENUATION IS RANGE (TWO-WAY) TIMES AVERAGE VALUE OF
C     ALPHA IN THE RANGE INTERVAL,
      ATTEN1=RNG*(ALPH(1,1) + ALPH(1,2))
      ATTEN2=RNG*(ALPH(2,1) + ALPH(2,2))
C     RADAR RANGE IS GEOMETRIC RANGE TIMES AVERAGE REFRACTIVE INDEX.
      RNG=RNG*(RP1 + 1. + REF0*EXP(-GRAD*H1)) * .5
      ISIG=2
      GO TO 7
    6 DS=RG1(DRDH3)
      RNG=RNG+DS
      DS1= DS/((AN1+AN2)*.5)
      ATTEN1=ATTEN1+ATT1(Y3)
      Y1=Y12
      Y2=Y22
      ATTEN2=ATTEN2 + ATT1(Y32)
    7 RG(K+1)=RNG
      ATTN(1,K+1)= ATTEN1
      ATTN(2,K+1)=ATTEN2
      ATTN(3,K+1)=ATTEN1 + ATTEN2
      GO TO (10,11) ISIG
   11 PR0D=2.*CC*H
      RNG=CC1*PR0D/(SQRTF(PR0D+SS)+SN)
      DS2=RNG-DS1
      ATTEN1=RNG*(ALPH(1,1) + ALPH(1,3))
      ATTEN2=RNG*(ALPH(2,1) + ALPH(2,3))
      RNG=RNG*(RP1 + 1. + REF0*EXP(-GRAD*H )) * .5
      ISIG=1
      GO TO 12
   10 DS=RG2(DRDH3)
      RNG=RNG+DS
      DS2=DS/((AN2+AN3)*.5)
      Y1=Y11
      Y2=Y21
      ATTEN1= ATTEN1 + ATT2(Y3)
      Y1=Y12
      Y2=Y22
      ATTEN2= ATTEN2 + ATT2(Y32)
   12 RG(K+2)=RNG
      ATTN(1,K+2)=ATTEN1
      ATTN(2,K+2)=ATTEN2
      ATTN(3,K+2)=ATTEN1 + ATTEN2
      ALOSS=10.**(-ATTN(3,K+2)*.05)
```

06/23/72

```
      TP3=ALPH(3,K+2)*TT(K+2)*ALOSS
      DS1 = (RG(K+1)-RG(K))/((AN1+AN2)*.5)
      DS2 = (RG(K+2)-RG(K+1))/((AN2+AN3)*.5)
      IF (K.EQ.1) 70,71
C     APPROXIMATION EMPLOYED IN PLACE OF FIRST INTEGRATION STEP.
C     TRIED TO GIVE VALID RESULTS IN HIGH-ATTENUATION CASES.  ANALYTIC
C     APPROXIMATION STARTS AT STATEMENT 70.
   70 CEX=0.5*CONST*(ALPH(3,1)+ALPH(3,2))
      CEY=0.5*CONST*(ALPH(3,2)+ALPH(3,3))
      ALOS1=EXPF(-CEX*DS1)
      ALOS2=EXPF(-CEY*DS1)
      ALOS3=EXPF(-CEY*(DS1+DS2))
      DIEMP=(0.5/CONST)*((TT(1)+TT(2))*(1.-ALOS1) + (TT(2)+TT(3))*(ALOS2
     1    -ALOS3))
      GO TO 72
   71 ALOSS=10.**(-ATTN(3,K+1)*.05)
      TP2=ALPH(3,K+1)*TT(K+1)*ALOSS
      CALL INTGRT(DS1,DS2,TP1,TP2,TP3,DIEMP)
   72 TEMP = TEMP+DIEMP
      DRDH1=DRDH3
      TP1 = TP3
      Y1=Y11=Y3
      Y12=Y32
      AN1 = AN3
   81 CONTINUE
   80 CONTINUE
      AIMP=TEMP*CONST
      END
```

```
                                                                  06/29/72
      SUBROUTINE ALPHA(PP,Z)
      COMMON /PTR/ PP(75), TT(75), RP(75),ALPH(3,75)
      COMMON/H2O/RWSFAC
      DIMENSION FTRP(23),FTRH(23)
      DIMENSION DELH(4),IMAX(4)
      DATA(DELH=100.,1000.,2000.,5000.),(IMAX=21,25,20,6)
      DATA(AL2=.1),(AL3=.27),(H1=24000.),(H2=42000.),(PWR=.5)
      DATA(CONST=3.7148),(CONST2=0.29685E)
      DATA(CSTH2O= 4.693  E-3),(FRH2O=22.235),(GAL7E80=17.99)
      DATA(CVP=.750064),(SMXI=.20646)
      DATA(FTRP=56.2649,56.4466,59.5911,60.4348,61.1506,61.8002,62.4112,
     162.9980,63.5685,64.1272,64.6779,65.2240,65.7626,66.2978,66.8313,
     267.3627,67.8923,68.4205,68.9478,69.4741,70.0000,70.5249,71.0497)
      DATA(FTRH=118.7505,62.4663,60.3041,59.1642,58.3239,57.6125,56.9682
     1,56.3834,55.7839,55.2214,54.6728,54.1294,53.5960,53.0695,52.5458,
     252.0259,51.5091,50.9949,50.4830,49.9730,49.4648,48.9582,48.4530)
      DATA (PP=
     11.01325E+3,1.00959E+3,1.00595E+3,1.00231E+3,9.9868E+2,9.95076E+2,
     19.91473E+2,9.8788E+2,9.84299E+2,9.80728E+2,9.77167E+2,9.73617E+2,
     19.70077E+2,9.66548E+2,9.63029E+2,9.59521E+2,9.56023E+2,9.52536E+2,
     19.49058E+2,9.45591E+2,9.42135E+2,9.3869E+2,8.75129E+2,8.43109E+2,
     18.12047E+2,7.81921E+2,7.52710E+2,7.24391E+2,6.96943E+2,6.70347E+2,
     16.44581E+2,6.19629E+2,5.95459E+2,5.72065E+2,5.49422E+2,5.27513E+2,
     15.06319E+2,4.85822E+2,4.66003E+2,4.46845E+2,4.28334E+2,4.10449E+2,
     13.93176E+2,3.76497E+2,3.60398E+2,3.44862E+2,3.29874E+2,3.15420E+2,
     13.01484E+2,2.75110E+2,2.50541E+2,2.27969E+2,2.07148E+2,1.88230E+2,
     11.71043E+2,1.55428E+2,1.41241E+2,1.28352E+2,1.16641E+2,1.06000E+2,
     19.63319E+1,8.75472E+1,7.95450E+1,7.23119E+1,6.57212E+1,5.97323E+1,
     15.42901E+1,4.93447E+1,4.48504E+1,3.53282E+1,2.78307E+1,2.19421E+1,
     11.73765E+1,1.38270E+1,1.10533E+1)
      DATA (TT=
     12.88160E+2,2.87956E+2,2.87764E+2,2.87566E+2,2.87368E+2,2.87169E+2,
     12.86971E+2,2.86773E+2,2.86575E+2,2.86377E+2,2.86179E+2,2.85981E+2,
     12.85783E+2,2.85585E+2,2.85387E+2,2.85188E+2,2.84990E+2,2.84792E+2,
     12.84594E+2,2.84396E+2,2.84198E+2,2.82217E+2,2.80237E+2,2.78256E+2,
     12.76276E+2,2.74296E+2,2.72316E+2,2.70337E+2,2.68357E+2,2.66378E+2,
     12.64399E+2,2.62420E+2,2.60442E+2,2.58463E+2,2.56485E+2,2.54507E+2,
     12.52529E+2,2.50551E+2,2.48574E+2,2.46597E+2,2.44620E+2,2.42643E+2,
     12.40666E+2,2.38689E+2,2.36713E+2,2.34737E+2,2.32761E+2,2.30785E+2,
     12.28809E+2,2.24859E+2,2.20909E+2,2.16960E+2,2.13010E+2,2.13010E+2,
     12.13010E+2,2.13010E+2,2.13010E+2,2.13010E+2,2.13010E+2,2.13010E+2,
     12.13010E+2,2.13010E+2,2.13010E+2,2.13010E+2,2.13010E+2,2.13010E+2,
     12.13010E+2,2.13010E+2,2.13010E+2,2.13010E+2,2.13010E+2,2.13010E+2,
     12.23602E+2,2.28134E+2,2.32664E+2)
C     THE FOLLOWING DATA CARDS WERE GENERATED 6/28/72. MINOR REVISION.
      DATA(RR= 7.50000E  0, 7.43584E  0, 7.37179E  0, 7.30779E  0,
     1 7.24387E  0, 7.18004E  0, 7.11630E  0, 7.05267E  0, 6.98913E  0,
     1 6.92575E  0, 6.86247E  0, 6.79933E  0, 6.73633E  0, 6.67347E  0,
     1 6.61077E  0, 6.54822E  0, 6.48585E  0, 6.42364E  0, 6.36162E  0,
     1 6.29978E  0, 6.23814E  0, 6.17668E  0, 6.11540E  0, 6.05432E  0,
     1 5.98936E  0, 5.90702E  0, 3.04673E  0, 2.62039E  0, 2.23850E  0,
     1 1.90459E  0, 1.61971E  0, 1.38096E  0, 1.18125E  0, 1.01091E  0,
     1 8.64635E -1, 7.38447E -1, 6.29176E -1, 5.34311E -1, 4.53215E -1,
     1 3.83598E -1, 3.23824E -1, 2.75746E -1, 2.31430E -1, 1.91777E -1,
     1 1.56023E -1, 1.23607E -1, 9.44502E -2, 7.08040E -2, 5.23315E -2,
     1 3.86489E -2, 1.70220E -2, 1.03701E -2, 6.45199E -3, 4.04284E -3,
```

06/29/72

```
     1 2.38249E -3, 1.46690E -3, 1.05209E -3, 9.02707E -4, 8.40642E -4,
     1 7.91078E -4, 7.14460E -4, 6.37848E -4, 5.79962E -4, 5.51107E -4,
     1 5.44362E -4, 5.50855E -4, 5.64024E -4, 5.87972E -4, 6.21432E -4,
     1 7.06726E -4, 8.03642E -4, 9.09155E -4, 7.32574E -4, 5.65102E -4,
     1 4.40224E -4)
      DATA(RHOFAC=1.)
      FGHZ=FMHZ*1.E-3
      FGHZ2=FGHZ*FGHZ
      FRATIO=FGHZ/FRH20
      FSUM2=(FGHZ+FRH20)**2
      FDIF2=(FGHZ-FRH20)**2
      I=0
      H=-100.
      DO 100 J=1,4
      IM=IMAX(J)
      DO 100 K=1,IM
      I=I+1
      RO   =RR(I) * RHOFAC
      PPW=RO   *TT(I)/216.75
C     TOTAL PRESSURE IS DRY-ATMOSPHERE PRESSURE + PARTIAL PRESSURE OF
C     WATER VAPOR (MILLIBARS).
      PR=PP(I) + PPW/CVP
      TSQ=TT(I)**2
      H=H+DELH(J)
      IF (H.LE.H1)  10,11
   10 AL1=.64
      GO TO 15
   11 IF (H .GT. H2) 12,13
   12 AL1=1.357
      GO TO 15
   13 AL1=.64 + .717*(H-H1)/54000.
   15 HAL1=CONST2*AL1*PP(I)/TT(I)
      HSA1=HAL1*HAL1
      FO=HAL1/(FGHZ2+HSA1)
      SUM=0.
      DO 50 M=1,23
      AN=2.*M-1.
      AN1=AN+1.
      ANP2=AN*(2.*AN+3.)/AN1
      ANM2=AN1*(2.*AN-1.)/AN
      AN02=2.*(AN*AN+AN+1.)*(2.*AN+1.)/(AN*AN1)
      FNP=HAL1/((FTRP(M)-FGHZ )**2+HSA1)+HAL1/((FTRP(M)+FGHZ)**2+HSA1)
      FNM=HAL1/((FTRM(M)-FGHZ )**2+HSA1)+HAL1/((FTRM(M)+FGHZ)**2+HSA1)
      TERM=(FNP*ANP2+FNM*ANM2+FO*AN02)*EXPF(-2.06844*AN*AN1/TT(I))
      SUM=SUM+TERM
   50 CONTINUE
C     ALPHO2=ALPH(1,I) IS ABSORPTION COEFFICIENT FOR OXYGEN
      ALPHO2 = CONST*(PR    /TT(I)**3)*FGHZ2*SUM
      ALPH(1,I)=ALPHO2
      TRO=300./TT(I)
      DELF=DEL/DEL0*(PPW*TRO+ PP(I)*CVP      *SMX1*TRO**.63)*1.E-3
      DELF2=DELF*DELF
      FPR2=FRATIO*DELF*(1./(FSUM2+DELF2)+1./(FDIF2+DELF2))
      ALPH22=CST22*FGHZ*PPW*TRO**3.5*EXPF(2.144*(1.-TRO))*FPR2
      ALFRES=1.3E1F-2 * FGHZ2 * RO * PR * TT(I)**(-2.5)
C     ALPH(2,I) IS ABSORPTION COEFFICIENT FOR WATER VAPOR
```

06/29/72

```
      ALPH(2,I) = ALPH2C + ALPRES
C     ALPH(3,I) IS TOTAL ABSORPTION COEFFICIENT
      ALPH(3,I)= ALPH(1,I) + ALPH(2,I)
  100 CONTINUE
      END
```

06/23/72

```
      SUBROUTINE DDH(H)
      COMMON /RRG/REFQ,RAD,GRAD,U
      COMMON/DRS/ DSDH3,DRDH3,AN
      EX=REFQ*EXP(-GRAD*H)
      AN=1.+EX
      V=EX*(2.+EX)
      W1=H/RAD
      W=W1*(2.+W1)
      DSDH3=AN*(1.+W1)/SQRT(U+V*W+V*W)
      DRDH3=AN*DSDH3
      END
```

06/23/72

```
      SUBROUTINE INTGRT (H1,H2,Y1,Y2,Y3,AREA)
      H12=H1*H1
      H22=H2*H2
      HH=H1*H2
      HPH=H1+H2
      AFAC=(Y1*H2 + Y3*H1-Y2*HPH)/(HH*HPH)
      AREA = (AFAC/3.)*(H22*H2 + H12*H1) + (Y3-Y2-AFAC*H22)*(H22-H12)/
     1    (2.*H2)  + Y2*HPH
      END
```

## REFERENCES


1. Blake, L.V., "A Fortran Computer Program to Calculate the Range of a Pulse Radar," NRL Report 7448, August 1972.
2. Blake, L.V., "Radar Attenuation by Atmospheric Oxygen," paper presented at URSI Commission 2 meeting of May 6, 1959, Washington, D.C.
3. Blake, L.V., "Interim Report on Basic Pulse-Radar Maximum-Range Calculation," NRL Memorandum Report 1106, Nov. 1960.
4. Blake, L.V., "Curves of Atmospheric-Absorption Loss for Use in Radar Range Calculation," NRL Report 5601, Mar. 1961.
5. Blake, L.V., "Recent Advancements in Basic Radar Range Calculation Technique," IRE Trans. *MIL-5* (No. 2), 154-164 (Apr. 1961).
6. Blake, L.V., "Tropospheric Absorption Loss and Noise Temperature," Trans. *IRE AP-10* (No. 1), 101-102 (Jan. 1962).
7. Blake, L.V., "A Guide to Basic Pulse-Radar Maximum-Range Calculation, Part 1 — Equations, Definitions, and Aids to Calculation," NRL Report 5868, Dec. 1962, and Second Edition, NRL Report 6930, Dec. 1969; and "Part 2 — Derivations of Equations, Bases of Graphs, and Additional Explanations," NRL Report 7010, Dec. 1969.
8. Blake, L.V. "Prediction of Radar Range," Chapter 2 of *Radar Handbook*, M.I. Skolnik, editor, McGraw-Hill, New York, 1970.
9. Van Vleck, J.H., "The Absorption of Microwaves by Oxygen," Phys. Rev. 71 (No. 7), 413-424 (Apr. 1, 1947).
10. Van Vleck, J.H., "The Absorption of Microwaves by Uncondensed Water Vapor," Phys. Rev. 71 (No. 7), 425-433 (Apr. 1, 1947).
11. Meeks, M.L., and Lilley, A.E., "The Microwave Spectrum of Oxygen in the Earth's Atmosphere," J. Geophys. Res. 68 (No. 6):1683-1703 (Mar. 15, 1963).
12. Reber, E.E., Mitchell, R.L., and Carter, C.J., "Attenuation of the 5-Mm Wavelength Band in a Variable Atmosphere," IEEE Trans. *AP-18* (No. 4), 472-479 (July 1970).
13. Straiton, A.W., and Tolbert, C.W., "Anomalies in the Absorption of Radio Waves by Atmospheric Gases," Proc. IRE 48 (No. 5), 898-903 (May 1960).
14. Liebe, H.J., "Calculated Tropospheric Dispersion and Absorption Due to the 22-GHz Water Vapor Line," IEEE Trans. *AP-17* (No. 5), 621-627 (Sept. 1969).
15. Bean, B.R., and Abbott, R., "Oxygen and Water Vapor Absorption of Radio Waves in the Atmosphere," Geofisica Pura E Applicata (Milano) 37, 127-144 (1957).
16. Hogg, D.C., "Effective Antenna Temperatures Due to Oxygen and Water Vapor in the Atmosphere," J. Appl. Phys. 30, 1417-1419 (Sept. 1959).
17. Schulkin, M., "Determination of Microwave Atmospheric Absorption Using Extraterrestrial Sources," NRL Report 3843, Oct. 1951.
18. Le Fande, R.A., "Attenuation of Microwave Radiation for Paths Through the Atmosphere," NRL Report 6766, Nov. 1968.

19. Ulaby, F.T., and Straiton, A.W., "Atmospheric Absorption of Radio Waves Between 150 and 350 GHz," IEEE Trans. *AP-18* (No. 4), 479-485 (July 1970).

20. Van Vleck, J.H., and Weisskopf, V.F., "On the Shape of Collision-Broadened Lines," Rev. Mod. Phys. 17 (Nos. 2 and 3), 227-236 (Apr.-July 1945).

21. Minzner, R.A., Ripley, W.S., and Condron, T.P., "U.S. Extension to the ICAO Standard Atmosphere," Dept. of Commerce Weather Bureau and USAF ARDC Cambridge Research Center, Geophysics Research Directorate, Government Printing Office, Washington, D.C., 1958.

22. Sissenwine, N., Grantham, D.D., and Salmela, H.A., "Humidity up to the Mesopause," Air Force Cambridge Research Laboratories Report AFCRL-68-0550 (Air Force Surveys in Geophysics No. 206), Oct. 1968.

23. Blake, L.V., "A 'French Curve' Computer Plotting Subroutine," NRL Memorandum Report 2335, Sept. 1971.

24. Bean, B.R., and Dutton, E.J., "Radio Meteorology," National Bureau of Standards Monograph 92, Government Printing Office, Mar. 1966, pp. 65-73.

25. Blake, L.V., "A Modified Simpson's Rule and Fortran Subroutine for Cumulative Numerical Integration of a Function Defined by Data Points," NRL Memorandum Report 2231, Apr. 1971.

26. Blake, L.V., "Ray Height Computation for a Continuous Nonlinear Atmospheric Refractive-Index Profile," Radio Science 3 (New Series) (No. 1), 85-92 (Jan. 1968).

27. Dicke, R.H., et al., "Atmospheric Absorption Measurements with a Microwave Radiometer," Phys. Rev. 70, 340-348 (Sept. 19.6).